MSc Thesis

Deterministic vessel motion prediction based on a wave radar forecast

S.M. Hillenius

Technische Universiteit Delft

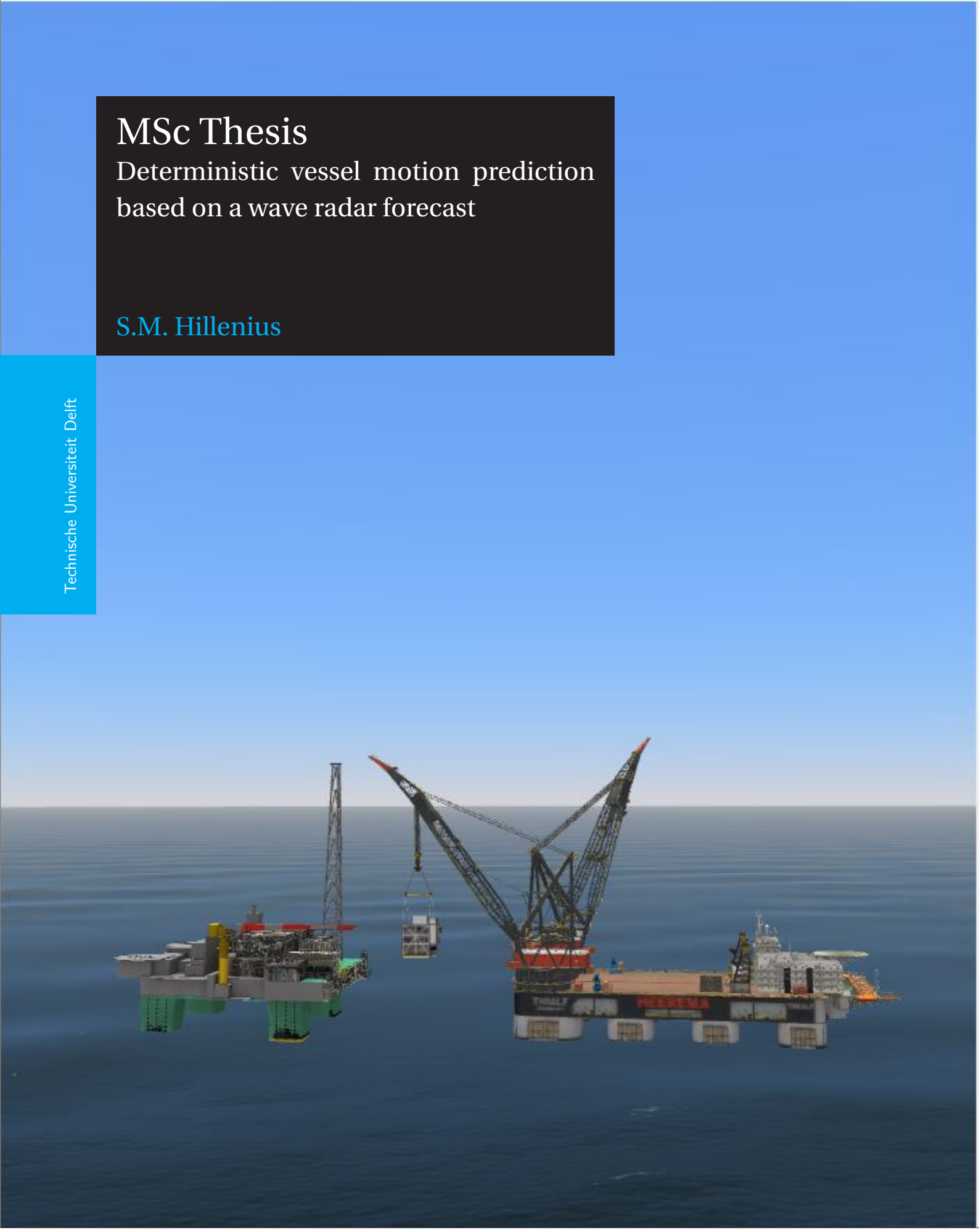

TU Delft Delft University of Technology

Challenge the future

“Front cover: Screen-shot of the Skarfjell exercise simulated in K-Sim.”

MSc Thesis

Deterministic vessel motion prediction based on a wave radar forecast

by

S.M. Hillenius

in partial fulfillment of the requirements for the degree of

Master of Science
in Offshore & Dredging Engineering

at the Delft University of Technology,
to be defended publicly on 15 November 2017 at 14:30 PM.

Supervisor:	Prof. Dr. Ir. A. V. Metrikine	TU Delft
Thesis committee:	Ir. J.S. Hoving	TU Delft
	Ir. G. Meskers	Heerema Marine Contractors
	Ir. T. Deelen	Heerema Marine Contractors

This thesis is confidential and cannot be made public until November 15, 2022.

TU Delft Delft University of Technology

PREFACE

Before you lies the thesis "Deterministic vessel motion prediction based on a wave radar forecast". This is the result of the 9 month graduation internship at Heerema Marine Contractors as part of my master program Offshore & Dredging Engineering at the TU Delft. With my graduation, an end has come to my student career which started in 2010 at the faculty Technology, Policy and Management.

First of all I would like to thank the people who helped me at HMC throughout my research and made it what it is today. I would like to thank my daily supervisor - Thomas Deelen - who has supported me on a daily basis and with whom I have had many discussions about the route to take. Geert Meskers who was willing to share his experience and knowledge with me and guided me throughout my research. Ruben de Bruin and Sjoerd de Jong, who have boosted my programming skills to a level I could not have dreamed of. Furthermore, I would like to express my gratitude to the whole HSC department who have helped me when 'the computer said no'.

Secondly I would like to thank Andrei Metrikine, my graduation professor and Jeroen Hoving for their willingness to be part of my thesis committee and guidance with an academic point of view.

To the reader: I sincerely hope you enjoy reading this!

S.M. Hillenius
Delft, November 2017

ABSTRACT

A new development aiming to improve the safety and/or operability of offshore operations is deterministic motion forecasting. Various parties target at developing a radar which is able to detect wave trains. This deterministic wave forecast can be used to forecast vessel motions up to several minutes ahead. With such a forecast a quiescent period can be searched for, where ship motions are at a minimum. Possible advantages considered for a heavy lift operation are: Safer operations, less waiting on weather and extended lifetime of equipment. With the use of the Heerema Simulation Center (HSC), the possibilities to extend a deterministic wave forecast into a motion forecast is investigated. The wave components are known in the HSC, so a perfect wave radar is available and the focus is entirely on (1) predicting motions and (2) presenting it in a useful way.

The first part of the objective is approached by investigating the possibilities and limitations of making a motion forecast in the frequency domain. This method is convenient since the calculation is easy to understand and very fast, a quality which is most wanted when making a future prediction. To quantify the quality of a wave- and motion forecast, the correlation coefficient (ρ) and RMS ratio (σ) are used (forecasted- vs logged motion).

The model showed good results for heave roll and pitch (ρ 0.85 - 1.0, σ 0.86 - 1.15) for mild, severe and complex sea-states (all wave directions, respectively). For extreme swell a forecast could not be made. This can be explained by the fact that when motions become larger, a frequency domain approach is no longer valid. However, it should be noted that it is very unlikely a lift operation will take place with Hs > 2m.

The sensitivity of the model to variations in the center of gravity and radii of gyration of the vessel (model input), is found to be within acceptable bounds. The impact is negligible on the phase and small (<10%) on the amplitude of the forecast. With data offshore available with an accuracy of +- 2m, this is acceptable.

Two test cases are investigated. A single crane lift (1000 mT module) and a dual crane (7000 mT module). In both cases the model proved to be well capable of forecasting the motion of interest (Heave) of the module (relative to a fixed and floating platform).

The second part of the objective has a more qualitative character, where the use of a forecast is tested in the HSC by using a tool that is created for this purpose: the Virtual Wave Radar Tool (VWRT). This tool is able to make and display a forecast in the HSC. The tests executed in the HSC showed positive results for the use of a forecast in the crane cabin during a lift operation. A reduction of secondary impact loads in a challenging environment was realized due to the use of the VWRT. Furthermore, a forecasted time span of two minutes (current performance of wave radars on the marked) proved to be long enough to benefit from during a lift operation. The tool demonstrated that simplicity of the dashboard is key and should be understandable at a glance.

With many possible sources causing a forecast to deviate from the actual motion, a self learning, optimization model could reduce the need for exact model input offshore (not always available), even without knowing the source of deviation.

ACRONYMS

API Application Programming Interface.

APS Applied Physical Sciences.

CoG Center of Gravity.

DCV Deepwater Construction Vessel.

EOM Equation of motion.

ESMF Environmental and Ship Motion Forecasting.

FEED Front End Engineering Design.

FPU Floating Production Platform.

HMC Heerema Marine Contractors.

HSC Heerema Simulation Center.

JIP Joint Industry Project.

LPP Lenghth Between Perpendiculars.

OWME On board Wave and Motion Estimator.

POI Point of Interest.

PS Portside.

RAO Response Amplitude Operator.

RMS Root Mean Square.

SB Starboard.

SSCV Semi-Submersible Crane Vessel.

TU Delft Delft University of Technology.

VWRT Virtual Wave Radar Tool.

NOMENCLATURE

Physics Constants

g	Gravitational Constant	$9.80665\,m/s^2$
ρ	Water Density	$1.025\,kg/m^3$

Other Symbols

ϕ_{shift}	Phase shift	rad
ω	Angular Frequency	rad/s
λ	Wave length	m
l	Traveled distance wave	m
k	Wave number	rad/m
d	Water depth	m
T	Period	sec
A	Wave amplitude	m
A_{comp}	Complex wave amplitude	m
t	Time	sec
T_{start}	Correction internal time HSC	sec
ρ	Correlation coefficient	–
σ	Root Mean Square Ratio	–

SIGN CONVENTIONS

K-SIM

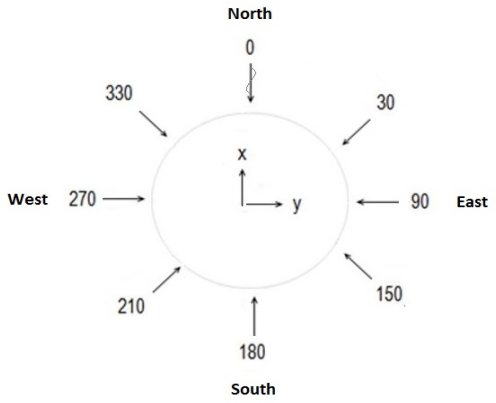

Figure 1: Sign convention K-Sim: Wave direction coming from, clock wise w.r.t. north. Global coordinate system X to north, Y to east

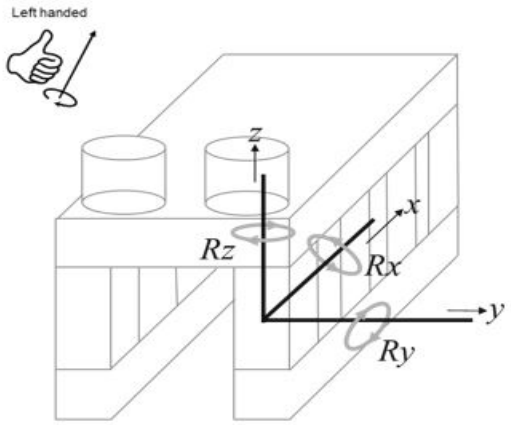

Figure 2: Sign convention K-Sim: Left handed coordinate system, Positive: Z up, x to bow, y to SB, yaw clock wise, roll PS down, Pitch bow down

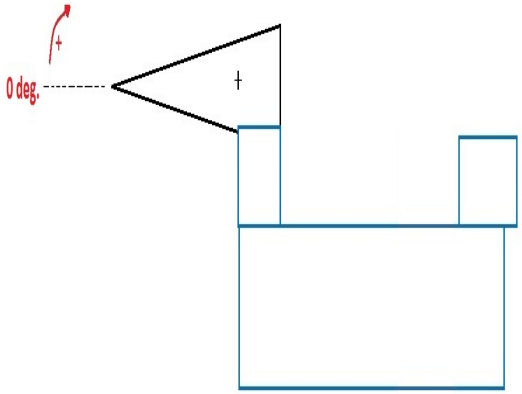

Figure 3: Sign convention K-Sim: Crane boom angles positive upwards, 0 deg horizontal.

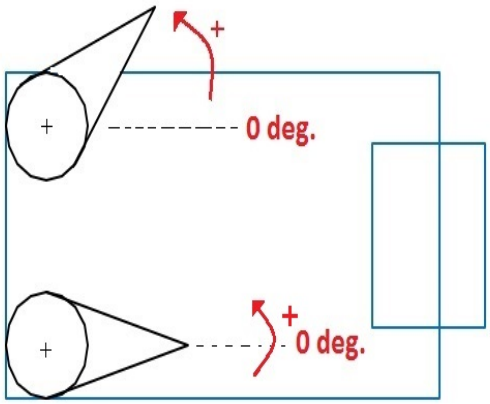

Figure 4: Sign convention K-Sim: Crane slew angles positive C.C.W, 0 deg in cradle pointing to bow.

LIFTDYN

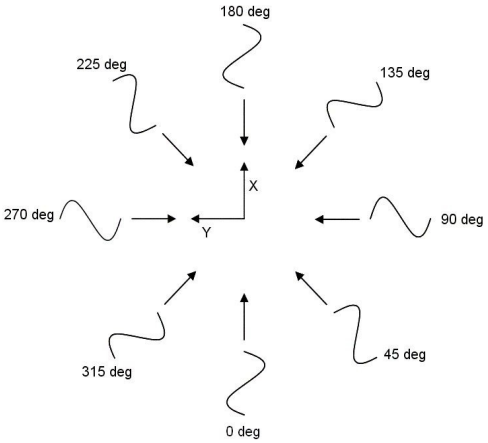

Figure 5: Sign convention LiftDyn: Wave direction coming from, counter clock wise w.r.t. local body axis, 0 deg wave following vessel

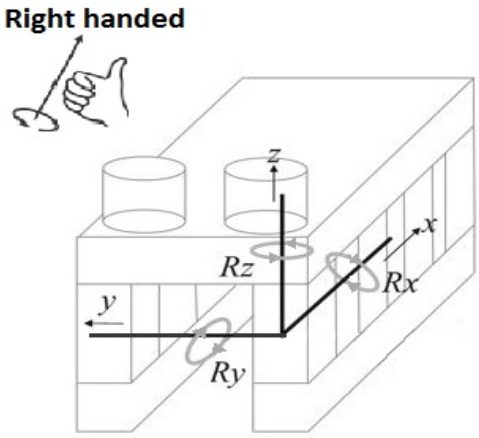

Figure 6: Sign convention LiftDyn: Right handed coordinate system, Positive: Z up, x to bow, y to PS, yaw counter clock wise, roll SB down, Pitch bow down

ORCAFLEX

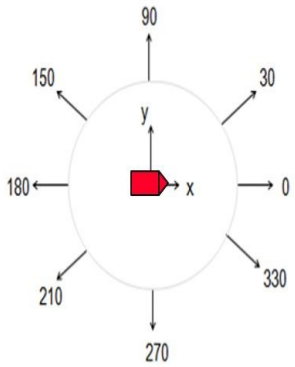

Figure 7: Sign convention OrcaFlex: Wave direction going to, counter clock wise w.r.t. local body axis, 0 deg wave following vessel.

CONTENTS

1

INTRODUCTION

1.1. INTRODUCTION

Heerema Marine Contractors (HMC) is a world leading marine construction company for the oil and gas industry and is specialized in design, transportation, installation and removal of all types of fixed and floating offshore structures, subsea pipelines and infrastructures in shallow and deep water. HMC owns and operates her own fleet consisting of the Semi-Submersible Crane Vessel (SSCV) Thialf, Deepwater Construction Vessel (DCV) Balder, DCV Aegir, anchor handling tugs/supply vessels and cargo/launch barges.

1.2. PROBLEM DEFINITION

In the oil and gas industry, safety is a main priority and becomes even more important when working offshore in conditions where risks can be high. HMC's most valuable assets, are its people. Therefore the company strives to create an incident and injury free work place (Rijtema, 2017, 00:26).

One of HMC's key operations is the lifting of objects with it's crane vessels. A suspended load is directly influenced by vessel motions and can be very dangerous when not handled with care. Based on load calculations and infield experience, workability limits are defined to ensure a successful operation and create a safe work environment.

Vessel motions are affected by the metocean conditions (wind, wave, climate, etc.). To find a period of workable weather required to perform an operation, a 'stochastic longterm prediction' is made with the use of weather data (note this is a probability distribution). In case one of the forecasted responses is exceeding the limit, the start of the operation will be postponed. This is known as 'Waiting on weather'. With high vessel rates, weather related downtime has a significant affect on the project's total costs.

A new development to improve the safety and/or Operability of offshore operations is deterministic motion forecasting. Various parties and Joint Industry Project (JIP)'s target at developing a radar which is able to detect wave trains. With the output of this wave radar, a model can be constructed to make a deterministic wave forecast. This wave forecast is then used to forecast vessel motions up to several minutes ahead. In contrary to a 'stochastic longterm motion prediction', the magnitude of both wave and vessel motions are now forecasted in time. With such a forecast a quiescent period can be searched for, where ship motions are at a minimum. Possible advantages considered for a heavy lift operation are: Safer operations, Less waiting on weather and an Extended lifetime for equipment. This leads to the following research question:

Research question: "(How) Can the safety and / or operability of offshore lifting operations be increased by deterministic motion forecasting?."

1.3. OBJECTIVES

HMC is interested in the possible advantages of deterministic motion forecasting of vessels, lifted items, barges and support vessels during offshore operations. A test campaign is planned for the summer of 2018 were a 'FutureWave™' system on board the Thialf will be tested (section 2.2.2). This thesis is aiming to investigate the possibilities for the use of deterministic motion forecasting during offshore lift operations. The objective of this thesis can be divided in two:

1. Determine the most suitable way of predicting vessel motions based on a wave forecast.
2. Make a preliminary design for a 'dashboard' presenting the forecast based on user preferences.

By reaching the first objective, a suitable method to make a forecast based on a wave forecast, is found and evaluated. The second objective has a more qualitative character and will determine the way a forecast should be presented in order to benefit from during a lift operation. With completion of both objectives, an answer to the research question as stated in 1.2 can be formulated.

1.4. APPROACH

Together with Kongsberg Digital, HMC has developed a simulation center (Heerema Simulation Center (HSC)) to to train offshore operators, prepare for specific projects and test new innovative solutions. Within this research, the HSC will be used to test the possibilities to extend a deterministic wave forecast into a motion forecast. To do so, a tool will be created which is compatible with the HSC, referred to as the Virtual Wave Radar Tool (VWRT). The wave components are known in the HSC (section 3.2.1), so a perfect wave radar is available and the focus can be entirely on predicting motions and presenting it in a useful way to operators.

1.4.1. SUBQUESTIONS

To answer the stated research question 1.2, subquestions are formulated and grouped by the objective they are related to:

1. Determine the most suitable way of predicting vessel motions based on a wave forecast.
   - 1.1. What are the requirements for a vessel motion prediction model?
   - 1.2. Do the environmental conditions influence the accuracy of the forecast ?
   - 1.3. Do (heavy) lift operations effect the accuracy of a motion forecast ?
   - 1.4. What should a 'wave radar system' be capable of for a lifting operation to benefit from?
2. Make a preliminary design for a 'dashboard' presenting the forecast based on user preferences.
   - 2.1. What operations can potentially benefit from a forecast?
   - 2.2. What parameter is relevant to forecast and how to present it?
   - 2.3. To whom is the forecast presented ?
   - 2.4. How can confidence in the motion forecast be created?

1.5. THESIS OUTLINE

This thesis consists of eight chapters. The first chapter gives an introduction to the thesis subject. The second chapter gives background information on deterministic motion forecasting and marine wave radars in particular. This will help the reader to understand the challenges of making a deterministic vessel motion forecast. Chapter three will give information about the HSC and its purpose within this research. In chapter four a model able to make a motion forecast based on a wave forecast is discussed. This model is tested in chapter five where two lift operations are investigated. In chapter six a tool is build which is able to display the forecast in the HSC. This tool is tested and the results are presented in chapter seven. In the final chapter conclusions and recommendations are given.

2

LITERATURE - THEORY OF WAVE RADAR SYSTEMS

This chapter will give background information on deterministic motion forecasting and marine wave radars in particular. This will help the reader to understand the current challenges of making a deterministic vessel motion forecast.

2.1. DETERMINISTIC MOTION FORECASTING

As mentioned in the introduction (section 1.2), several applications are thinkable for the use of (real-time) deterministic motions forecasting, in which (vessel) motions are predicted in time. The duration of the forecasted period and accuracy are related and depend on the method used (decreasing accuracy for an increasing timespan). An interesting development is the prediction of vessel motions with the use of 'Neural Networks', were a data driven self learning algorithm uses measured vessel motions to make a prediction up to 10 seconds in the future [1], [2]. A method getting more attention in recent years, is the forecasting of vessel motions based on a wave forecast. Deterministic vessel motion prediction based on a wave forecast, can be summarized in three general steps which are continuously solved in real time:

1. **Sea surface measurement:** A device measures the (directional) sea state at a certain distance from the vessel (section 2.1.1).

2. **Wave propagation:** The sea state at the location of the vessel is predicted using a wave propagation model (section 2.1.2).

3. **Vessel motion prediction:** The vessel motions are predicted based on the forecasted sea state at the location of the vessel (section 2.1.3) .

2.1.1. SEA SURFACE MEASUREMENT

Sea surface measuring techniques can be divided into "in situ techniques" (positioned in the water) and "remote sensing techniques" (positioned above the water). The most common in situ - and remote sensing surface measuring techniques are the waverider buoy (figure 2.1) and wave radar (figure 2.2). For more information about other surface measuring techniques I refer to [3].

Figure 2.1: Directional waverider buoy, picture taken from the RS Aqua website

Figure 2.2: Schematic representation of a X-Band radar (antenna). Picture taken from the Kongsberg website.

WAVERIDER

A waverider buoy is commonly used in the offshore industry to derive stochastic wave characteristics (e.g. significant wave height (Hs), peak period (Tp), most probable maximum (mpm), etc.) at a location close to the vessel. The use of a waverider for making a deterministic motion forecast has the clear disadvantage that the positioning of the buoy needs to be carefully selected w.r.t the vessel and with a multi modal sea-sate (e.g. swell coming from different direction than wind seas), more than one buoy is needed. Furthermore, deploying and collecting these buoys is time consuming and for moving vessels this method cannot be used.

WAVE RADAR

The use of a radar to measure the sea surface (referred to as 'wave radar'), has the clear advantage over 'in situ techniques' of monitoring a much larger area with the use of a single radar and does not need to be deployed once on board installed. Therefore, the use of a wave radars has become a topic of interest in recent years and will be focused on in this research. More information about the wave radar is given in section 2.2.

2.1.2. WAVE PROPAGATION

To understand the concept of making a motion forecast based on a wave forecast, one must have basic knowledge of the linear wave theory and the propagation of waves. For a more in-depth explanation about ocean waves and the linear wave theory, I refer to [3], [4].

LINEAR WAVE THEORY

The linear wave theory (Airy wave theory) gives a linearized description of the propagation of gravity surface waves. The exclusion of non-linear wave-to-wave interactions, is valid when propagation distances are relatively small [5], [6]. The following assumptions are made:

- **Ideal fluid:** The fluid is incompressible with a constant density (i.e no stratification).
- **Continuous fluid:** No discontinuities within the fluid (e.g. no air bubbles), and therefore not valid when wave breaking becomes significant.
- **A single external force:** The water is only subjected to gravity. The generation of waves by wind is excluded.
- **Small amplitude:** The wave amplitude is small relative to the wave length and water depth (not valid for steep waves and shallow water).

Within the linear wave theory, an irregular sea-state can be described by a superposition of a large number of stochastically independent sinusoidal wave components (Fourier series, equation 2.1).

$$\eta(x,y,t) = \sum_{n=1}^{N}\sum_{m=1}^{M} A_{n,m} cos(\omega_n t - k_n x cos\theta_m - k_n y sin\theta_m + \phi n,m) \tag{2.1}$$

Where:

η Surface elevation [m]	ω Angular Frequency [rad/s]	ϕ Phase angle [rad]
k Wave number [m].	t Time [s]	θ Wave direction [rad]
M Wave directions [-].	N Wave frequencies[-]	n,m indices wave frequencies and directions [-]

The frequency and wavenumber are uniquely related through the dispersion relation (equation 4.4). It should be noted that due to this relation, two indices are sufficient in equation 2.1.

$$\omega^2 = gktanh(kd) \tag{2.2}$$

$$\omega = \frac{2pi}{T} \qquad k = \frac{2pi}{L} \qquad c_p = \frac{L}{T} = \frac{\omega}{k} \tag{2.3}$$

Where:

g Gravitational constant [m/s^2]	ω Angular Frequency [rad/s]	d Water depth [m]
k Wave number [rad/m]	L Wave length [m]	$TWaveperiod[s]$
c_p Phase speed [m/s]		

As a result of this relation, the propagation velocity (phase velocity,c_p) of a wave is dependent on its frequency, low frequency waves travel faster than high frequency waves. The dispersion relation forms the basis for wave propagation models within the linear wave theory.

WAVE PROPAGATION AND PREDICTABILITY

With the use of a propagation model, the surface elevation (η) at location A(x,y) can be forecasted in time(t) with knowledge of the wave component characteristics (ω,ϕ,k,θ) at location B (equation 2.1). Without applying restrictions to the time- (t) and space domain (x,y), the surface elevation at an arbitrary distance from the measured location can be described for an unlimited timespan [7]. Obviously this is not possible in reality and limits apply as is illustrated in figure 2.3.

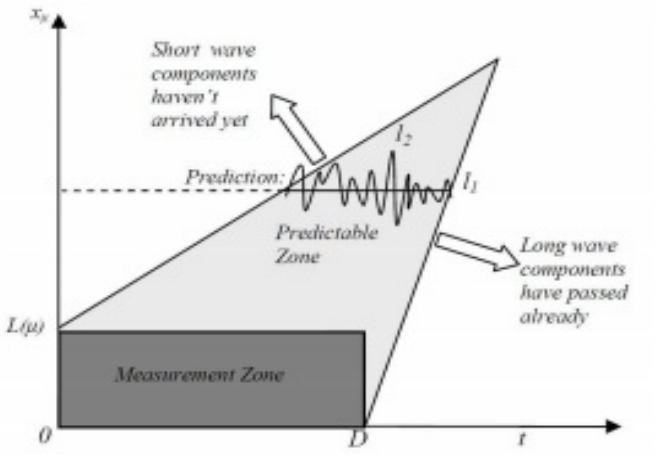

Figure 2.3: Predictable timespan for a measured zone by a wave radar, image taken from [8]

The limits that apply to the predictability of the surface elevation for a certain location (dotted line) based on the sea state at another location (Measurement Zone), is only valid for the part within the predictable gray zone. This zone is bounded by the group velocity (c_g, velocity with which the overall shape of the wave amplitudes propagate through space) of the highest- and lowest wave frequencies (l_2 and l_1) [9]. This can be explained by the fact that the longest wave components are already passed the vessel and the shortest have not reached the vessel yet.

Note: The example is for a single wave traveling direction and can be extended for a three dimensional wave field with waves traveling in several directions.

As a result, the optimal time horizon of a prediction is depending on the distance of the measurement point to the vessels location, wave period and directional spreading. Outside the predictable zone, the accuracy of a forecast will decrease drastically. This means that for a deterministic forecast, a good spatial (and temporal) coverage (Measurement Zone) is necessary, something that hardly can be achieved with 'in situ' techniques (section 2.1.1).

Summarizing the above, an answer to subquestion 1.1 (section 1.4.1, stated below), is found. The main requirement for a motion prediction is a low computational time.

Subquestion 1: "What are the requirements for a vessel motion prediction model?"

2.1.3. VESSEL MOTION PREDICTION

The most practical way of making a motion forecast based on a wave forecast, would be a frequency domain calculation. The calculation is easy to understand and very fast, a quality which is most wanted when making a future prediction (section 2.1.2).

A calculation in the frequency domain is only valid when forces are linear depending on motion, velocity and acceleration. In general a problem can be solved with a frequency domain approach when satisfying the following statements:

- **Linear process:** The output is linear with respect to the input meaning that a double input amplitude (e.g. wave amplitude) results in a double output amplitude (e.g. vessel motion) without a change in the phase shift between in- and output.
- **Stationary process:** The system does not change in time and therefore the response characteristics do not change in time.
- **Harmonic nature:** Forces are harmonic and proportional to sinusoids.

Several studies have validated a frequency domain approach for the the use of deterministic motion forecasting [8], [6], [10],[11],[10]. More information about these studies and results can be found in section 2.2.2.

2.2. THE WAVE RADAR

A wave radar measures sea characteristics of a large area with the use of a electromagnetic waves transmitted by the antenna of the radar. The returning signal is modulated by the encounter of a wave. The Doppler shift is used to derive intensity characteristics, resulting in a radar image (figure 2.4).

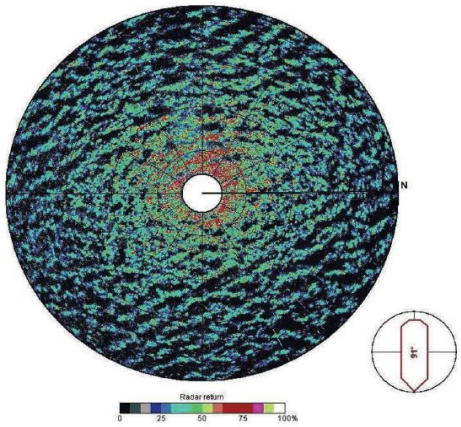

Figure 2.4: X-band radar image of surrounding sea, image taken from [12]

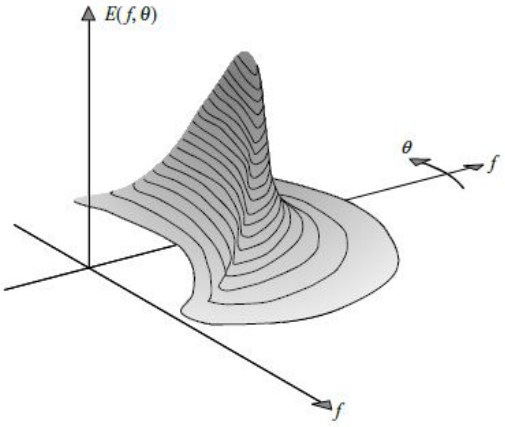

Figure 2.5: Two-dimensional spectrum of wind generated waves in polar co-ordinates. Picture taken from [3].

In contrary to for instance a wave buoy, the surface itself is not disturbed and the radar system can be deployed on either a fixed platform or a moving vessel. A typical radar system setup is shown in figure 2.6 and consists of a rotating antenna, a computer processing the radar images and a display and/or storage device. Furthermore, (motion) sensors are connected to compare the forecasted- with measured motion.

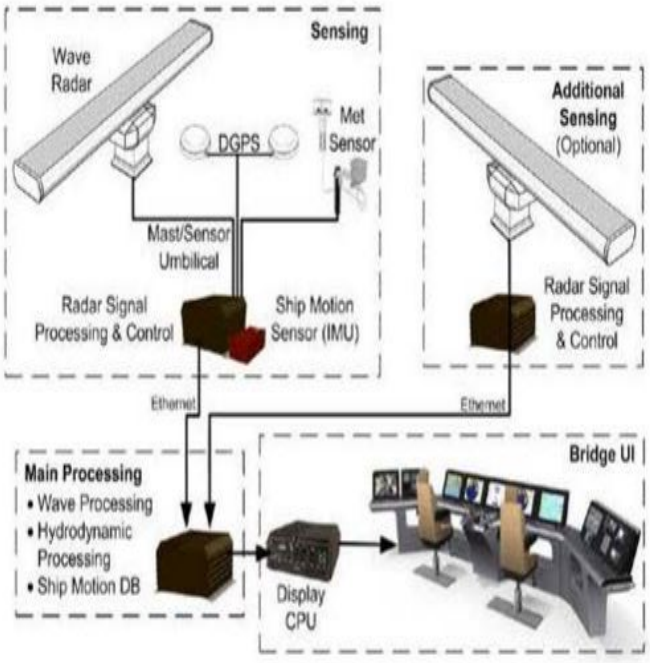

Figure 2.6: Wave radar system schematically illustrated, picture taken from the FutureWaves brochure

A marine radar is conventionally used for marine navigation were the reflection of the signal by waves ('sea-clutter') is unwanted and brought to a minimum. In contrary, a wave radar is making use of the 'sea-clutter' in order to make a wave forecast and therefore, this effect is enhanced. There are two mechanisms that mainly cause the reflection of magnetic wave on the sea surface [13]:

- **Specular reflection:** Radar is measuring the echo by reflection of the sea surface (Mirror-like reflection). This mechanism is important when the angle of incidence is small normal to the wave surface. Radars that look straight down use this mechanism (e.g. altimeter).

- **Bragg scattering:** Occurs for electromagnetic wave lengths equal to half the electromagnetic wave length (Bragg scatter criterion). For X-band marine radars this means that the high frequency gravity capillary waves are responsible for the return.

The later method is used when making a forecast and requires a certain surface roughness (gravity capillary waves) created by the wind to ensure backscattering. Therefore, favorable environmental conditions for a wave radar to operate in would be wind speeds and significant wave heights greater than 3 m/s and 0.5 m, respectively [14]. When the signal is reflected, the backscatter signals have a different amplitude, phase or frequency. This modulated signal carries information about the sea surface which can be extracted by processing the signal. Due to this modulation, longer (swell and wind) seas can be made visible. Typical X-band radar specifics are summarized in the table below:

	Frequency range [GHz]	Wavelength range [cm]	Rotation period [sec]	Range [m]
X-Band	8.0 – 12.0	2.5 - 4	1-3	2000

Table 2.1: X-band radar specifics

2.2.1. RADAR IMAGE PROCESSING

The first reports stating the use of a marine radar for the purpose of collecting ocean data, date back to the sixties [15]. Radar images were visually inspected to estimate the wave direction, wavelength and period. Young *et al.* [16] describes a method (used in todays wave radar systems) in which radar images (figure 2.4 are translated into a 3 dimensional directional (unambiguous) wave spectra E(f,θ) (figure 2.5). The radar image processing flow is schematically illustrated in the figure below:

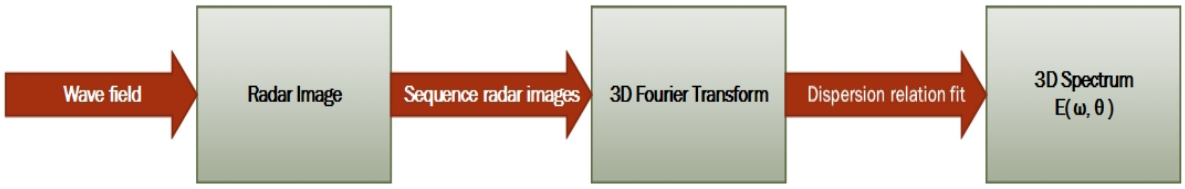

Figure 2.7: Radar image processing schematically illustrated

A sequence of radar images is used as input for a 3 dimensional Fast Fourier Transform, which delivers with knowledge of the dispersion relation (equation 4.4) a 3 dimensional directional wave spectra E(ω,θ). This spectra, describing how the mean sea-surface elevation is distributed as function of frequency and propagation direction. For more information about the three-dimensional analysis of (marine) wave radar images is refer to [16], [17],[14].

The acquisition and processing of radar images are two continuous parallel processes. This is illustrated in figure 2.8. A wave radar makes a number of images in a certain amount of time (Δt_1), depending on its repetition rate (typical 1-3 seconds). These images form a sequence which is analyzed. When a cycle (Δt_2, typical 10 seconds) is finished, the next (newest) sequence is analyzed. These cycles have a certain overlap which is used to correct for errors resulting in a changing forecast. To reduce the time needed to analyze the radar images, a radar is focused only on the area of interest (waves reaching the vessel).

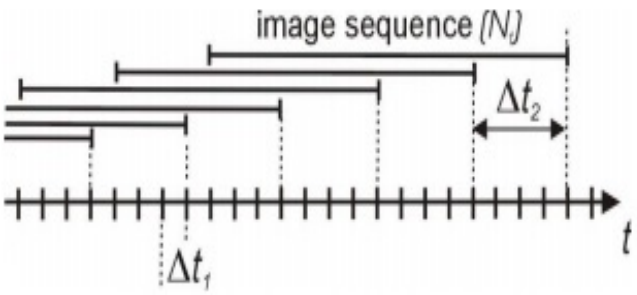

Figure 2.8: Update rate of wave radar, image taken from [8]

2.2.2. CURRENT DEVELOPMENTS OF WAVE RADAR SYSTEMS

This paragraph gives an overview of several wave radar products on the market, their specifics and claimed results. Further more the work of previous JIP's is summarized.

ON BOARD WAVE AND MOTION ESTIMATOR (OWME)

The OWME project was a JIP in which SBM, Shell, MARIN, OceanWaveS and the Delft University of Technology (TU Delft) were directly involved. The objective of the project was to develop, test and demonstrate a system that is able to predict a quiescent periods of ship motions up to 120 seconds ahead, in a mild to moderate sea state at zero forward speed [8]. To do so the Wave Monitoring System (WaMoS II, X-band radar) was used to derive the wave profiles at a distance of 500-2000m from the vessel. Table 2.2 gives a summary of the full scale tests results (80 m single hull support vessel), where the use of the WaMoS II radar is validated with a waverider buoy. The project concluded that although significant deviations between forecasted- and measured motions occurred, the OWME system proved capable of identifying quiescent periods. More research was needed to increase the accuracy and validate a wider range of sea states including a sea state in which both wind- and swell components are present.

WaMoS II	Range	Standard Deviation
Significant wave height	0.5-20 [m]	10% or 0.5 [m]
Wave period	3.5 - 40 [sec]	0.5 [sec]
Wave direction	0-360 [deg]	2 [deg]

Table 2.2: Summary of WaMos II parameters

WAMOS II RADAR

Several projects used the Wave and Surface Current Monitoring System (WaMoS II). Correlations of wave elevation measured and forecasted up to 0.87 have been reported by Hilmer and Thornhill [18]. The validation of a real-time prototype wave prediction system developed by OceanWaves GmbH is described in [6]. The predictive skill of the algorithm was tested with the use of data from several prior sea trials. Correlations exceeding 0.8 were realized between the predicted- and measured sea surface elevations. Figure 2.9 shows the correlation between the predicted- and measured sea surface elevation for the OWME trial.

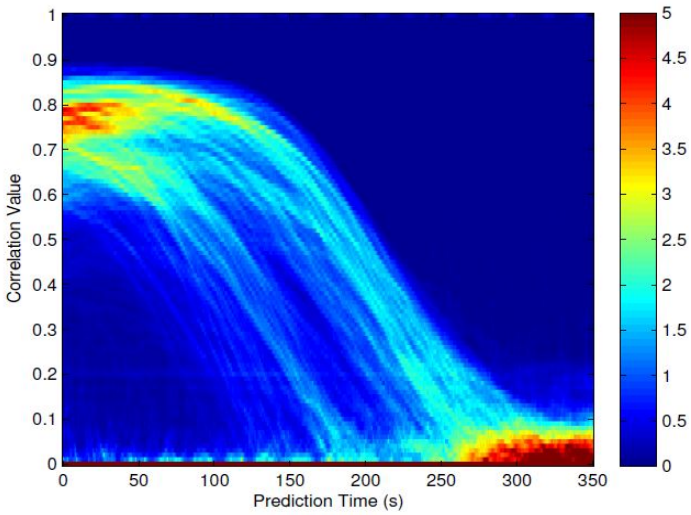

Figure 2.9: Correlation between the predicted- and measured sea surface elevation for the OWME trial. The color scale indicates the percentile of all results. Image taken from [6].

FUTUREWAVES

'FutureWaves is a standalone system that predicts vessel motion time-series based upon wide-area ocean-surface radar operational observations' [10]. The system is based on a development project lead by the University of Michigan where a Environmental and Ship Motion Forecasting (ESMF) system featuring a commercial of the shelf X-band marine radar was designed and tested. A nonlinear wave model (VORTWAVE) is used to propagate the radar-measured wave-field to the location of the vessel. Three vessel motion prediction models are incorporated in the ESMF system:

- **Pre-Computed RAO Model:** A pre-computed Response Amplitude Operator (RAO) approach using linear transfer functions to relate the ship response to the incident wave forcing (section 4.1.
- **Adaptive Filter Model:** A model using measured motions to 'tune' pre-computed RAO in real time, minimizing the uncertainties for the vessel mass- and damping characteristics (model input).
- **Autoregressive Model:** A model making a forecast based on measured vessel motions, designed for low-wind/swell dominated sea states when radar measurements of the wave field are unreliable due to a lack of sea surface roughness (backscatter criterion, section 2.2).

The system makes forecasts in real time for three time scales:

- **0 - 30 seconds:** A phase resolved wave- and motion forecast.
- **1 - 5 minutes:** A envelope of the wave- and motion time traces.
- **24-48 hours:** Statistically-averaged characteristics of wave- and ship motions.

Performance:

During sea trials (October 2013) on board the R/V Melville (a 85m long single hull vessel), a forecast by the FutureWaves system is compared with 'in-situ' waverider measurements. For a thirty seconds forecast with stern-quartering seas and a ship speed of 6 knots, the following correlation coefficients and RMS-ratios (section 4.2) have been reported. [11],[19]:

ESMF system	Correlation Coefficient(ρ) [-]	RMS Ratio (σ) [-]
Sway velocity	0.61	0.70
Heave	0.72	1.14
Pitch	0.77	1.05
Roll	0.52	1.22

Table 2.3: Summary of results reported for the ESMF system for a 30 second forecast, stern-quartering seas with a ship speed of 6 knots [11],[19].

Note: The above described results are obtained using the 'Pre-Computed RAO Model'. No results have been reported for the other models.

Similar results are reported for sea trials in October 2015 [10], figure 2.10. The left plot shows the evolution of the RMS for heave over time. The right plot shows the correlation between the forecasted- and measured heave motion as function for the forecast time . This plot shows a decreasing correlation for increasing forecast time as one would expect. Distinctive is the degraded system performance for small RMS values.

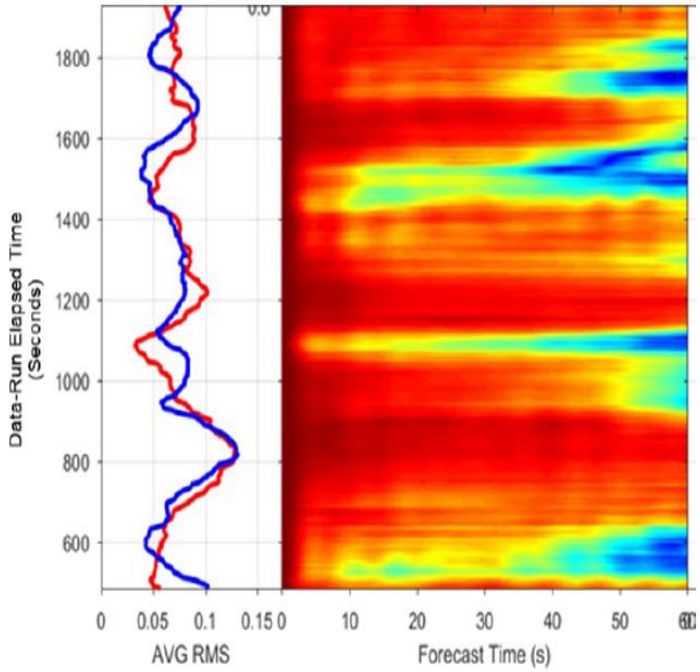

Figure 2.10: Results sea trials in October 2015 making a heave motion forecast with the use of a FutureWaves system, image taken from [10].

2.3. DETERMINISTIC MOTION FORECAST IN THE OFFSHORE INDUSTRY

Within the offshore industry, the following applications and advantages for the use of deterministic motion forecasting are identified:

- **Safer operations:** The execution of offshore operation without unexpected vessel motions would would improve the overall safety.
- **Vessel crossing:** The safe transport of personnel (and material) from one vessel to another without unexpected movements.
- **Extreme wave prediction:** Extreme waves (freak waves) can have a damaging effect on vessels and offshore operation. Real-time prediction of wave groups leading to such an extreme wave could mitigate this risk [20],[21],[11], [22].
- **Less waiting on weather:** When vessel motion exceed prescribed limits, an operation will be postponed. These limits can be broadened when able to forecast a quiescent period within a period of limit exceeding vessel motions.
- **Extended lifetime equipment:** By anticipating on vessel motions, loads can be reduced on equipment. E.g. second impact loads (a lifted objects hitting the surface several times due to a limit in hoisting- and lowering speed of the crane in combination with a moving vessel), can be reduced when anticipating on vessel motions.
- **Helicopter landing:** Landing a helicopter in offshore environments can be challenging. Predicting a quiescent period were vessel motions are at minimum would be beneficial for a safe landing [23].
- **Optimal Cruising speed:** The frequency of encounter is depending on the cruising speed of the vessel (e.g. with increasing speed, head seas become steeper with decreasing wave length). By adjusting the cruising speed of a vessel, the sea state spectrum can be shifted out of the area with peak periods of the RAO (section 4.1.1, resulting in a less critical response [22] .

3

THE HSC - INFORMATION ABOUT THE HEEREMA SIMULATION CENTER

3.1. THE HSC

The HSC was build by Kongsberg and delivered in the fourth quarter of 2015. It is located in the Heerema Leiden head office on the second floor. The simulator rooms (figure 3.1) are one-2-one with the actual offshore equipment of the HMC fleet and include:

- A bridge, incl. DP console
- A DP back-up room (full DP3)
- 2x crane dome's adjustable for the Thialf, Balder and Aegir
- A ballast control room
- 2x deck position
- A winch control room with 12 mooring winches
- 2x Instructor station
- 2x Debriefing room

Figure 3.1: HSC floor plan

The HSC is a project preparation tool different from most engineering tools. The simulations are run in real time and include dynamic environments with accurate hydrodynamics and physics. The interior of the crane cabins (figure 3.2) are adjustable to the different cranes on the HMC vessels. Furthermore, a simulation in the HSC includes the human element, an important factor in offshore operations. With the use of the HSC, project risks can be reduced by practicing critical procedures and operations, train in severe environmental conditions, test the implementation of a new design or improve operational performances.

3.2. K-SIM INSTRUCTOR

HMC has several (heavy-duty) laptops with stand alone software able to run a simulation outside the actual HSC environment. The K-Sim Instructor software, referred to as 'K-Sim', is an exact copy of the software in the HSC and has been used throughout this assignment to run simulations and test the VWRT. Furthermore, recordings of simulations can be replayed with K-Sim, allowing the user to analyze a simulation made in the

Figure 3.2: Interior crane dome HSC

past.

3.2.1. K-SIM IN- AND OUTPUT

K-Sim is an advanced software package with many options. This subsection will only describe features that are used for this research and need explanation.

SIGN CONVENTION

With K-Sim, any offshore environment of interest can be reconstructed (referred to as 'exercise'). An exercise can contain several bodies (referred to as 'objects') such as vessels and platforms. Each object has its own body-fixed coordinate system, local origin and heading with reference to the global origin. K-Sim uses a left-handed coordinate system, with for the global coordinates x-axis pointing North, y-axis East and z-axis upwards. The local body axis origin is typically chosen at the base of the body in the center of the top projection with x-axis pointing forward, y-axis to the right (starboard) and z-axis upwards (figure 1 and 2).

TIME IN K-SIM

Time in K-Sim is indicated in three ways:

- **Simulation time:** Time elapsed since start of simulation, displayed in the upper left area (top bar) of the application window.
- **Exercise time:** Local time (actual clock) in the exercise. Presented in the top bar – smaller digits.
- **Internal time:** Total time elapsed since creation of exercise. When an exerciser is saved and reopened, the simulation time is reset but the internal time not.

THE ENVIRONMENT

K-Sim has very detailed options to specify the environmental conditions (air, sea, seabed, waves, precipitations, tide and ice). Waves can be either generated automatically, based on specified wind or by defining a custom spectra. At the start of a simulation, 70000 [1] wave components are generated with each an amplitude, phase, frequency and direction. The location where the components are generated (referred to as 'wave

[1] At start research 5000 components, increased during a system update in September 2017

origin') is the origin of the first object created in the exercise at t=0. Throughout the simulation, these components remain unchanged. Within K-Sim the phase shift of the wave components is based on the deep water dispersion relation (section 4.1.2).

WAVE LOADS

WAMIT is an engineering software package that uses linear and second-order potential theory to analyze the interaction of waves with vessels or other structures. A standard WAMIT file is used as input in K-Sim to load the hydrodynamic properties of each object. This file is used for the calculation of wave loads on objects and contains added mass, potential damping and wave forces. Within HMC, a large quantity of WAMIT files is available (all objects used in this research). For more detailed information about WAMIT or its use, I refer to the WAMIT web page.

MOORING SYSTEMS

There are several ways an object in K-Sim can be kept in place. Next to a common mooring system (taut, catenary) or Dynamic Positioning, two additional mooring options in K-Sim need further explanation:

- **Turret Well Device**: The Turret Well Device is a tool in K-Sim consisting of a fictional mooring system designed to keep a vessel or object on the same geographical position, without using it's propulsion- or anchoring systems. The object can move in a circle of which the size (radius) can be defined. It should be noted that 1st order motions are correctly captured but 2nd order motions (drift forces) are not.

- **Mooring Through API**: The Application Programming Interface (explained in section 3.2.2), allows the user to keep a vessel or object on the same location by tuning its stiffness matrix. Furthermore, by using frictional mooring, object characteristics can by tuned in such a way that it matches offshore data provided by for example a client.

3.2.2. APPLICATION PROGRAMMING INTERFACE

To process data from K-Sim or log and present data that K-Sim is not able to do with its standard features, HSC engineers have developed an application to connect with the K-Sim interface, referred to as 'Application Programming Interface (API)'. With this application it is possible to apply external forces on- and retrieve body states of objects in K-Sim in real time. For this thesis assignment, the API is used for:

- **Wave Analysis:** The wave components used to build the wave spectrum can be extracted in a standard '.csv' format. With these components, an exact time-trace of the wave elevation at a location of choice can be reconstructed.
- **Retrieve Body State:** While connected with K-Sim, the body state (information) of an object of choice can be retrieved in real time (6-DOF). For example, vessel motions can be displayed in real time while simulating. For a vessel the motion is given for 1/2 Lenghth Between Perpendiculars (LPP) (standard).
- **Restrict Motions:** The motions (6-DOF) of an object can be restricted by tuning the stiffness- or damping matrix. For example, keeping a vessel in place without need of mooring lines or DP.

3.3. MAKING A FORECAST FOR THE HSC

In order to answer the research question stated in 1.2, the VWRT is created. The VWRT is a tool that is able to make and display a wave and motion forecast in the HSC. The tool imitates a wave radar system that can be used offshore but has some important differences compared to an actual system:

- **Forecast time**: At the start of a simulation, wave components are made available through the API socket. These wave components are used to make the forecast and will not change during the simulation. Therefore, a forecast can be made for an unlimited amount of time in contrary to a maximum of several minutes in reality (section 2.1.2).

- **Forecast update-rate**: A wave radar system gives an updated forecast in a certain frequency (typical 10 seconds, section **??**). Every new forecast is more accurate than the one before. Since the VWRT gets all wave components at the start of a simulation, the accuracy of a forecast is constant over time.
- **Forecast error**: A wave forecast made by a real wave radar system is never a hundred percent accurate and has a certain error. Therefore, the input used for making a motion forecast already contains a certain error (section 2.2). Within the HSC, the wave components are known exactly and waves can be forecasted without an error. Therefore, we can speak of a 'perfect wave radar'.

Making a forecast for the HSC can be divided in to two steps:

- A model making the forecast, referred to as 'The Model' (chapter 4 and 5)
- A tool to displaying the forecast, referred to as 'Virtual Wave Radar Tool' (chapter 6 and 7)

4

THE MODEL - A DETERMINISTIC MOTION FORECAST

This chapter explains the model making a motion forecast for the Thialf (referred to as 'The Model'). The first two sections describe the modeling approach that is used to make the forecast. The third section describes a test model of a simplified barge, which is used to familiarize with K-Sim and the deterministic motion forecast idea. In section 4.4 a motion forecast for the Thialf is made and the results are verified and discussed.

4.1. FREQUENCY DOMAIN ANALYSIS

Part of the assignment is to investigate the most suitable way of predicting vessel motions based on a wave forecast. The most practical way of making a motion forecast based on a wave forecast, would be a frequency domain calculation (section 2.1.3). The calculation is easy to understand and very fast, a quality which is most wanted when making a future prediction (section 2.1.2). Therefore this research will investigating the possibilities and limitations for making a motion forecast during a lift operation in the frequency domain

Within the linear wave theory, an irregular sea-state can be described by a superposition of sinusoidal waves as a Fourier series. The response of a vessel to ocean waves can be linearized for small motions and therefore described as a Fourier series as well:

$$\zeta(t) = \sum_{n=1}^{N} \zeta_{a,n} cos(\omega_n t + \phi_{\zeta,n}) \qquad \text{(Wave elevation)} \tag{4.1}$$

$$Z(t) = \sum_{n=1}^{N} Z_{a,n} cos(\omega_{\zeta,n} t + \phi_{z\zeta,n}) \qquad \text{(Vessel response, heave)} \tag{4.2}$$

Where:

ζ_a Wave amplitude [m]	ω Angular Frequency [rad/s]	ϕ Phase angle [rad]
Z_a Motion amplitude (heave) [m].	t Time [s]	N Number of samples

When vessel motions become larger, this linearization is no longer valid as more terms in the Equation of motion (EOM) become non-linear (e.g. Non-linear damping). A time domain approach would allow to (in principle) solve any dynamic problem. However, this approach is far more time consuming than a frequency domain approach. A few examples of (marine) problems that require a time domain approach are:

- **Impact loads:** Impact on guiding system of stabbing cones when lowering platform to set down point.
- **Vessel ballasting:** By ballasting a vessel, the draft of a vessel changes. Therefore, the GM changes and the hydrodynamic properties are no longer stationary. When this is done during a simulation the system is not stationary and a frequency domain approach will not be valid.

- **Mooring studies:** When analyzing forces or motions of a moored vessel, higher order wave drift forces can not be neglected. Therefore, the behavior of a vessel in a mooring pattern is very non-linear and can not be solved within the frequency domain.

4.1.1. RESPONSE AMPLITUDE OPERATOR

The wave elevation (equation 4.1) and vessel response (equation 4.2) are linear proportional. This means that the ratio of the force and response amplitude and phase is constant, respectively. Therefore, the response of a vessel to an external force (wave elevation), can be calculated by multiplying the wave amplitude by a linear transfer function, so called RAO (equation 4.3). For the complete derivation of RAO's I refer to [4]. An example for heave is provided below:

$$Z(t) = \sum_{n=1}^{N} RAO_z(\omega_n, \mu_n) \cdot \zeta_{a,n} cos(\omega_n t + \phi_{\zeta,n}) \qquad and \qquad Z_a(\omega) = RAO_z \cdot \zeta_a \tag{4.3}$$

Where:

ζ_a Wave amplitude [m]	ω Angular Frequency [rad/s]	ϕ Phase angle [rad]
Z_a Motion amplitude (heave) [m].	t Time [s]	N Number of samples
μ Wave direction [rad]		

Note: RAO is depending on wave direction (μ) and frequency (ω). The Model uses linear interpolation to match the RAO's with the wave components.

RAO's can be determined with model tests in a test basin, full scale measurements or CFD (computational fluid dynamics) analysis. HMC has an extensive database with RAO's of their vessels which is continuously updated. For this research, an in-house tool called LiftDyn is used to construct and analyze RAO's which are needed as model input to make a motion forecast.

LIFTDYN

LiftDyn is an in-house software package of HMC that is designed to solve linear hydrodynamic problems in the frequency domain. The equation of motion for an object in LiftDyn is formed by defining a mass matrix, damping matrix and stiffness matrix. Within HMC standard LiftDyn models are available for each vessel at several drafts and will be used for this research and adapted for purpose. These models use the following input:

- **Center of Gravity:** Position of the Center of Gravity (CoG) of the body, specified in local body coordinates [m].
- **Local Origin:** Position of the local origin, specified in global coordinates (illustrated in figure 4.1).
- **Hydrostatic Properties:** Hydrodynamic data base (Hyd-File, origin in local body coordinates) of body including hydrostatic stiffness parameters, added mass and damping matrices for a number of wave frequencies and wave directions. A free surface correction factor can be defined (reduction of stability due to free fluid surface is captured by correcting GM).
- **Radius of Gyration:** The radii of gyration about local x-, y- and z-axis at CoG [m].
- **Crane Specifics:** The following crane specifics can be defined: Slew angle [deg], crane radius [m] (horizontal distance crane hub to block), type of block (main, aux, whip), hook load [mT], hook height [m] (vertical distance block to global origin) and type of hoist reeving (for Portside (PS) and Starboard (SB), respectively).

LIFTDYN VS K-SIM

The body state of an object in K-Sim is logged for 1/2LPP (standard output). Therefore, the LiftDyn model is shifted in such a way that the global origin is located at 1/2 LPP. By doing so, a RAO w.r.t. global origin can directly be compared with K-sim loggings. An example of a Thialf model with the origins marked is illustrated in figure 4.1.

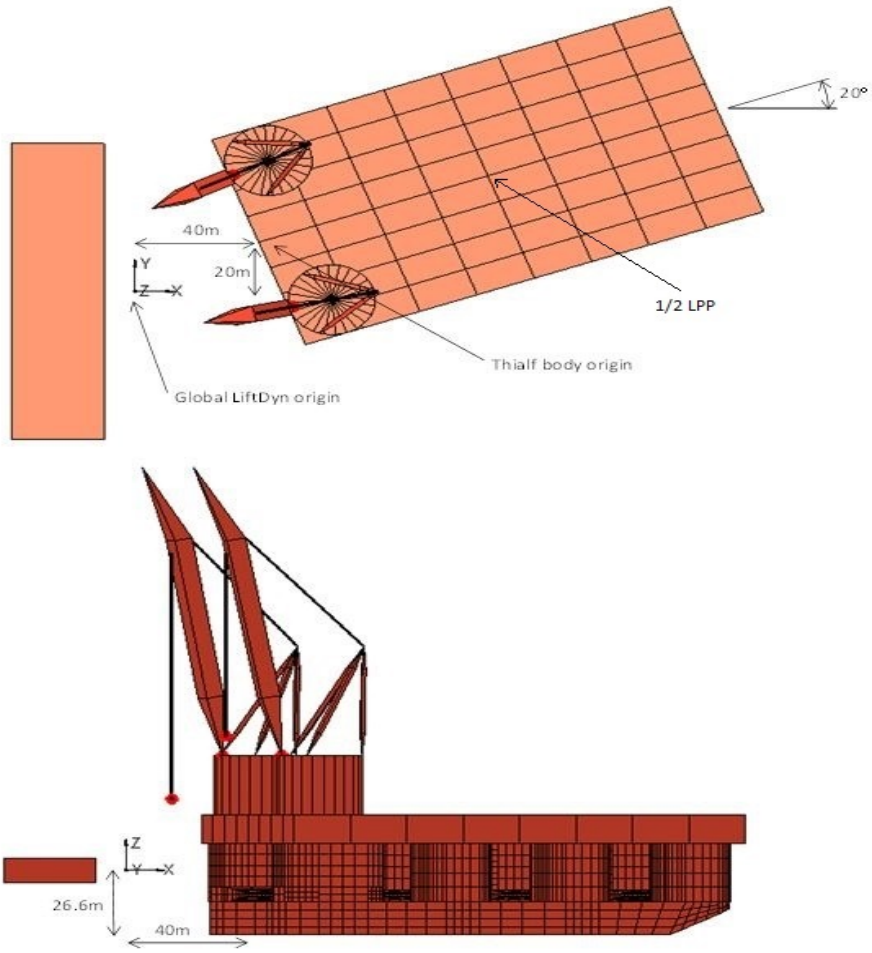

Figure 4.1: LiftDyn origin example

4.1.2. WAVE PROPAGATION

As described in section 3.2.1, K-Sim generates 70000 wave components at the start of a simulation at the wave origin. Within the linear wave theory, the wave elevation can be calculated by a superposition of its wave components (equation 4.1). Within K-Sim and The Model, the phase shift for a propagating wave is based on the deep water dispersion relation [3]. Below the calculation of the wave elevation at location vessel is summarized:

$$\omega^2 = gktanh(kd) \quad \text{(Arbitrary depth)} \quad \rightarrow \quad \omega = \sqrt{gk_{deep}} \quad \text{(Deep water)} \tag{4.4}$$

Where:

g Gravitational constant [m/s^2] ω Angular Frequency [rad/s] d Water depth [m]
k Wave number [rad/m]

The water depth is considered as deep water when larger than half the wave length. The phase shift is calculated for the distance a wave has to travel from the wave origin to the location of the vessel.

$$\phi_{shift} = \frac{2\pi l}{\lambda} \tag{4.5}$$

Where:

ϕ_{shift} Phase shift [rad] ω Angular Frequency [rad/s] l Traveled distance wave [m]
λ Wave length [m]

It should be noted that the distance a wave has to travel to location vessel, is only depending on the direction of the wave (linear wave theory, long-crested waves). The complex wave amplitude for each frequency is used to calculate the total wave elevation (super position principle):

$$A_{complex} = Acos(\phi - \phi_{shift}) + iAsin(\phi - \phi_{shift}) \tag{4.6}$$

$$\zeta = \sum_{n=1}^{\infty} A_{complex} \exp(i\omega(t - T_{start})) \tag{4.7}$$

Where:

A Wave amplitude [m] A_{comp} Complex wave amplitude [m] ϕ_{shift} Phase shift [rad]
ω Angular Frequency [rad/s] T_{start} Correction internal time HSC [s] t Time [s]

4.2. PREDICTION VS MEASUREMENT

A motion forecast does not have to be perfect to predict a quiescent period. E.g. when the amplitude of the forecasted signal is overestimated, a calmer period can still be identified when the phase is corresponding to the measured signal (showing a correct trend). However, when deviating too much, a motion exceeding a limit would be falsely identified. Therefore, to quantify the quality of a wave- and motion forecast, two measures that are widely used are adopted in this research [24] [19] [11]:

- **Correlation Coefficient (ρ):** The correlation coefficient, also referred to as the Pearson correlation coefficient, is a measure of how well the phase of the measured motion and the forecasted motion agree, illustrated in figure 4.2, upper plot. It measures the linear association between forecasted and measured signal (equation 4.8). Values scale from -1 (perfect negative correlation) to 1 (perfect positive correlation). Table 4.1 provides a (rule-of-thumb) scale for evaluating the strength of the the correlation coefficient as presented in [25].

$$\rho = \frac{\sum(x - \bar{x})(y - \bar{y})}{(n-1)s_x s_y} \tag{4.8}$$

$$s = \left(\frac{1}{n}\sum_{i=1}^{n}(x_i - \bar{x})^2\right)^{\frac{1}{2}} \tag{4.9}$$

Where:

x Predicted value y Measure value s_y Standard deviation (eq. 4.9) measured value
$\bar{y}$ Mean of measured value n Number of samples s_x Standard deviation (eq. 4.9) predicted value
$\bar{x}$ Mean of predicted value

Size of ρ	Interpretation
0.90 to 1.00	Very high correlation
0.70 to 0.89	High correlation
0.50 to 0.69	Moderate correlation
0.30 to 0.49	Low correlation
0.90 to 0.29	Little if any correlation

Table 4.1: Scale for evaluating the strength of the the correlation coefficient

Note: The correlation coefficient is depending on the number of samples analyzed. However, within this research a minimum simulation time of 30 minutes is used which is equal to 1800 samples for which the correlation coefficient is stable.

- **RMS Ratio (σ):** A measure of how well the amplitude of the measured motion and the forecasted motion agree, illustrated in figure 4.2 lower plot. A value of 1 would indicate that both signals have the exact same Root Mean Square (RMS) values. A value larger than 1 indicates the predicted RMS value being larger than the measured RMS value. A value smaller than 1 indicates the predicted RMS value being smaller than the measured RMS value (equation 4.10).

$$RMSratio = \frac{RMS_{predicted}}{RMS_{measured}} = \frac{\sqrt{\frac{x_{p1}^2+x_{p2}^2+...+x_{pn}^2}{n}}}{\sqrt{\frac{x_{m1}^2+x_{m2}^2+...+x_{mn}^2}{n}}} \tag{4.10}$$

Where:

x_{pn}: Predicted value x_{mn}: Measured value n: Number of samples

Note: The RMS ratio is depending on the amount of sample analyzed. Therefore, the ratio can be different for various durations of a forecast looked at. For this research a minimum of 1800 samples is used.

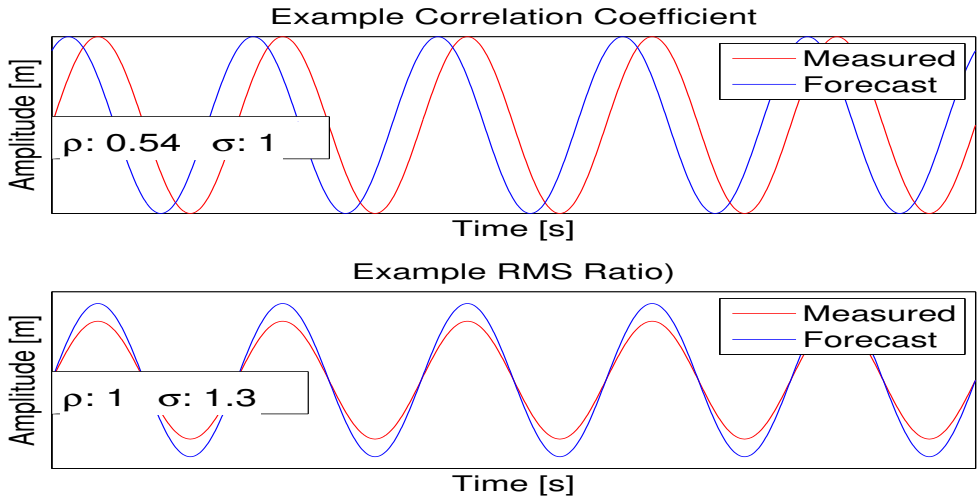

Figure 4.2: Example wave signal illustrating accuracy of a forecast measured by the Correlation Coefficient and RMS Ratio

4.3. THE TEST BARGE H400 MODEL

To familiarize with the HSC and its output, a simplistic model of a barge is used (referred to as 'Test Barge'), shown in figure 4.3. A summary of the simulation specifics and environment used is given in table D.1 and 4.2.

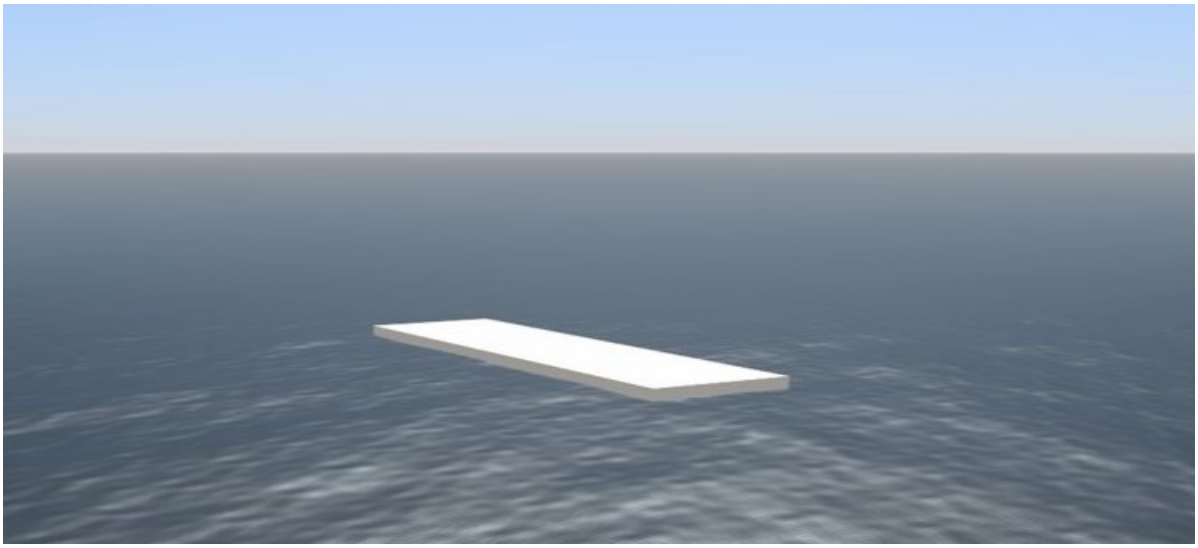

Figure 4.3: Test Barge H400

	Spectrum [-]	Hs [m]	Tp [sec]	$HsTp^2$ [ms^2]	Heading [deg]	Spreading [-]
Test Barge	JONSWAP	1.5	7	73.5	0 (head waves)	cos2

Table 4.2: Environment used in simulation

4.3.1. MODEL INPUT

By using a simplified vessel (squared beam) with all specifics known, a good match between the forecasted and measured motions is expected. I.e. with correct input, the linear model is expected to give correct results (an accurate forecast). A summary of the LiftDyn model input is given in table 4.3.

	Trim/Heel [deg]	Displ. [m^3]	CoG [x,y,z] [m]	radii of gyration [x,y,z] [m]	Local Origin [x,y,z]
Test Barge	0.00/0.00	12600	[0, 0, 7.5]	[6.9, 18.4, 18.1]	[0, 0, -3.5]

Table 4.3: Summary of input LiftDyn Test Barge H400, local origin is w.r.t. global origin.

4.3.2. RESULTS

The simulation results show that when the origin of the vessel is positioned at the wave origin (Barge1, figure 4.6), the logged- and forecasted motions give an accurate match (upper two plots figure 4.4). However, when the vessel is no longer positioned at the wave origin (Barge 2), the measured and forecasted motions no longer agree (lower two plots figure 4.4).It should be noted that the wave does not correlate for the full 100%. This is due to the barge being moored via the turret device(3.2.1), allowing it to move in a sway circle (figure 4.5) with small deviations in the measured and forecasted wave elevation as a result (measuring different locations, forecasted for fixed location).

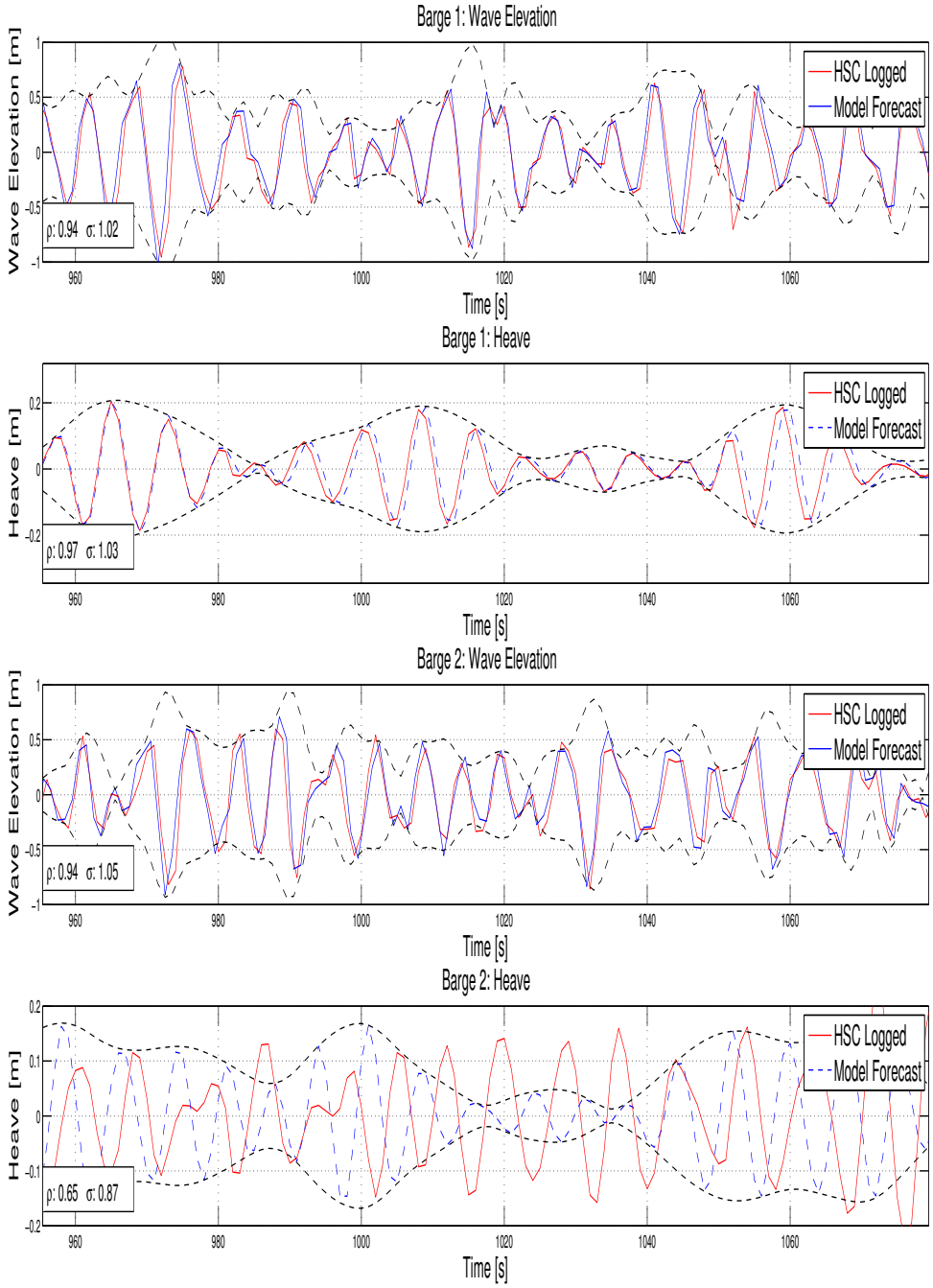

Figure 4.4: Test Barge 1 at wave origin, test barge 2 not at wave origin.

Note: Wave elevation agrees for both barges but heave motion is not.

VERIFICATION RESULTS WITH ORCAFLEX

The only difference between Barge 1 and 2 is the location and thus the wave elevation used to calculate the vessel motions (same wave components with different phase, section 4.1.2, 4.1.1). However, since the wave elevation does agree for both locations and the motions agree for Barge 1 but not 2 (figure 4.4), something else must be causing the odd results. To verify the results obtained, the Test Barge was modeled in OrcaFlex, which is a common engineering tool to analyze dynamic offshore marine systems. With the same wave components as used in K-Sim, OrcaFlex gave the exact same results as the forecast made by The Model.

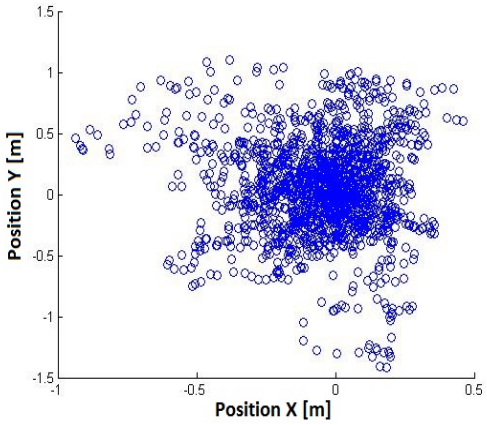

Figure 4.5: Test Barge location logging, moored via the turret device(3.2.1), allowing it to move in a sway circle.

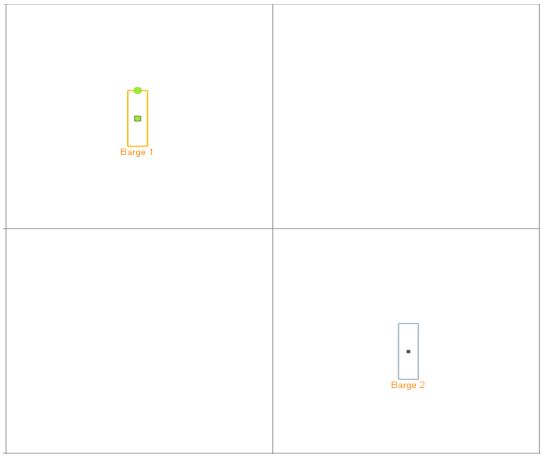

Figure 4.6: Screen-shot of simulation in K-Sim Chart view: Barge 1 (at wave origin) and Barge 2.

BUG HSC: SWAP X EN Y COORDINATE

The test results in OrcaFlex could indicate that a bug was causing the mismatch. An extra test in the HSC indicated that indeed a bug was found. For the motion calculations, the x and y coordinates in the HSC are swapped. This bug is reported to Kongsberg Digital and temporary solved by simply (wrongly) calculating the vessel motions with swapped x and y coordinates [1] (not influencing results when corrected). More information about the bug, test setup and the results can be found in Appendix B.

RESULT TEST BARGE

With the correction for the bug, a very high correlation for Heave, Roll and Pitch is achieved by the model (table 4.4). The 'sway circle' of the Turret (section 3.2.1), is most likely the reason why the wave and thus the motions do not correlate for the full 100 percent.

	Correlation Coefficient [-]	dT Shift [sec]	RMS Ratio [-]	Standard Deviation [*]
Wave Elevation	0.94	-0.44	1.02	0.34[m]
Heave	0.97	-0.39	1.03	0.07[m]
Roll	0.96	-0.29	1.05	0.30[deg]
Pitch	0.96	-0.30	1.03	0.12[deg]

Table 4.4: Result Test Barge H400.

Note: Correlation achieved with corrected for dT Shift (section 4.4.2).

[1] Bug is acknowledged by Kongsberg and fixed during a system update in September 2017

4.4. THE DEFAULT THIALF

In the previous section the results of the Test Barge model and a (pragmatic) solution for the bug found is discussed. This sections describes a model of the Thialf, ballasted to an even keel at 26.6m draught and with its cranes in the cradle (Referred to as 'Default Thialf). This model will form the basis for exercises with a load in the cranes (chapter 5). A summary of the simulation specifics and environment used is given in table D.2 and 4.5.

Figure 4.7: Default Thialf

	Spectrum [-]	Hs [m]	Tp [sec]	$HsTp^2$ [ms^2]	Heading [deg]	Spreading [-]
Default Thialf	JONSWAP	1.5	7	73.5	0	cos2

Table 4.5: Environment used in simulation

4.4.1. MODEL INPUT

The results with the 'standard' LiftDyn model of the Thialf available at HMC showed a clear mismatch. The input for the LiftDyn model was clearly not in alignment with the K-Sim object. With the Test Barge model all specifics were known and easily matched to the K-Sim object. However, for the Default Thialf (and all other objects in K-Sim) exporting object specifics (location of CoG, radii of gyration, etc.) directly from K-Sim is not possible.

CENTER OF GRAVITY

The exact coordinates of the CoG of the K-Sim object can be calculated by hand. However, an in-house HMC application called SSCV Ballast is used to speed up the process. The input needed is the fillings of the ballast tanks that is available in the K-Sim Ballast scheme.

RADII OF GYRATION

The radii of gyration for the Thialf with standard ballasting, are known. The actual radii for the used tank fillings is calculated by first subtracting the radii for the 'default ballast' tanks to "lightship weight" and then adding the radii for the actual ballast back. In chapter 5, the same method will be used to calculate the radii for models with objects in the cranes. A summary of the recalculated LiftDyn input variables are given in table 4.6.

	Cranes [-]	Trim/Heel [deg]	CoG [x,y,z] [m]	radii of gyration [x,y,z] [m]	Local Origin [x,y,z]
Default Thialf	in cradle	0.00/0.00	[redacted]	[redacted]	[redacted]

Table 4.6: Summary of input LiftDyn Default Thialf, local origin is w.r.t. global origin.

4.4.2. RESULTS

BUG HSC: CONSTANT SHIFT

Distinctive is the plotted time trace showing a constant time shift between forecasted- and logged motion of 1.2 seconds (figure 4.8). With a similar test as described in Appendix B, a second bug was found and reported to Kongsberg Digital [2]. For the purpose of this thesis, the cross-correlation (also known as 'sliding correlation') is used to calculate the time shift between forecasted- and measured signal. This function calculates the maximum correlation between two signals by shifting one to the other (referred to as 'dT Shift'). By shifting the forecasted signal with this time shift, the bug is (pragmatically) solved an no longer affects the results. From here on all results are corrected for this dT shift of approximately 1.2 seconds.

Note: A time shift as described above between measured- and forecasted signal, can be found in reality. Sea trials described in [6] showed an offset of 10 seconds between the 'clocks' of two independent measuring systems. This offset was corrected in the same way as described above.

RESULT DEFAULT THIALF

With the newly recalculated LiftDyn input and the determined dT shift, a very accurate forecast is realized with correlations close to 1. Furthermore it should be noted that with the vessel kept in position by tuning its stiffness matrix instead of using a Turret device (section 4.3.2), a perfect wave correlation is realized (Table 4.7). The importance of the model input discussed in 4.4.1 demands to be further investigated (section D.3).

	Correlation Coefficient	dT Shift [sec]	RMS Ratio	Standard Deviation
Wave Elevation	0.99	0.08	1.01	0.34
Heave	1.00	1.18	1.10	0.01
Roll	0.86	1.14	0.98	0.01
Pitch	0.99	1.23	1.11	0.02

Table 4.7: Result Default Thialf, head waves.

Note: Correlation achieved with correction for dT Shift (section 4.4.2).

4.4.3. VERIFICATION

In the previous sections the results for the Default Thialf Model are presented for a single sea-state and relative heading. In order to check the ability of the model to deal with different environmental conditions, several verification runs have been analyzed. The easiest way to vary the wave conditions is using a JONSWAP spectrum, directly available in K-Sim (section 3.2.1). A JONSWAP spectrum is expected to be reasonable for the following parameters [26]:

$$\sqrt{13Hs} < T_p < \sqrt{30Hs} \quad \text{(Areas where swell is insignificant)} \tag{4.11}$$

$$\sqrt{12.4Hs} < T_p < 18.2 \quad \text{(Areas where swell is significant, } H_s < 5.7\text{)} \tag{4.12}$$

$$\sqrt{12.4Hs} < T_p < \sqrt{57.8Hs} \quad \text{(Areas where swell is significant, } H_s > 5.7\text{)} \tag{4.13}$$

Where:

H_s: Significant wave height [m] T_p: Wave peak period [sec]

Based on these guidelines, the following spectra have been selected for verification of the Thialf Default Model (specifics in table 4.8):

[2] Bug is acknowledged by Kongsberg and brought back to a time shift of 0.5 seconds during a system update in September 2017

- **Mild Sea-State:** A realistic environment for a lifting operation to take place, used for both the Test Barge and Default Thialf model (section 4.3, 4.4).
- **Moderate Sea-State:** A typical North Sea environment.
- **Swell:** Maximum environment reasonable for a JONSWAP spectrum, periods close to resonant frequency of the Thialf.
- **Combined Sea-State:** An environment with both wind- and swell components (double peaked spectrum), used in the Skarfjell test case (Chapter 5). To mimic this spectrum in K-Sim, two JONSWAP spectra are combined (appendix E.1).

	Spectrum [-]	Hs [m]	Tp [sec]	$HsTp^2$ [ms^2]	Heading [deg]	Spreading [-]
Mild	JONSWAP	1.5	7	73.5	0:45:180	cos2
Moderate	JONSWAP	5	10	500	0:45:180	cos2
Swell	JONSWAP	6	16	1536	0	cos2
Combined	Torsethaugen	1.5	8	88	315	cos2

Table 4.8: Environments used for verification

The motion forecast model showed good results for heave, roll and pitch (correlation coefficient 0.85 - 1.0 and RMS ratio 0.86 - 1.15) for mild, moderate and a combined sea-states (all wave directions, respectively). The (small) differences in the results for different wave headings can be explained due to inaccuracies of the model input that become governing for certain directions. It should be noted that the model input for the Default Thialf model is calculated (section 4.4.1) but not optimized. The sensitivity of the model to this input is investigated in the next section.

For the swell case the model was no longer able to make a usable forecast. This can be explained by the fact that when motions become larger, a frequency domain approach is no longer valid. A linearization of the EOM is no longer accurate with non-linear terms becoming more important. Secondly, the superposition principle used to calculate the vessel motions does not hold due the vessel's body-state becoming dependent on time (section 4.1). Taking the above in account, an answer to subquestion 2 (section 1.4.1, stated below), is found.

Subquestion 2: "Do the environmental conditions influence the accuracy of the forecast ?"

Although the model is not able to make a forecast for extreme weather conditions, it should be noted that it is very unlikely a lift operation will take place with Hs > 2m. Furthermore, making a model that is able to forecast responses in all environmental conditions is not the objective of this thesis (section 1.3). A summary of the results of all verification runs can be found in Appendix D.

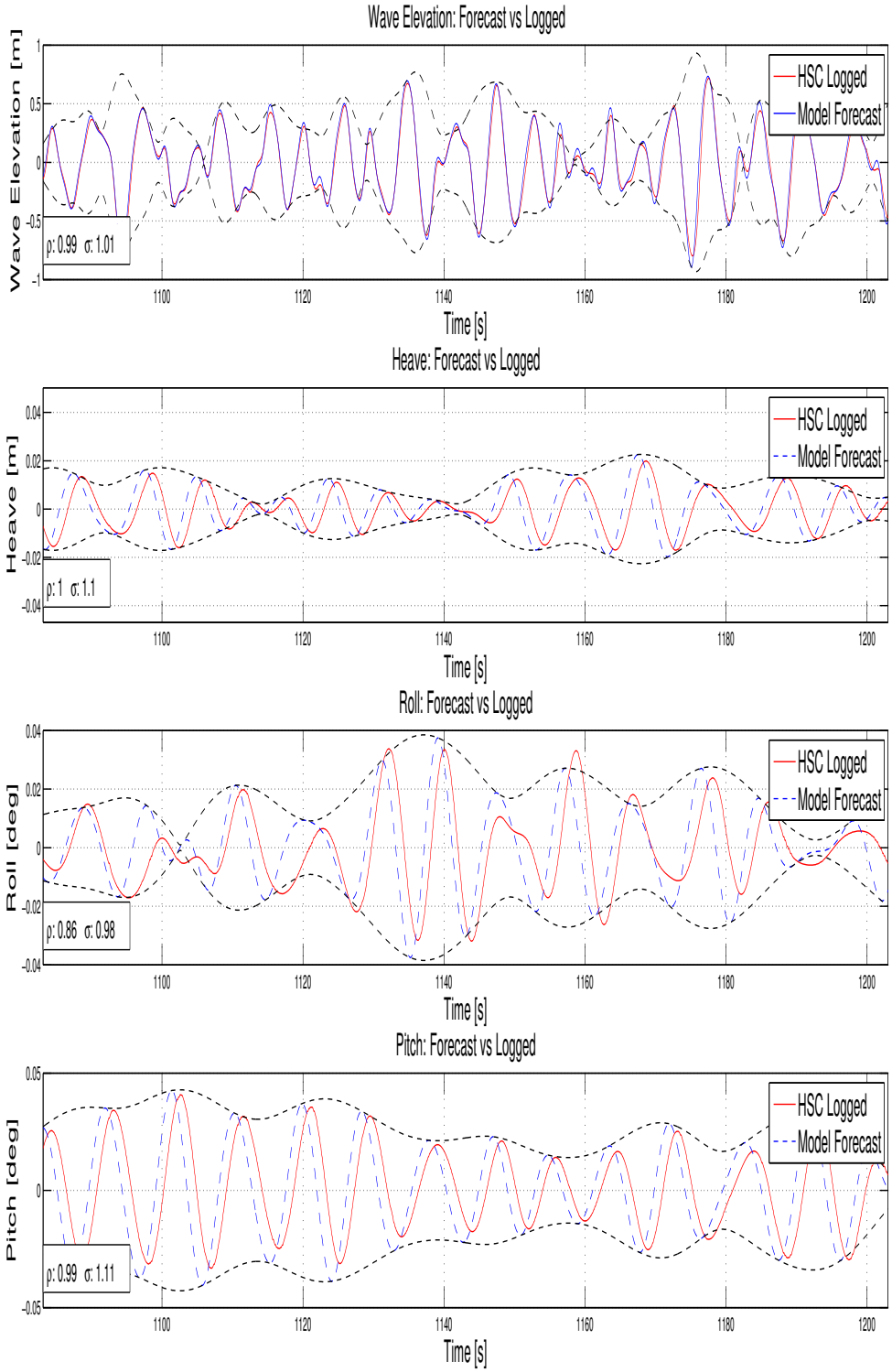

Figure 4.8: Time trace of Default Thialf, in head waves (0 deg), JONSWAP HS=1.5m Tp=7s Spreading=cos2. Note: constant time shift dT of 1.2 seconds can be seen between forecast and logged motion

4.5. SENSITIVITY ANALYSES

The model input discussed in section 4.4.1 and its effect on the forecast demanded further investigation. This is relevant since the model input values available offshore might deviate from the actual values. Therefore, the sensitivity of the model to (selected) input values is investigated. By doing so, the requirements for a wave radar system is established and a careful reflection on the VWRT w.r.t. a real system can be given. The following input parameters are investigated:

- **Center of Gravity:** For the CoG, the longitudinal (x) and transversal (y) coordinate is known accurately offshore (a deviation will result in trim and heel of the vessel). The vertical coordinate (z) however is not and therefore investigated.
- **Radii of Gyration:** A deviation in the radii of gyration showed to have an effect that cannot be ignored. Furthermore, these values are known to deviate from the actual value offshore.
- **Wave Elevation:** Since the wave correlation realized with The Model ($\rho = 0.95 - 1$) are not realistic (section 2.2.2), the performance of the model is tested with noise on the wave signal.

The model sensitivity for the CoG and radii of gyration, are investigated by letting the model input deviate from the actual value used in K-Sim. This is first done for each value separately and then all together. To magnify the effect of deviation in the model input, the moderate sea-state (section D.3) is used to compare. A summary of the results can be found in appendix D.3.

As previously mentioned, the model input used for the Default Thialf model is not optimized. Therefore, when the used input values deviate from the original values, the results sometimes improve. Therefore, to investigate the actual sensitivity of the model to its input, the 'tuned' forecast should be compared with the original forecast. However, the behavior of the model to changing input values is illustrated with the above described sensitivity analyses and a more thorough investigation is not required.

The test showed that when the model input is accurate within 2 meters, the impact on the forecast is negligible. When deviating more, it has still no serious impact on the phase (correlation coefficient) but a small impact on amplitude (RMS Ratio) of the forecast. We can clearly see that when radii of gyration are over estimated, the amplitudes are lower and the other way around (as expected). Furthermore, the variations in the model input demonstrated once more that there is room for optimization.

4.6. CONCLUSION

Based on the verification runs, the Default Thialf Model is found to be valid for all headings and relevant environmental conditions. For these environments, the sensitivity of the model to variations in the CoG and radii of gyration (model input) is negligible on the phase and small (<10%) on the amplitude of the forecast. With data offshore available within +- 2m this is found to be acceptable. However, the source of deviation between forecasted and logged motions is not further investigated. Furthermore, the model input is not optimized, but (roughly) calculated based on K-Sim object specifics. A higher accuracy of the forecast can possibly be achieved when optimizing the model input. Based on the above, the Default Thialf is found to be fit for purpose, and ready to be tested in a test case lift operation (chapter 5).

5

TEST CASES - MOTION FORECASTING DURING A LIFT OPERATION

The previous chapter showed the results of a motion forecast made by The Model for the Thialf's CoG (Default Thialf, cranes in the cradle). This chapter elaborates on two 'Test Cases' aiming to investigate the capabilities of The Model when making a forecast for an actual lift operation. The first case selected is the 'E1186 Skarfjell' study, in which a 1000 mT module is installed by the Thialf's SB crane on a Floating Production Platform (FPU). The second case is part of the 'I0477 Sable Island' project, a dual crane lift in which a 7000 mT topside is lifted and put on a barge. By investigating both a heavy lift dual crane- and a single crane lift operation, an answer to subquestion 3 (section 1.4.1, stated below), is searched for.

Subquestion 3: "Do (heavy) lift operations effect the accuracy of a motion forecast ?"

5.1. E1186 SKARFJELL - SINGLE CRANE LIFT

The Skarfjell project is chosen because of the small sized module to be installed, the interest in relative motions between the module and the FPU and the topicality of the study at HMC. Furthermore, during the actual Skarfjell study (executed while writing this thesis), the question arose if it was possible to assist the crane operator in the HSC with the moment of set-down.

The Skarfjell simulations were executed by HMC as part of a Front End Engineering Design (FEED) study commissioned by ENGIE E&P Norge AS, a European oil and gas company. A subsea tie-back of the Skarfjell oil and gas field to the Gjøa semi-submersible platform is considered. This subsea tie-back concept includes the installation of a new Skarfjell module of circa 1,000 mT (Figure 5.2) on the existing Gjøa FPU located in the Norwegian section of the North Sea (Figure 5.1). The goal of the FEED study was to investigate the design loads for the bumper and guide system used for installation of the new module on the semi-submersible platform. The installation can be summarized in five steps:

1. The Skarfjell module is lifted from Thialf deck and slewed to stern.
2. Thialf lines up the module in the centerline of the garage.
3. Thialf moves astern on dynamic positioning until the module is completely in the garage.
4. Final positioning of module is done by crane operator.
5. **Module is lowered by paying out hoist wire.**
6. Thialf moves away from the platform and the crane slews to keep the block over the module.

The speed at which the module is lowered is critical. A 'low' lowering speed will reduce dynamic platform response and decrease primary impact load, but may lead to multiple impact loads when contact with the

Figure 5.1: Location Gjøa platform, Norwegian section of the North Sea

Figure 5.2: Screen-shot of simulation in K-Sim: Gjøa platform and Thialf with Skarfjell module in crane

platform is lost again. A 'high' lowering speed will have a higher primary impact load but prevents secondary impact loads. Timing the right moment (a quiescent period with minimum relative heave motion between module and platform) for the lowering is therefore crucial. A deterministic motion forecast could possibly allow a low lowering speed and reduce the secondary impact loads to a minimum.

5.1.1. ENVIRONMENT

To define the operational limits, 8 weather conditions for various wave directions were simulated based on most occurring sea states in the area of the Gjøa platform. The maximum impact loads of the module, occurred at a wave direction of 315 degrees and is used in this test case. To mimic a TorsetHaugen spectrum (which is a double peaked spectrum and typically used to represent Northern North Sea conditions), the following two JONSWAP spectra are used with a combined $HsTp^2$ of 88:

	Hs [m]	Tp [s]	gamma [-]	$HsTp^2$ [ms^2]
JONSWAP 1	1.5	8.0	2.2	96
JONSWAP 2	0.1	2.5	1	0.63

Table 5.1: Wave spectrum used for Skarfjell test case.

5.1.2. TEST CASE SETUP

Since The Model is making a forecast in the frequency domain, it cannot cope with systems where the response characteristics change over time (section 4.1). A (dynamic) lift operation from start to end is very not stationary. However, one is only interested in timing the right moment to start lowering the module. Therefore, only step five of the lifting operation is investigated, in which the module is already brought in position and the system is stationary (until lowering starts). A summary of the simulation specifics can be found in table E.1

To make a forecast of the heave motion of the module w.r.t. the FPU, the heave motion of both module and platform need to be forecasted. To do so, the RAO's of the Gjøa FPU, Thialf and Skarfjell module are exported from a LiftDyn model (figure 5.3). The input used for the LiftDyn model can be found in appendix E.1. Several assumptions and simplifications are made:

- The motion forecast is only made for 'step 5' when the module is hovering in the final position above the set down point.
- When the lowering of the module has started, the motion forecast is no longer needed and will be disregarded.

- The rigging system in the LiftDyn model is simplified, using single point connectors.
- Tugger lines are not modeled in the LiftDyn model.

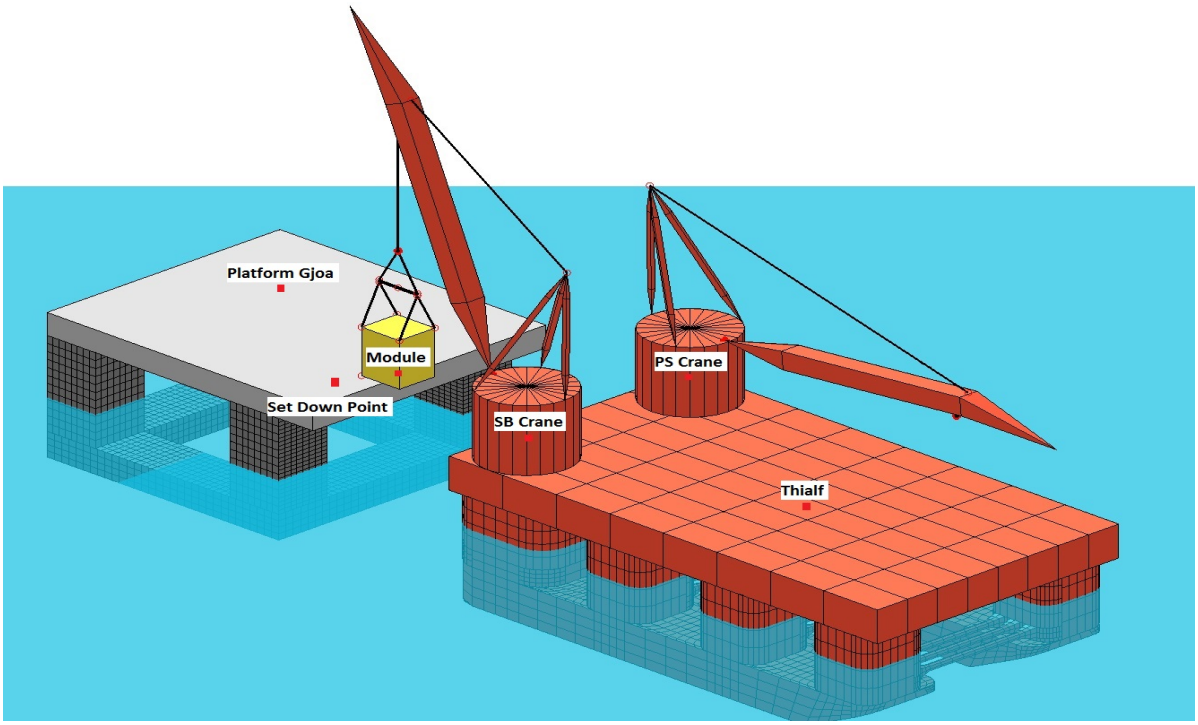

Figure 5.3: LiftDyn model used in Skarfjell test case

5.1.3. MOTION FORECAST

Aligning the LiftDyn model with K-Sim in order to make a forecast for the Skarfjell test case, proved to be quite challenging. At first, a complete mismatch between forecasted- and logged (module) motions (roll and pitch) were thought to be caused by the lack of tuggers in the LiftDyn model. However, when investigating the effect of tuggers on the motion of a module (figure E.3 and E.4), it became clear the tuggers mainly stopped the module from yawing (yaw movement) and barely affected the other motions.

Secondly, the effect of the simplified rigging was further investigated to see if this could cause the mismatch. By looking at the modes in which the module could move, it became clear that the natural periods of the modes that would be effected by simplifications in the rigging, are all smaller than 5 seconds and will barely (if not at all) be excited by wave induced vessel motions (figure E.1 and E.2). Therefore, one can state that the simplifications made in the model are valid and not causing the mismatch.

Having no reason why the model should not be able to forecast the roll and pitch of the module, a step by step debugging process finally solved the mismatch (definition hook distance: K-Sim w.r.t. crane tip vs LiftDyn w.r.t global origin). With the models aligned, an accurate forecast could be made for all objects ($\rho .81 - .96 \quad \sigma .92 - 1.17$) and the results are summarized in Appendix E.1.

	Correlation Coefficient [-]	dT Shift [sec]	RMS Ratio [-]	Standard Deviation [*]
Wave Elevation Thialf	0.95	-0.46	1.04	0.44[m]
Wave Elevation Platform	0.95	-0.54	1.04	0.37 [m]
Relative heave	0.86	1.8	1.08	0.09 [m]

Table 5.2: Summary test case Skarfjell, Relative heave (Module w.r.t. Platform), wave heading: 315 deg.

For this test case, the motion of interest was the relative heave of the module w.r.t. the FPU set down point. In figure 5.4, the center plot illustrates some deviations between the forecasted and logged signal. However, when looking at the lower plot (envelope of both signals), the model proved to be well capable of forecasting a quiescent period (figure 5.4).

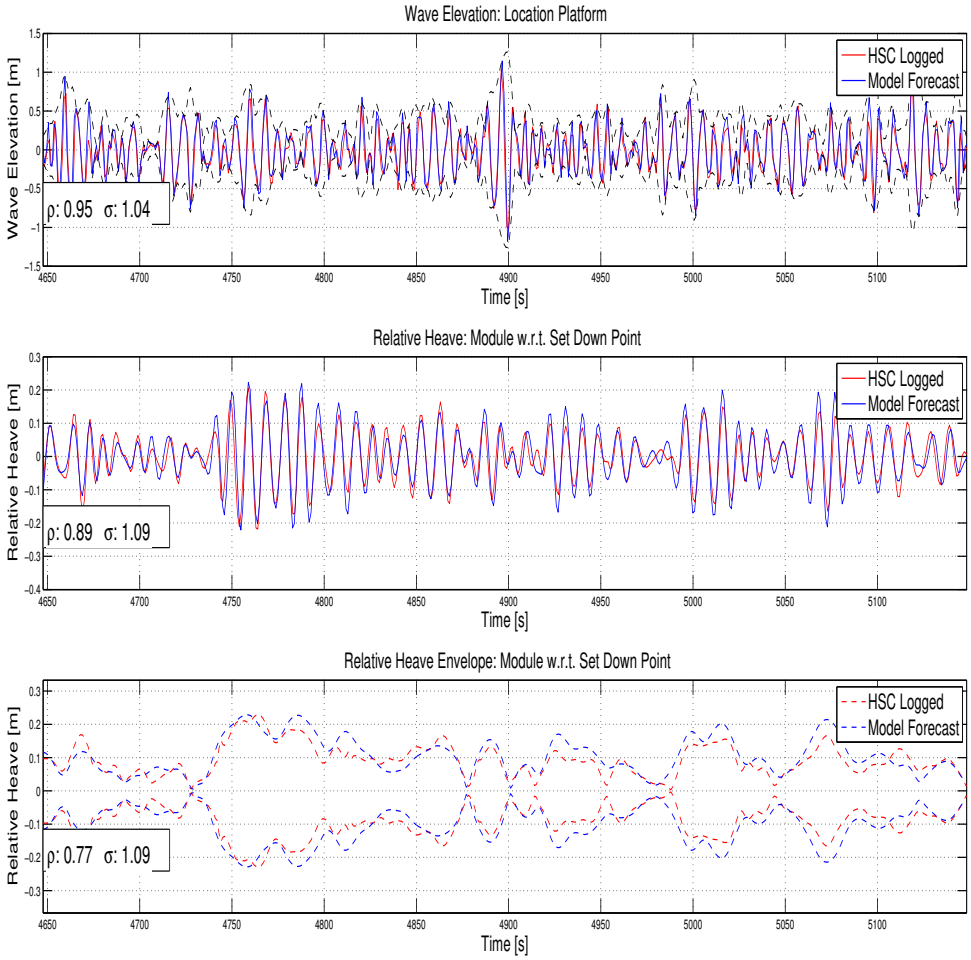

Figure 5.4: Time trace test case Skarfjell, Relative heave (Module w.r.t Platform), complex sea-state, wave heading: 315 deg.

Note: Better results were achieved for other environments (figure E.10 and E.9). As concluded in section 4.4.3, this is most likely due to model input being not accurate, having more influence with certain wave directions.

Figure 5.5: Location Sable Island, southeast of Nova Scotia in the Atlantic Ocean.

Figure 5.6: Screen-shot of simulation in K-Sim: H-541 Barge and Thialf with Theboud Compression Topside in cranes.

5.2. SABLE ISLAND - DUAL CRANE LIFT

The Sable Island project is chosen as second test case to see how well The Model is able to make a forecast for a dual crane (heavy) lift operation. The Sable Island project is part of a removal scope for ExxonMobil, to be executed by HMC in 2020 - 2021. The total project consists of the engineering, preparation, removal and disposal (EPRD) of all offshore facilities associated with the Sable Offshore Energy project. This includes 7 topsides and 7 jackets and is planned to be executed by the Thialf. The platforms are located southeast of Nova Scotia (near Sable Island), Canada in the Atlantic Ocean (figure 5.5).

For this test case, the removal of the 'Thebaud Compression' topside is investigated. This is the heaviest topside and weighs over 7500 mT. The topside will be lifted from its jacket and back loaded on the H-541 barge (figure 5.6). Engineering sessions in the HSC have taken place to test the design an effectiveness of bumper- and guide systems to increase workability. One option for guiding the platform safely on the barge is the usage of guide pins and receptacle cones. The alignment of the pins with the cones is foreseen to be difficult and time consuming. A motion forecast of the surge and sway movement could make it more easy and therefore the horizontal motions are of interest for this test case. The removal of the Thebaud Compression topside can be summarized in five steps:

1. Topside is cut lose from its jacket and lifted by the Thialf SB- and PS crane using spreader bars.
2. Thialf lines up with the platform in the centerline of the H-541 barge.
3. Thialf moves astern on dynamic positioning until the topside is hanging above the barge.
4. Final positioning of topside is done by crane operators.
5. **Module is lowered by paying out hoist wire of both SB- and PS crane.**
6. Barge is towed to mainland.

5.2.1. ENVIRONMENT

Several weather conditions for various wave directions were used during the engineering session in the HSC to determine the most suitable bumper design. The following environmental conditions proved to be realistic and is used for this test case:

	Hs [m]	Tp [s]	Heading [deg]	Spreading [-]	$HsTp^2$ [ms^2]
JONSWAP	1.5	8	30 (bow quartering)	2	150

Table 5.3: Wave spectrum used in the Sable Island test case.

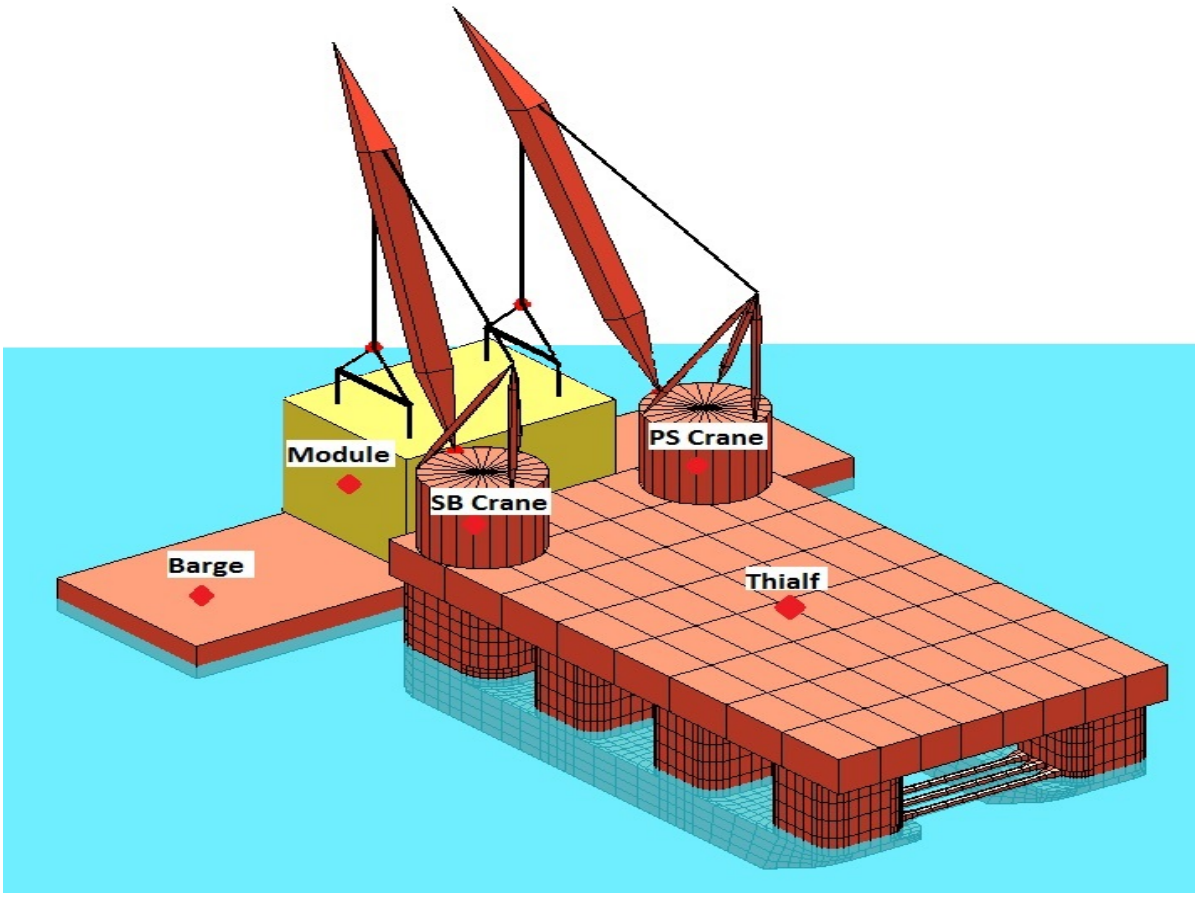

Figure 5.7: LiftDyn model Sable Island test case

5.2.2. TEST CASE SETUP

As for the Skarfjell test case, a forecast is made only for step five of the removal (the Topside is hanging above the barge and can be lowered at command). During the set down of the Topside, mooring winches of the Thialf are used to keep the Barge in place. These winches have non-linear characteristics and are not modeled in the LiftDyn model (figure 5.7). Due to this simplification, the relative movement w.r.t. the moored barge can not be investigated. A forecast for a barge floating on its own is made in section 4.3 (Test Barge). For simplification purposes, the barge is fixed to earth ('lashed', as if a bottom founded platform). The input used for the LiftDyn models can be found in appendix E.2.

The stabbing cones used for guiding the platform to its set down point are most likely positioned at the utmost end of a module/platform. At these positions, roll, pitch and yaw add to the surge, sway and heave motion. When comparing the forecast of the Gjoa platform CoG (table E.6) with the set-down point (table E.7), one can state that for both locations the forecast for roll and pitch are equally accurate (as expected for a stiff body). However, it should be noted that a deviation in the forecasted roll or pitch, will effect the accuracy of the surge, sway and heave forecast. Therefore, (for larger bodies/topsides) the forecast of a Point of Interest (POI) can be less accurate than for the CoG. Summarizing the above, the following simplifications are made:

- **Mooring Barge:** Instead of making a motion forecast w.r.t. a moving moored barge, the forecast is made to a fixed point.
- **Forecast POI**: A forecast is made for the CoG of the Topside.

A summary of the simulation specifics can be found in the appendix, table E.11.

5.2.3. MOTION FORECAST

The Model proved to be well capable of forecasting the heave, roll and pitch motion of both the topside and the Thialf's CoG (Appendix E.2). The forecasted- and logged sway- and surge motions matched in less extend. However, this is not caused by the inability of the model making a forecast, but the way of logging the actual vessel motions. With the location of a POI being logged instead of the distance relative to a certain point, (low frequent) motions of the Thialf (figure 5.8 and 5.9 upper plot) add to this motion (figure 5.8 and 5.9 second plot). By correcting for the Thialf's surge, sway, pitch and roll motions, the low frequent motion of the module is no longer present (figure 5.8 and 5.9 third plot). However, the 3th plot is clearly showing a difference in amplitude between forecasted- and logged motions. With an accurate forecast for heave roll and pitch (table 5.4), a forecast for sway and surge of the topside, is expected to be similar accurate (all motions are closely related). The error is most likely caused due to not accurately correcting the logged motion (e.g. offset point of rotation w.r.t. model origin and crane positions not taken into account). When correcting the logged signal with the RMS Ratio (scaling the response based on the motion history), the surge and sway behavior of the module is clearly visible (figure 5.8 and 5.9, lower plot).

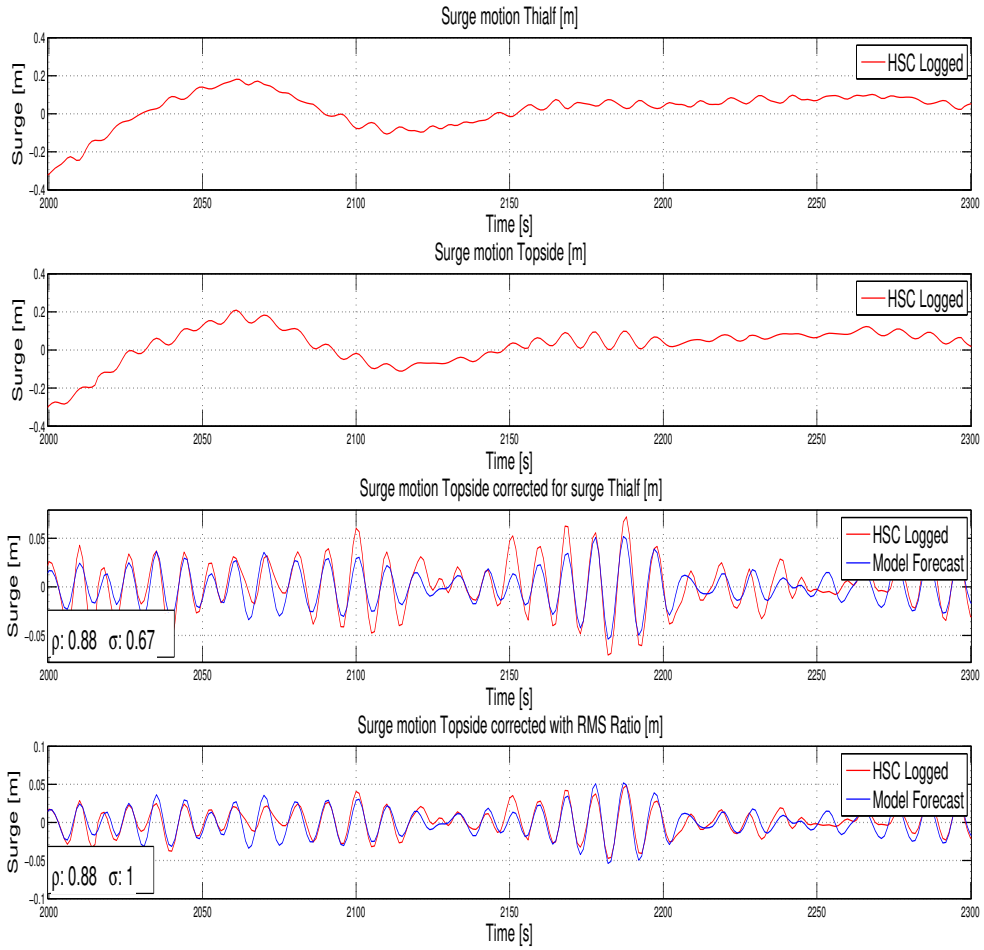

Figure 5.8: Time trace test case Sable Island, Surge topside CoG

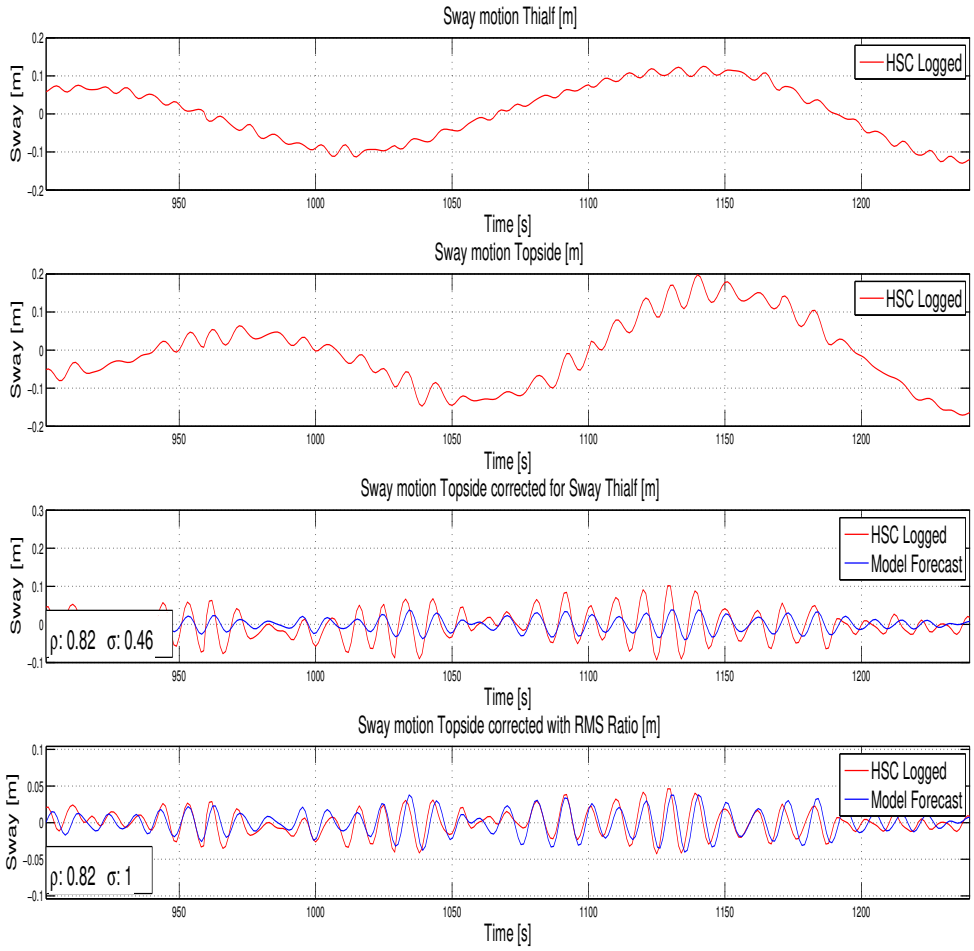

Figure 5.9: Time trace test case Sable Island, Sway topside CoG

	Correlation Coefficient [-]	dT Shift [sec]	RMS Ratio [-]	Standard Deviation [*]
Wave Elevation	0.96	-0.93	1.04	0.37[m]
Heave	0.96	1.26	1.37	0.04[m]
Roll	0.85	1.35	1.17	0.08[deg]
Pitch	0.89	1.35	1.16	0.05[deg]

Table 5.4: Summary test case Sable Island, Module CoG, stern quartering waves.

5.3. CONCLUSION TEST CASES

The model proved to be well capable of forecasting the heave, roll and pitch motion of a module (free hanging) for both a single- and dual crane lift operation. When comparing the results of the Default Thialf model (table D.4) with the Sable Island test case (table E.15), one could state that the load in the crane does barely influence the accuracy of the forecast for the Thialf's CoG.

Tugger lines showed to have no effect on the motions of the module (1000 mT Skarfjell), only preventing it from yawing. However, one should note that the natural frequency of the module lays around 15 seconds (pendulum length of 60m, equation 5.1, Huygens law).

$$T \approx 2\pi\sqrt{\frac{l}{g}} \qquad (\theta << 1 radian) \tag{5.1}$$

Where:

T: Natural period [sec] l: Length pendulum [m] g Gravitational constant [m/s^2]

With a wave peak period of 8 seconds (table 5.3), the motions of the module are mass dominated (figure 5.10) and the influence of tuggers is small. For longer wave periods (West Africa Swell area), closer to the natural frequency of the module, the effect of tuggers is expected to be bigger. For these scenarios, the effect of tuggers possibly need to be included in the model and need to be further investigated.

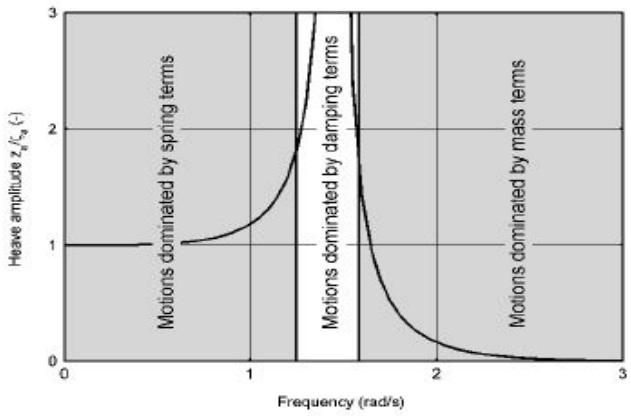

Figure 5.10: Frequencies areas with respect to motional behavior, picture from Journée and Massie [4].

Note: Preferably a setup (cranes position) is chosen in such way that the natural frequencies of the load lay outside the wave peak period.

More research is needed concerning a scenario in which a vessel is moored alongside the Thialf. With natural periods of a barge around 7 seconds, a scenario in which the Thialf barely moves and the moored barge is moving heavily (Sable Island) is known to be realistic. Forecasting the motions of the load in the crane will no longer be sufficient. For these scenarios, a frequency domain approach is expected to be no longer valid due to non-linear mooring forces.

A difference between forecasted- and logged motion amplitudes of the sway and surge motion of the Sable Island topside can be explained by the way motions are logged in K-Sim. One would expect that when the model is able to forecast heave, roll and pitch of a module, similar results would be achieved for sway and surge since these motions are closely related. The error is expected to be fixed when accurately correcting the logged motions for the roll and pitch motion of the Thialf. Furthermore, it would be easier to directly correct for motions of the crane tip instead of transposing motions from model origin. Another option is filtering low frequent motions from the logged signal.

Summarizing the above, the model is well capable of making a motion forecast for a lift operation, single- and dual crane. Although deviations between the amplitude of the forecasted- and measured motions (logged by HSC) are seen, a trend is clearly visible and quiescent periods can be identified. The Skarfjell scenario will be used for a test in the HSC with the use of the VWRT (chapter 7).

6

Graphical User Interface - Presenting A Motion Forecast

6.1. The Virtual Wave Radar Tool

This chapter describes the tool that is created to present a motion forecast in the HSC (referred to as 'the VWRT). Part of the thesis assignment was to determine the requirements for the users 'dashboard' based on preferences of possible users on the HMC fleet and make a (preliminary) design.

6.1.1. User of the Tool

Two possible users of a tool giving decision support have been identified within the HSC fleet, namely:

- **Super intendent:** For a supper intendent, a wave radar could be supportive in two ways. (1) Delivering stochastic wave characteristics (e.g. significant wave height (Hs), peak period (Tp), most probable maximum (mpm)) currently measured by waveriders. (2) The identification of a quiescent period for timing the optimal moment for lifting - and set down of objects.

- **Crane Operator:** The identification of a quiescent period for timing the optimal moment for lifting - and set down of objects.

The use of a radar to determine stochastic wave characteristics, has the clear advantage over a waverider monitoring a much larger area with the use of a single radar and no need to be deployed once on board installed. Therefore, when both methods are equally accurate (to be tested offshore), the use of a wave radar is preferred. The decision support during a lift operation can be used by both the super intendent and crane operator. An answer to subquestion 2.3 (section 1.4.1, stated below), will be searched for by investigating the possibilities for the use of a motion forecast in the crane cabin during a lift operation.

Subquestion 2.3: "To whom is the forecast presented ?"

6.1.2. Requirements tool

To test and demonstrate the use of a motion forecast in the HSC, a tool had to be created with the following requirements:

- Compatible with the HSC.
- Able to present the motion forecast in real-time.
- Satisfy requirements of possible user.

6.1.3. DESIGN PROCESS

The user requirements of the VWRT are determined in a structured process consisting of four steps. Each step included a feedback session with Stefan Adriaanse, an experienced crane operator of the SSCV Thialf.

- **Step 1**: Familiarize with lifting process and identify suitable operations for use of a motion forecast (section 2.3).
- **Step 2**: Generate ideas for a possible interface for the tool.
- **Step 3**: Make selection of generated ideas based on practical experience of HMC employee (section 6.2).
- **Step 4**: Test the final selection in the HSC (chapter 7).

USER REQUIREMENTS

Based on the insights of chapter 2 and feedback from Stefan Adriaanse, the following user requirements are defined:

- **Governing Motion**: During a heavy lift operation, seldom more than one motion is governing. Therefore, only one motion at a time (Heave, Roll, Pitch, Sway and Surge) needs to be forecasted. Preferably this would be the relative motion of the crane block w.r.t the set-down point. In chapter 7 is investigated if a forecast of the CoG of the vessel or module is sufficient to benefit from during a lift operation.
- **Layout Dashboard**: In a crane cabin, a lot of displays are present (figure 3.2). It is important that the forecast is understandable at a glance. Therefore, the user input should be hidden in tabs and only the necessary displayed. Using colors (green and red) to mark motions that exceed a prescribed limit is most wanted.
- **Confidence forecast**: Convincing the user of the capability of the system to make a forecast is necessary and will be challenging. Feedback on the accuracy of the forecast should be given to user.

6.2. FINAL DESIGN

The above described design process has led to a final design version A and B. Both versions are using the same model (chapter 4) but have a different simulation panel in the VWRT (display of forecast).

USER INPUT

The input needed by the VWRT (section 4.1), has to be specified by the user in the input panels at the top of the dashboard. The operation of the tool works intuitive from left to right. An extensive explanation of the input needed and how to use the tool can be found in Appendix C and is summarized in bullets below:

Mode Selection Panel: Select off-Line or on-line HSC mode (section C.1.1).

File Selection Panel: Select Wave-, Motion- (Off-Line mode) and RAO file (section C.1.1).

Plot Selection Panel: Select plotting options for each plot (section C.1.1).

Command Panel: Load files, connect to HSC, start and stop simulation (section C.1.1).

THE DISPLAY

An example of the final design of the VWRT while simulating (version A and B) is shown in figure 6.1 and 6.2. Both show a heave forecast with a limit of 0.1 meter marked. Below a short description of the display is given. Both versions are tested in the HSC (chapter 7).

Version A: (figure 6.1) Three plots are shown. The upper plot shows the wave forecast (wave elevation) for the next 300 seconds. The middle plot show a motion forecast for 300 seconds. The lower plot shows the same motion forecast for 120 seconds in the future and the measured motion as a reference for the past 60 seconds (blue line). This lower plot gives the user confidence in making decisions based on the forecast (if forecast and measured motions are aligned). A smiley is added just above the lower plot indicating the accuracy of the forecast in the past 60 seconds turning yellow ($\rho < 0.8$) and green ($\rho > 0.8$) (both limits and timespan to be defined by user).

Version B: (figure 6.2) Version B does not show the wave elevation (upper plot version A), but instead has a 'Traffic Light' function. This traffic light changes color depending on the time to next limit exceedance. Furthermore, the lower plot is only used as reference, showing a larger span of logged motions. As for version A, a smiley feature is added to give feedback on the accuracy of the forecast.

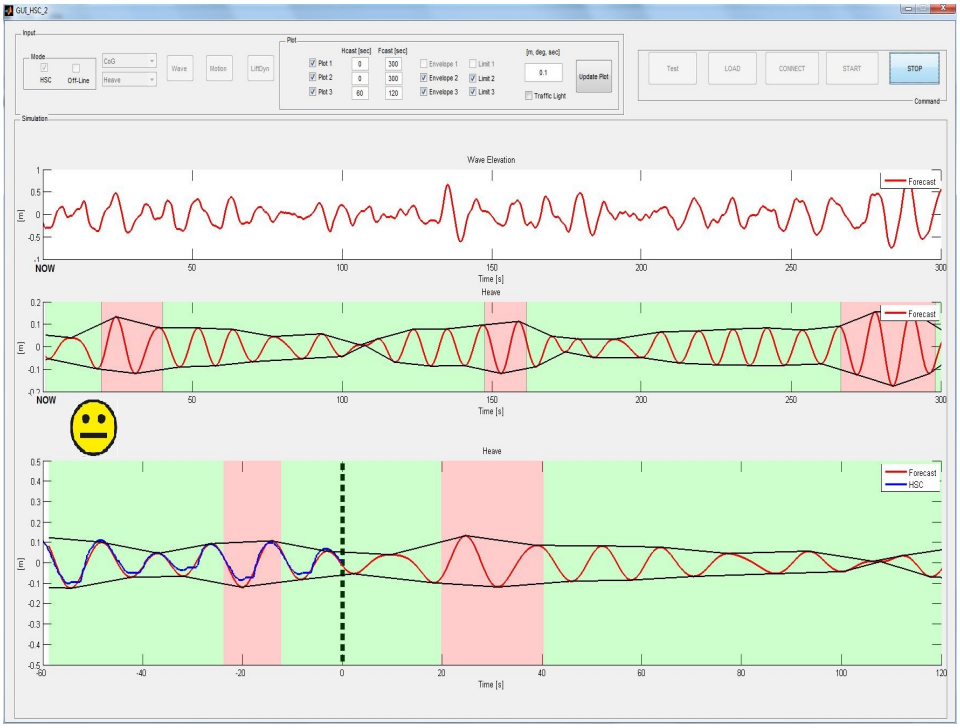

Figure 6.1: Display Version A: Example of a plotted Heave forecast, limit of 0.1 meter (marked with red panels).

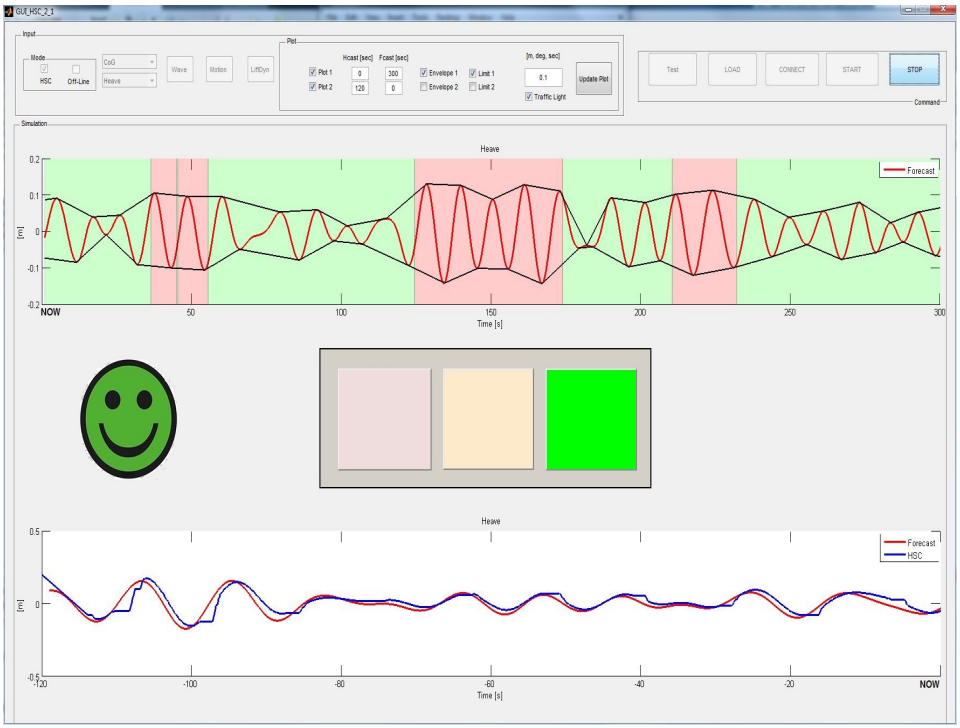

Figure 6.2: Display Version B: Example of a plotted Heave forecast, limit of 0.1 meter (marked with red panels).

6.3. DATA MANAGEMENT

To create a tool that satisfies the above described requirements, several 'data flows' need to be managed in a structured way. To do so, the programming platform MATLAB was chosen to construct the tool since this platform is well supported by the TU Delft and HMC.

6.3.1. OBJECT-ORIENTED PROGRAMMING

To manage the different data flows, 'Object-oriented programming' has been used. This is an approach that combines data and associated actions (methods) into logical structures (objects). It's a well known approach that has advantages when developing large applications and data structures. Furthermore, it enables the programmer to easily add more functionality to the application in later stages. For more detailed information about 'Object-oriented programming' or the use of MATLAB, I refer to the MathWorks MATLAB web page.

The VWRT consists of twelve objects, each with a specific task. Figure 6.3 shows a flow diagram of the data handled by the VWRT. A short description of each object and its function is stated in bullets. A more in depth description can be found in appendix C

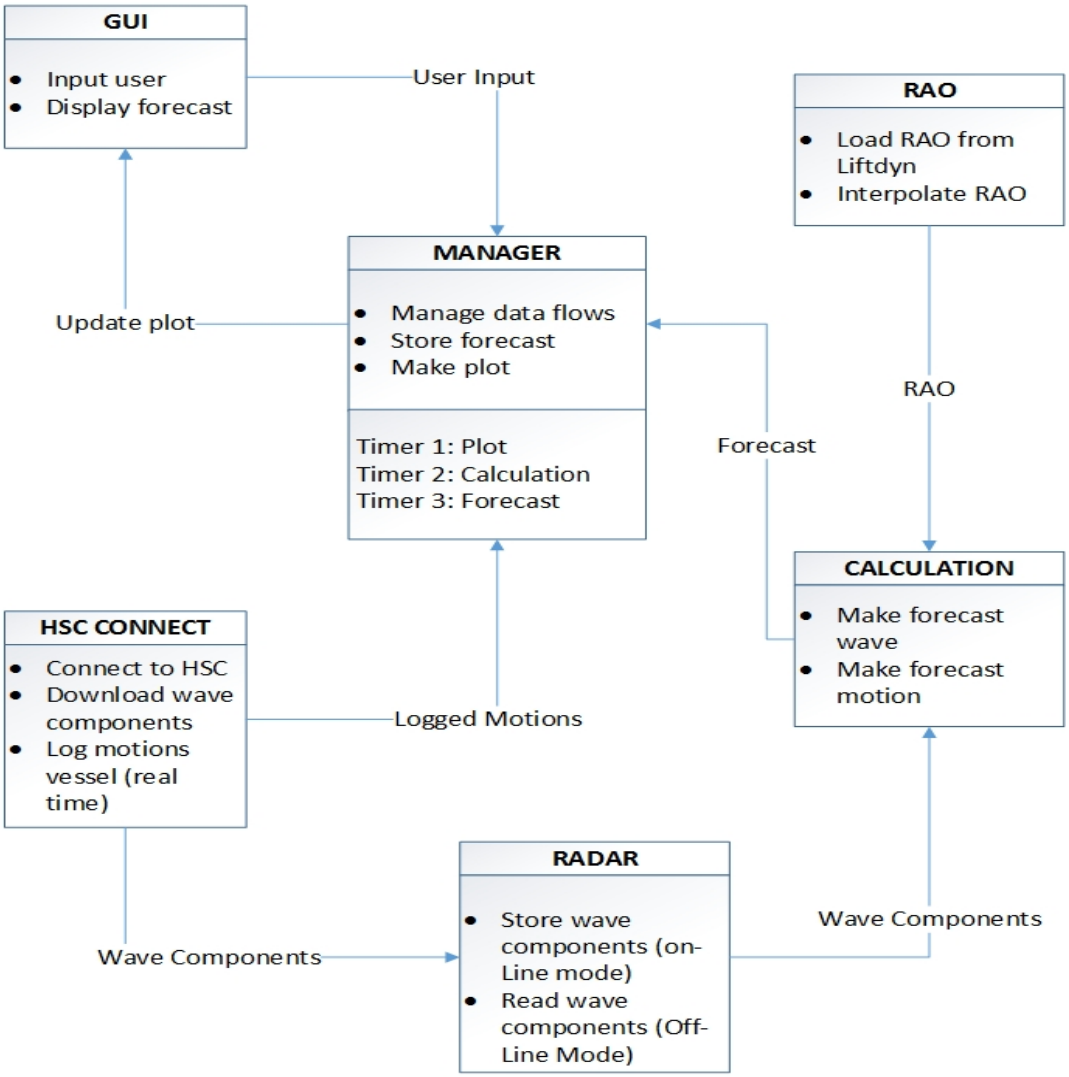

Figure 6.3: GUI Object Flow

7

DEMONSTRATION - A TEST IN THE SIMULATION CENTER

7.1. TESTING THE VWRT

The test case results (Skarfjell and Sable Island) discussed in chapter 5, showed that a motion forecast of a module (single- and dual crane), both relative to a floating or fixed platform / vessel, can be made by The Model. The in the previous chapter described tool is now ready to be tested in the HSC. By doing so, the following is demonstrated / tested:

- The usefulness of a motion forecast during a lift operations.
- The preferred presentation of a motion forecast.

7.1.1. UPDATE OF THE HSC

A planned update of the HSC by Kongsberg in November affected this research in the following way:

- The bugs found are fixed (section 4.3.2 and 4.4.2).
- Old exercises / recordings cannot be used anymore.
- The wave spectrum in K-Sim is build with more components (5000 to 70000).

In the course of this research this imposed some challenges. Not only is the test case, investigated in chapter 5 no longer available, the VWRT as described in chapter 6 does not work anymore due to insufficient computing force (overload of wave components). Attempts to use less components (only the ones that actual excite the vessel) did not have sufficient effect (45000 components remained). Therefore, a simplified tool had to be build (figure 7.1). This tool no longer makes a forecast in real time. A forecast is made on forehand and synchronized when displayed with the logged motions. With this tool only exercises which are carefully prepared can be tested. With this simplified tool, the usefulness and presentation of a motion forecast is tested in the HSC.

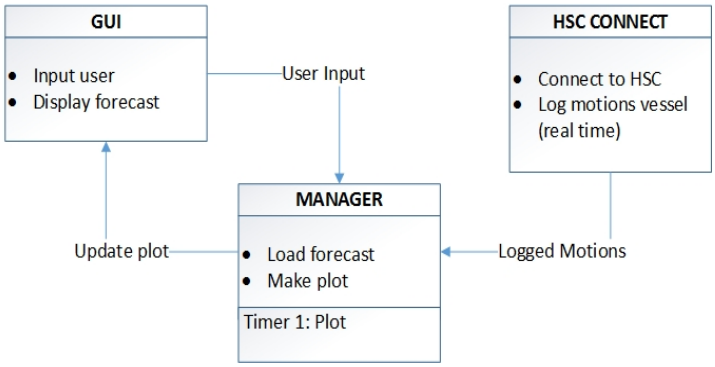

Figure 7.1: Simplified Tool after update HSC

7.1.2. TEST SETUP IN THE HSC

As described in section 7.1.1, exercises previously used in the test cases (chapter 5) are no longer available. For the purpose of testing the VWRT in the HSC, the Skarfjell exercise is rebuild. However, due to unknown reasons, no forecast could be made for two objects in the same exercise (Thialf and Gjoa platform). Therefore, the Gjoa platform is fixed to earth ('lashed') and the motions are forecasted to a fixed platform. The Skarfjell study was challenging due to the relative heave motion (module in crane w.r.t. floating platform). Without the platform moving, a more challenging environment had to be selected (table 7.1).

	Hs [m]	Tp [s]	Heading [deg]	Spreading [-]	$HsTp^2$ [ms^2]
JONSWAP	2	8	0 (Head waves)	30	128

Table 7.1: Wave spectrum used for test in HSC.

The following is tested by using the VWRT on carefully prepared exercises:

- **Advantage motion forecast:** The use of a motion forecast displayed in the crane cabin during a lift operation is tested. The (adapted) Skarfjell test case is used to test the advantage of a motion forecast during a single crane lift operation. Without the platform moving, a challenging environment (table 7.1 is selected to magnify the need for a motion forecast. It should be noted that in real life a lift operation would be delayed for the chosen environment.
- **Forecasted time span:** By varying the time span for which a forecast is displayed (30 seconds, 1 minute, 2 minutes and 5 minutes), one can reflect on current wave radar systems (claimed results presented in section 2.2.2) and the use of such a system for a lift operation.
- **Response of forecast to interference:** When an object is lifted from deck and put on a barge, the crane has to make a slewing motion. When the object is positioned above the barge, a motion forecast should indicate the right moment to lower the object. However, it is expected that the slewing motion would result in a disturbance of the object's motion. The time needed for the model forecast to be accurate after slewing is investigated. Note that attempts to test this in K-Sim, resulted in unrealistic motions of the object (without a crane driver using his skills to damp the motions of the object).

The following feature of the VWRT are tested and reviewed w.r.t. the experience of the user:

- **Layout dashboard:** The in section 6.2 discussed displays version A and B.
- **Decision support:** The use of a 'traffic light' as decision support (section 6.2).
- **Feedback accuracy:** Both the 'smiley'- and logged motion feature (section 6.2).

7.2. TEST RESULTS

The preparation needed for the tests in the HSC (aligning RAO with K-Sim), clearly show the need for more adaptable system when used offshore. Furthermore, as mentioned in section 7.1.1, a simplified tool is tested in the HSC with a forecast made on forehand. This forecast is synchronized with the HSC at the start of a simulation. K-Sim does not supply time info during the simulation. Therefore, when the simulation is not running in real time, the forecast is out of phase with the simulation. This proved to be a real problem during the tests with simulations not running in real time. Therefore, for further improvement of the VWRT, a real time-stamp in K-Sim / HSC is needed.

USING A MOTION FORECAST

The advantage when using a motion forecast during a lift operation is demonstrated by executing the same operation twice. First the crane operator is free to chose a moment to start lowering the module (step 5, section 5.1) without the use of the VWRT (Try 1). Subsequently, a retry with the tool switched on (Try 2) is performed where a quiescent period is selected to start lowering the module. Both 'Try 1' and 'Try 2' are marked on the motion forecast in figure 7.2. One can see clearly that 'Try 2' is carefully timed in order to have first contact (between the module and platform) in a period with minimum vessel motions.

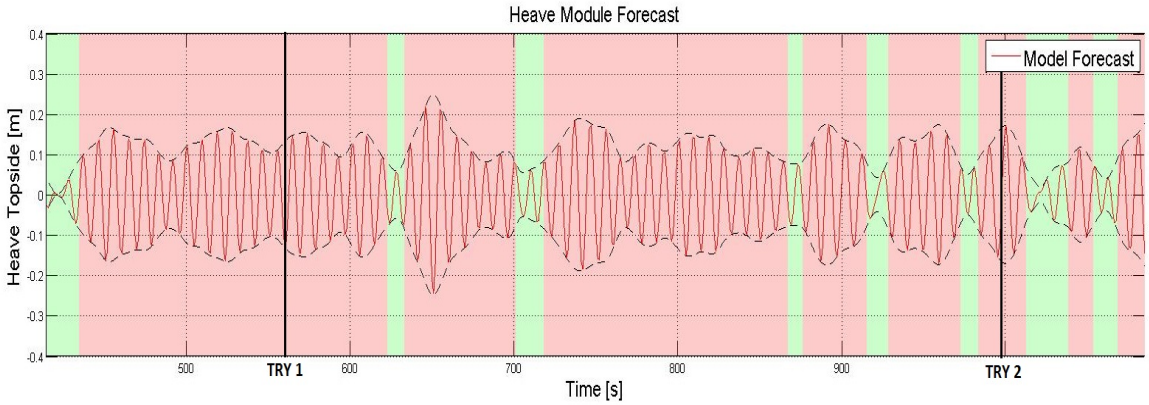

Figure 7.2: Heave of module w.r.t. platform. Marked with red panels when limit is exceeded. Moment of set-down Try 1 and 2 marked with black line.

As can be seen in figure 7.2, 'Try 1' started lowering the module at an unfavorable time. Due to the large vessel motions at the moment of first contact between the module and platform, several secondary impacts are registered (figure 7.3 lower plot, small bumps after t = 580). It should be noted that the heave motion of the module is logged in the HSC as 'altitude'. Therefore, one can see the actual lowering of the module in the lower plot (t = 558).

The results of Try 2 are shown in figure 7.4. The moment of lowering (t =993) is chosen in such a way that the first contact between the module and platform is during a quiescent period with vessel motions at a minimum (upper plot). The lower plot illustrates that there are no secondary impacts for Try 2. Therefore, one may conclude that the use of a motion forecast has proven to be useful in the above described example.

Furthermore, variations in the forecasted timespan (30 seconds, 1 minute, 2 minutes and 5 minutes) did not have any effect on the ability of the crane operator to select a quiescent period. However, it is clear that with a larger time span, the user can select the most suitable moment out of a larger selection. Therefore, one may conclude that (w.r.t. the timespan of future telling) wave radar systems currently available on the marked (section 2.2.2) could very well be used in the advantage of a lift operation.

The 'slewing' exercise did not show significant deviations after moving the crane. The 1000 T module is handled with care by the crane driver. Therefore, when arriving above the set down point, no excessive motions are present.

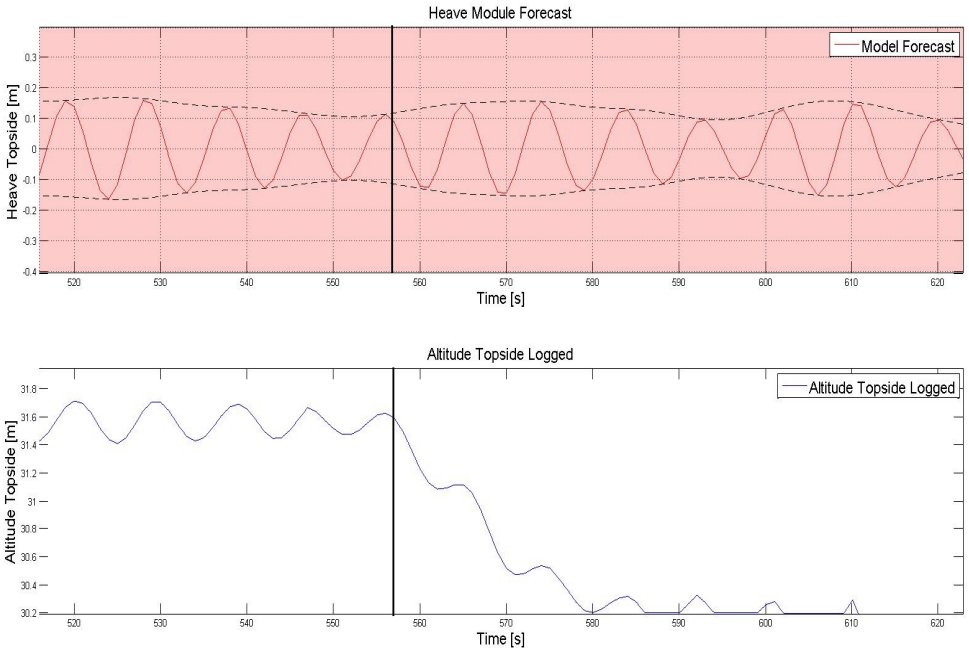

Figure 7.3: Upper plot: Heave of module. Moment of set-down Try 1, random chosen. Lower plot: Altitude of module. Note the secondary impacts (4 times) after set-down.

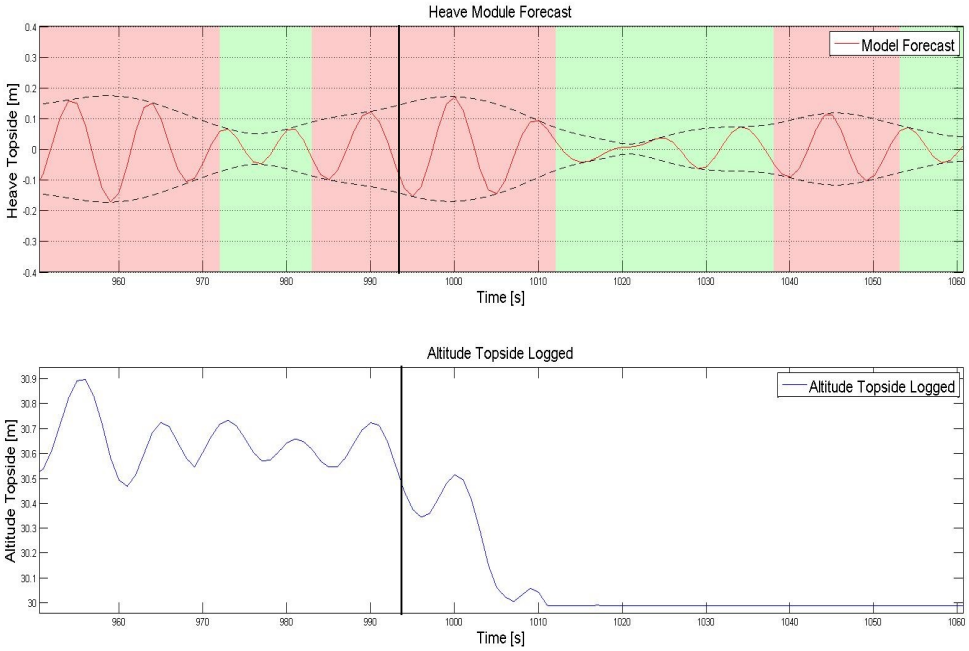

Figure 7.4: Upper plot: Heave of module. Moment of set-down Try 2, chosen with use forecast. Lower plot: Altitude of module. Note that there are no secondary impact after set-down.

EVALUATING THE DESIGN:
It became once more clear that a motion forecast displayed in a crane cabin has to be understandable at a glance. Furthermore, the position of the display should be in front of the operator. Timing the right moment to start the lowering was a two-man job with the current configuration. The use of a 'traffic light' decision support could be the solution to this problem. In addition to the current traffic light feature, the time to- and duration of a quiescent period should be marked clearly. Furthermore, only quiescent periods with a duration long enough to successfully set down (or lift) an object should be marked. Therefore the hight of the module and lowering speed should be incorporated.

As stated in section 6.1.3, feedback on the accuracy of a forecast should be given to user. During the test, more than once the simulation lagged, resulting in a forecast being no longer correct. The tested 'feedback features' (smiley and displayed logged motions) did indicate the incorrect forecast but were not noticed by the crane operator. Therefore, when a forecast is wrong, the display should turn off or freeze, mitigating the risk of making a decision on false information.

Summarizing the above, version A of the VWRT proved to be most suitable for using a motion forecast during a lift operation. However, improvement of the design is needed concerning:

- Less info in display.
- Mark duration quiescent period.
- Freeze display when forecast incorrect.

8

CONCLUSIONS AND RECOMMENDATIONS

During the 2018 summer campaign, HMC will test a wave radar system from Applied Physical Sciences (APS) aboard the SSCV Thialf. This thesis has aimed to investigate the possibilities for the use of a wave forecast during an offshore lift operation. The focus lays on predicting motions and how to present it in a useful way.The objective of this thesis can be divided in two:

1. Determine the most suitable way of predicting vessel motions based on a wave forecast.
2. Make a preliminary design for a 'dashboard' presenting the forecast based on user preferences.

The first part of the objective is approached by investigating the possibilities and limitations of making a motion forecast in the frequency domain. This method is convenient since the calculation is easy to understand and very fast, a quality which is most wanted when making a future prediction. The second part has a more qualitative character, where the use of a forecast is tested in the HSC by using a tool that is created for this purpose (the VWRT).

8.1. CONCLUSION

Conclusions and recommendations are separately given for objective one an two and stated in bullets below:

8.1.1. MAKING A MOTION FORECAST

- The motion forecast made by The Model showed good results for heave roll and pitch (correlation coefficient 0.85 - 1.0 and RMS ratio 0.86 - 1.15) for mild, severe and a combined sea-states (all wave directions, respectively). However, for the (extreme) swell case the model was no longer able to make a forecast. This can be explained by the fact that when motions become larger, frequency domain approach is is no longer valid. Based on the performed analyses, it can be concluded that for sea-states used during (heavy) lift operations, the motion forecast made by the model is providing accurate results.
- The model showed that the accuracy of a forecast is not influenced by environmental conditions itself. However, model input being not accurate has more influence in certain environments. Therefore, one can not conclude that the input of the model is correct based on a accurate forecast. Furthermore, offshore the model input, generated by a wave radar, is most certainly influenced by the environmental conditions and therefore will influence the accuracy of the forecast.
- The sensitivity of the model to variations in the CoG and radii of gyration of the vessel, is investigated and found to be within acceptable bounds. The impact is negligible on the phase and small (<10%) on the amplitude. Data offshore is said to be accurate to +- 2m and therefore the model sensitivity to its input is acceptable.
- The model proved to be well capable of forecasting the heave motion of a module relative to the set down point on a floating platform. Simplifications made w.r.t. the rigging of a module proved to be valid when forecasting the heave, roll or pitch movements of the module.

8.1.2. PRESENTING A MOTION FORECAST

- The tests in the HSC showed positive results for the use of a forecast in the crane cabin during a lift operation. A reduction of secondary impact loads in a challenging environment was realized due to the use of a forecast. A forecasted time span of two minutes proved to be more than enough.
- During a heavy lift operation, seldom more than one motion is governing. Therefore, only one motion has to be forecasted simultaneously for decisions support. The relative motion of the crane block w.r.t set-down point would be preferable.
- A motion forecast displayed in a crane cabin, should be understandable at a glance and positioned in front of the operator. Time to- and duration of quiescent period should be clearly marked.
- The length of the quiescent period needed for a successful lift is based on the distance of the module to set-down point and the lowering speed. Therefore, the speed of the crane block should be included in the decisions support marking only calm periods long enough for e successful lift / set down.
- Feedback on the accuracy of the forecast should be given to user. When the forecast is wrong, the display should turn off mitigating the risk of making a decision on non accurate forecast.

8.2. RECOMMENDATIONS AND FOLLOW UP

- Surge and Sway of a module is forecasted with less accuracy ($\rho 0.82 - 0.88$ and $\sigma 0.5 - 0.7$) than the other motions ($\rho 0.85 - 1.0$ and $\sigma 0.86 - 1.15$). With an accurate forecast for heave roll and pitch, a forecast for sway and surge of the topside, is expected to be similarly accurate since all motions are closely related. The deviation between forecasted- and logged motion can possibly be explained by logging inaccuracies, which when accurately corrected for could result in a higher accuracy.
- The source of deviation between forecasted and logged motions is only investigated to a certain level. For instance, the model input is not optimized, but (roughly) calculated based on K-Sim object specifics. Higher accuracy can be achieved with further optimization.
- The source of deviation between forecasted and logged motions is only investigated to a certain level. For instance, the model input is not optimized, but (roughly) calculated based on K-Sim object specifics. Higher accuracy can be achieved with further optimization.
- There are many possible sources causing a forecast to deviate from the actual motion. A self learning (adaptive model), could reduce the need for exact model input offshore (not always available), even without knowing the source of deviation.
- The update-rate of a wave radar system is not tested within this research. With in reality, a forecast becoming more accurate for waves closer to the vessel, handling the display of a changing forecast should be further investigated.
- This thesis demonstrated the possible advantage of a motion forecast during a lift operation. To whom a forecast should be presented (superintendent / crane operator / both) should be decided on operational level.
- For further improvement of the VWRT, a real time-stamp in K-Sim / HSC is needed. With simulations not running in real time, the API work around does not work. Furthermore, the enormous amount of wave components demands more computer capacity when making a forecast real time.

BIBLIOGRAPHY

[1] A. Khan, K. Marion, and C. Bil, *The Prediction of Ship Motions and Attitudes using Artificial Neural Networks,* (2017).

[2] W. Zhang and Z. Liu, *Real-time ship motion prediction based on time delay wavelet neural network,* Journal of Applied Mathematics (2014), 10.1155/2014/176297.

[3] L. H. Holthuijsen, *L. H. Holthuijsen 2007_Waves_In_Oceanic_and_Coastal_Waters_ISBN-10 0-521-86028-8.1.1,* .

[4] J. M. J. Journée and W. W. Massie, *OFFSHORE HYDROMECHANICS,* (2001).

[5] M. S. Longuet-Higgins and O. M. Phillips, *Phase velocity effects in tertiary wave interactions,* Journal of Fluid Mechanics **12**, 333 (1962).

[6] T. Hilmer and E. Thornhill, *Observations of predictive skill for real-time Deterministic Sea Waves from the WaMoS II,* (2015).

[7] P. Naaijen, R. R. T. Vandijk, R. H. M. Huijsmans, and A. A. El-Mouhandiz, *Real Time Estimation of Ship Motions in Short Crested Seas,* 10.1115/OMAE2009-79366.

[8] J. Dannenberg, K. Hessner, P. Naaijen, H. Van Den Boom, and K. Reichert, *The On board Wave and Motion Estimator OWME,* Proceedings of the International Offshore and Polar Engineering Conference **3**, 424 (2010).

[9] G. Wu, *Direct Simulation and Deterministic Prediction of Large-scale Nonlinear Ocean Wave-field,* Massachusetts Institute of Technology (2004).

[10] J. G. Kusters, K. L. Cockrell, B. S. Connell, J. P. Rudzinsky, and V. J. Vinciullo, *FutureWaves™: A real-time Ship Motion Forecasting system employing advanced wave-sensing radar,* in *OCEANS 2016 MTS/IEEE Monterey, OCE 2016* (2016).

[11] L. K. Alford, R. F. Beck, J. T. Johnson, D. Lyzenga, O. Nwogu, and A. Zundel, *A REAL-TIME SYSTEM FOR FORECASTING EXTREME WAVES AND VESSEL MOTIONS,* .

[12] J. M. Giron-Sierra and J. F. Jimenez, *State-of-the-Art of Wave Measurement for Ship Motion Prediction,* IFAC Proceedings Volumes **43**, 295 (2010).

[13] G. R. Valenzuela, *Theories for the interaction of electromagnetic and oceanic waves — A review,* Boundary-Layer Meteorology **13**, 61 (1978).

[14] B. Lund, C. O. Collins, H. Tamura, and H. C. Graber, *Multi-directional wave spectra from marine X-band radar,* Ocean Dynamics **66**, 973 (2016).

[15] F. F. Wright, *Wave observation by shipboard radar,* Ocean Sci. Ocean Eng **1**, 506 (1965).

[16] I. Young, W. Rosenthal, and F. Ziemer, *A Three-Dimensional Analysis of Marine Radar Images for the Determination of Ocean Wave Directionality and Surface Currents,* JOURNAL OF GEOPHYSICAL RESEARCH **90**, 1049 (1985).

[17] J. C. Borge, G. Rodríquez Rodríguez, K. Hessner, and P. I. González, *Inversion of marine radar images for surface wave analysis,* Journal of Atmospheric and Oceanic Technology (2004), 10.1175/1520-0426(2004)021<1291:IOMRIF>2.0.CO;2.

[18] T. Hilmer and E. Thornhill, *Deterministic wave predictions from the WaMoS II,* in *OCEANS 2014 - TAIPEI* (2014).

[19] B. S. H. Connell, J. P. Rudzinsky, C. S. Brundick, W. M. Milewski, J. G. Kusters, and G. Farquharson, *DEVELOPMENT OF AN ENVIRONMENTAL AND SHIP MOTION FORECASTING SYSTEM,* .

[20] G. F. Clauss, M. Klein, and M. Onorato, *Formation of Extraordinarily High Waves in Space and Time,* 10.1115/OMAE2011-49545.

[21] G. F. Clauss, M. Klein, and D. Testa, *Spatial Evolution of an Extreme Sea State With an Embedded Rogue Wave,* (2008).

[22] G. F. Clauss, S. Kosleck, and D. Testa, *Critical Situations of Vessel Operations in Short Crested Seas—Forecast and Decision Support System,* Journal of Offshore Mechanics and Arctic Engineering (2012), 10.1115/1.4004515.

[23] X. Yang, *Displacement motion prediction of a landing deck for recovery operations of rotary UAVs,* International Journal of Control, Automation and Systems **11**, 58 (2013).

[24] A. P. Wijaya, P. Naaijen, Andonowati, and E. V. Groesen, *Reconstruction and future prediction of the sea surface from radar observations,* Ocean Engineering (2015), 10.1016/j.oceaneng.2015.07.009.

[25] A. G. Asuero, A. Sayago, and A. G. González, *The Correlation Coefficient: An Overview,* Critical Reviews in Analytical Chemistry **36**, 41 (2006).

[26] E. .-. DNVGL-ST-N001, *Marine operations and marine warranty,* (2016).

A

DEFINITIONS

Default Thialf	Standard model of Thialf with no loads in cranes, cranes in cradles and draft of 26m
Exercise	A scenario build in K-Sim.
K-Sim	Stand alone software able to run a simulation from a laptop.
Object	An object in K-Sim exercise (vessel, crane block, etc.).
Model	The script / model behind the interface of the virtual wave radar tool.
Net API	Application Programming Interface developed by HMC to connect with the K-Sim interface.
Object	An object in K-Sim exercise (vessel, crane block, etc.) / A programming structure used for data manag
Test Barge	A model of a simplified barge, consisting of a symmetrical uniform beam.
The Model	Model able to make a vessel motion forecast based on a wave forecast. **Wave Origin**
Virtual Wave Radar Tool	Tool created to make and show a vessel motion forecast in the HSC.
Wave Radar	Actual radar reading wave patterns.
Wave Radar System	Full System including wave radar, making a motion forecast.

B

THE HEEREMA SIMULATION CENTER

B.0.1. BUG HSC

The results of the 'Test Barge runs' were not as expected. When the vessels origin is positioned at the wave origin, the logged- and forecasted motions give an accurate match. However, when the vessel is no longer positioned at the wave origin, the measured and forecasted vessel motions no longer agree. As can be seen in figure **??**, the wave elevations does match but the motions do not. To investigate the source of this odd result, the same Test Barge has been modeled in Orcina OrcaFlex (figure B.1).

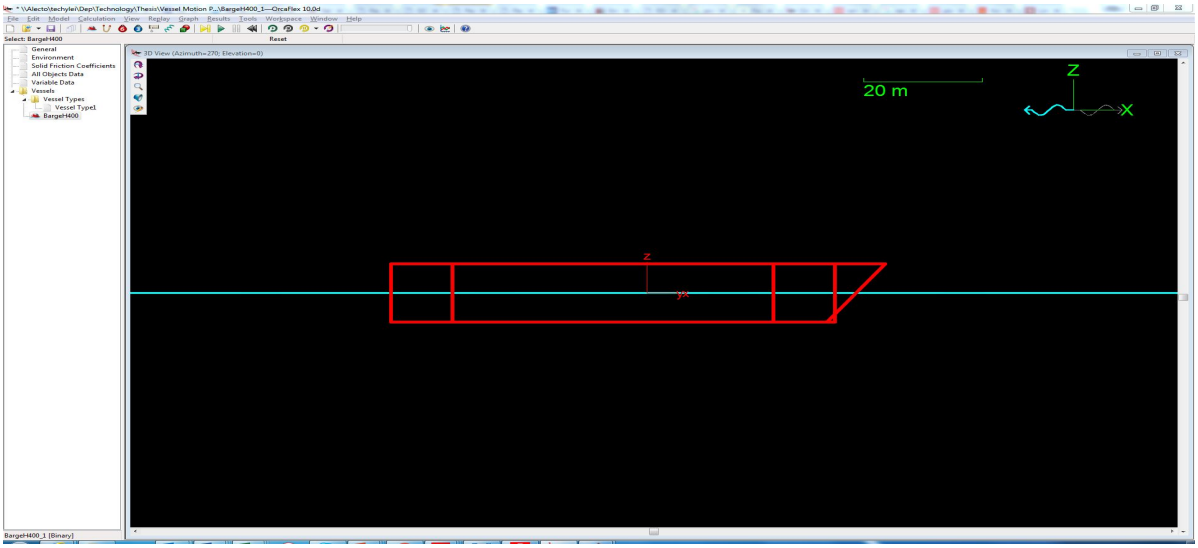

Figure B.1: Model of Test Barge H400 modeled in OrcaFlex to verify odd results obtained in HSC simulations

The same 5000[1] wave components that were used for the simulation are used as input for OrcaFlex. Each component has an amplitude, phase, frequency and direction. However, OrcaFlex does not have the option to add a unique wave direction to each wave component. As a solution to this problem, separate wave trains with different directions are added one by one. To do so, Matlab is used to add the wave components, run OrcaFlex and extract the result for each wave component separately. The results are than summed together (superposition principle) to get the total wave elevation and response.

The result of the OrcaFlex run was identical to The Model calculations (different from the HSC simulation). The measured wave elevation at the origin of the vessel agreed with the logged elevation of the HSC but the vessel motions did not. However, when the 'x' and 'y' coordinates where swapped, the vessel motions did agree but the measured and forecasted wave elevation did not. Therefore, it was expected that a bug in the

[1] At start research 5000 components, increased to 70000 during a system update by Kongsberg in September 2017

HSC was found.

To proof the bug in the HSC, a straight forward test with four barges and a single wave (a wave with a single amplitude, frequency, phase and direction) was executed. The arrangement of the test can be seen in figure B.2.

With the wave coming from 0 degree (north, figure 1), the wave elevation at the location of Barge 1, Barge 2 and Barge 3 should be identical and therefore also the vessel motions. In figure B.3 we see that the wave elevation indeed agree for the three barges and differ for Barge 4. However, in figure B.4 we see that the heave motion of Barge 1, Barge 2 and Barge 3 are not the same. Furthermore, we see that Barge 4 is overlapping Barge 2 what proves that indeed the 'x' and 'y' coordinates for the calculation of the vessel motion in the HSC are swapped.

This bug is reported to Kongsberg Digital and temporarily solved by simply (wrongly) calculating the vessel motions with swapped x and y coordinates in The Model [2].

[2] Bug is acknowledged by Kongsberg and fixed during a system update in September 2017

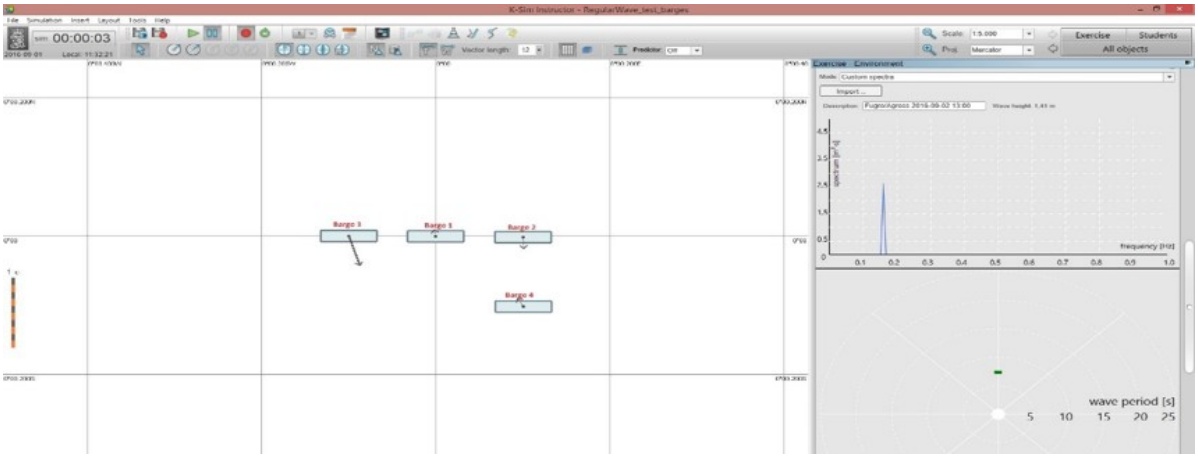

Figure B.2: Singel Wave Test

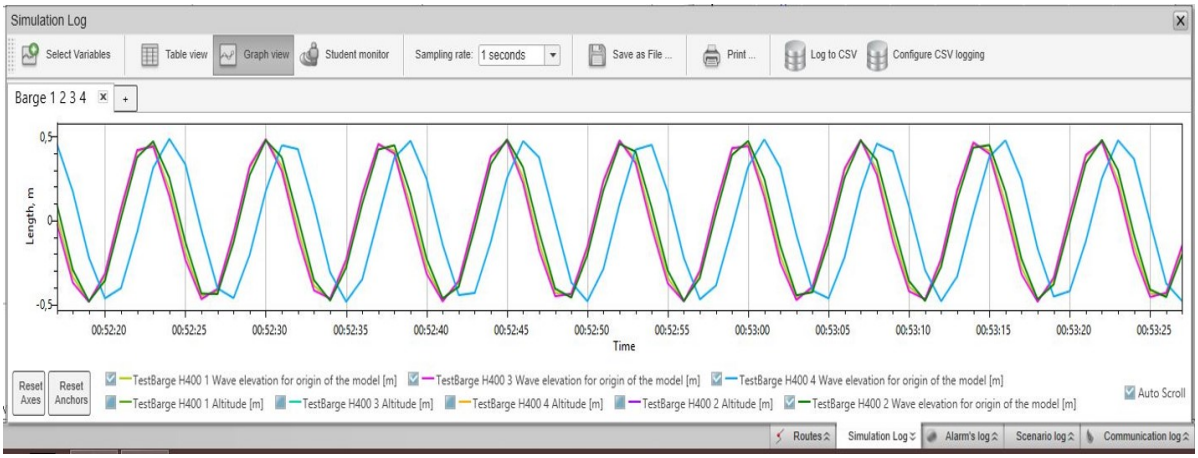

Figure B.3: Logged wave elevation location barges

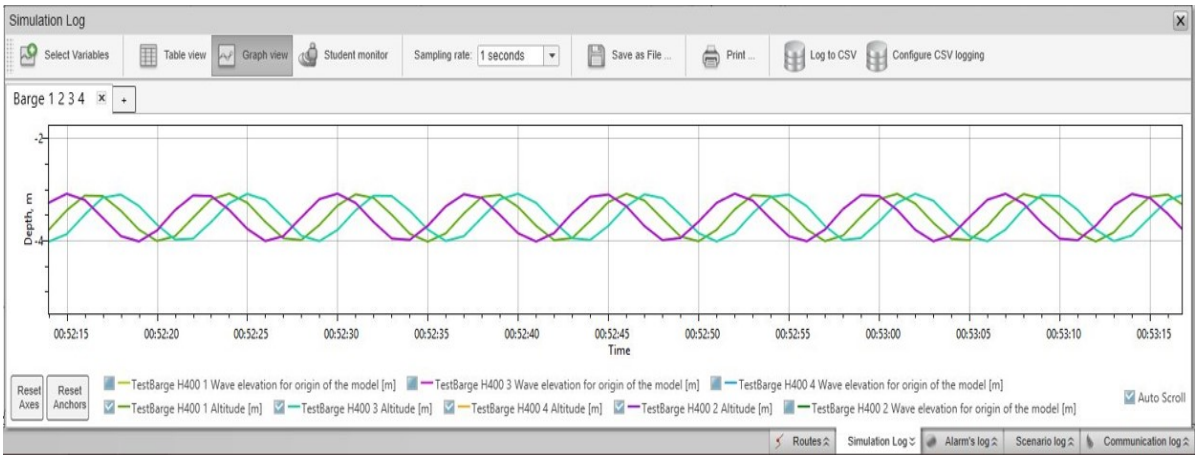

Figure B.4: Logged Heave (Altitude) with Barge 4 in overlap Barge 2 (orange is behind purple)

C

GRAPHICAL USER INTERFACE

This appendix describes the VWRT in detail, how the tool should be used and what input is necessary to make a forecast. Furthermore, the tasks of each object modeled in matlab (figure 6.3) handling the data flows while simulating is summarized.

C.1. DATA MANAGEMENT

The VWRT consists of twelve objects, each with a specific task. Figure 6.3 shows a flow diagram of the data handled by the VWRT. A description of each object is given below.

C.1.1. GUI

The 'GUI' object creates the dashboard for the user when opening the VWRT. It receives the users input at the start of a simulation and displays the forecast while simulating. One of the requirements determined in the 'design phase' was a simple interface only showing the information needed. Therefore, it would be desirable to have different tabs in the display to hide input information while simulating (figure: **??**). Unfortunately 'matlab 2013b' does not support a 'tab' function. Instead there are three panels positioned at the top of the display: An 'input panel', a 'command panel' and a 'simulation panel' (C.1).

INPUT PANEL

The input panel (C.2) contains three sub-panels named: 'Mode Selection', 'File Selection' and 'Plot Selection'.

Mode Selection By switching between 'HSC' and 'Off-Line' in the 'Mode Selection' sub-panel, the user can choose between connecting to the HSC or using a recorded simulation in the 'off-line mode'. When operating in 'off-line mode', an excel file containing the recorded wave components and logged motions need to be selected in the 'File Selection' sub-panel by clicking on the pushbuttons.

File Selection The sub-panel 'File Selection' contains three push-buttons named: 'Wave', 'Motion' and 'RAO'. The 'Wave' and 'Motion' push-buttons are only available when operating in 'off-line mode' and open a pop-up dialog which enables the user to either select a 'wave.csv' or a 'motion.xlsx' file . To be compatible with the VWRT, both files should be in the standard format of the HSC. An example of these formats is shown in C.3 and C.4. The drop down boxes 'Select Motion' and 'Select POI' will let the user define the degree of freedom to be forecasted at the POI.

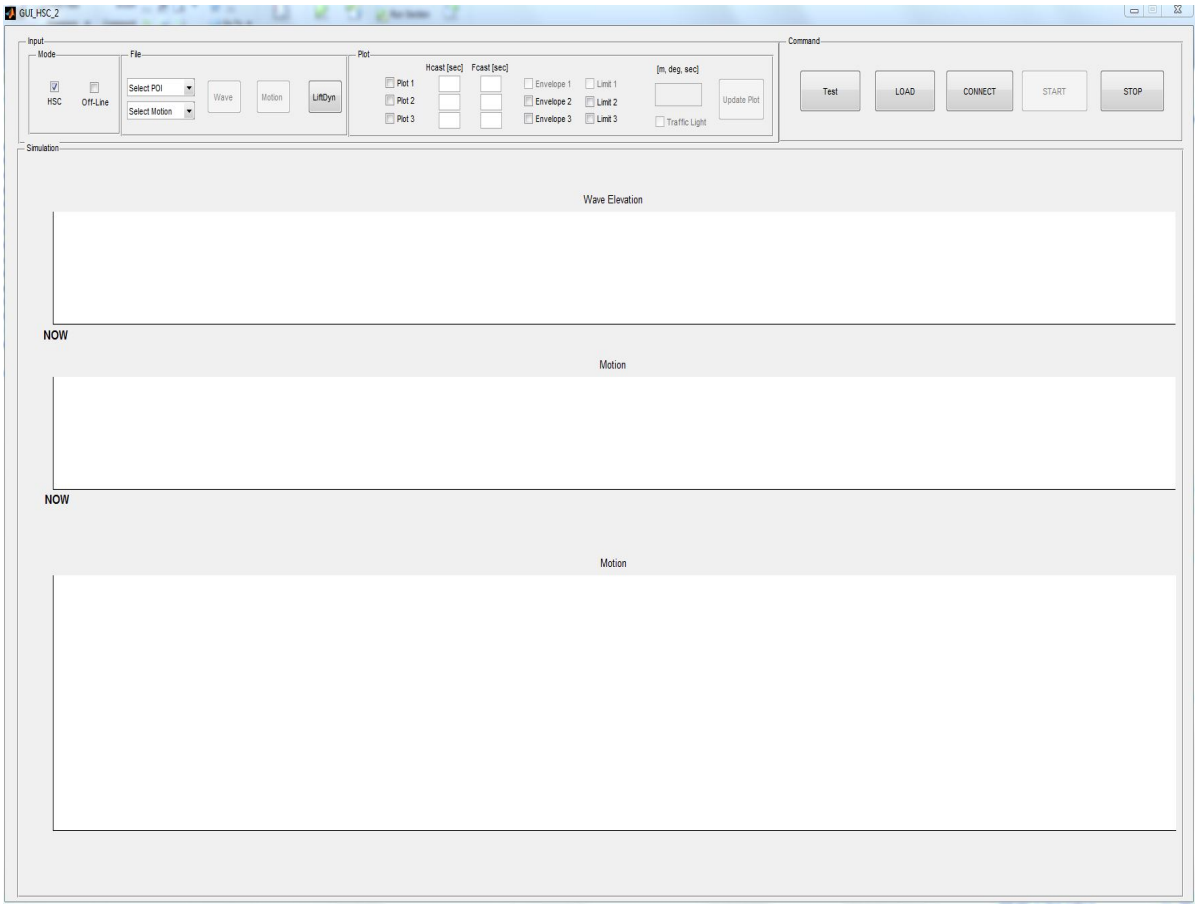

Figure C.1: GUI 2

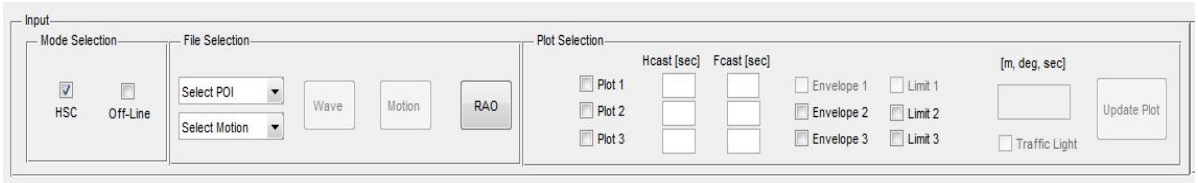

Figure C.2: Input Panel

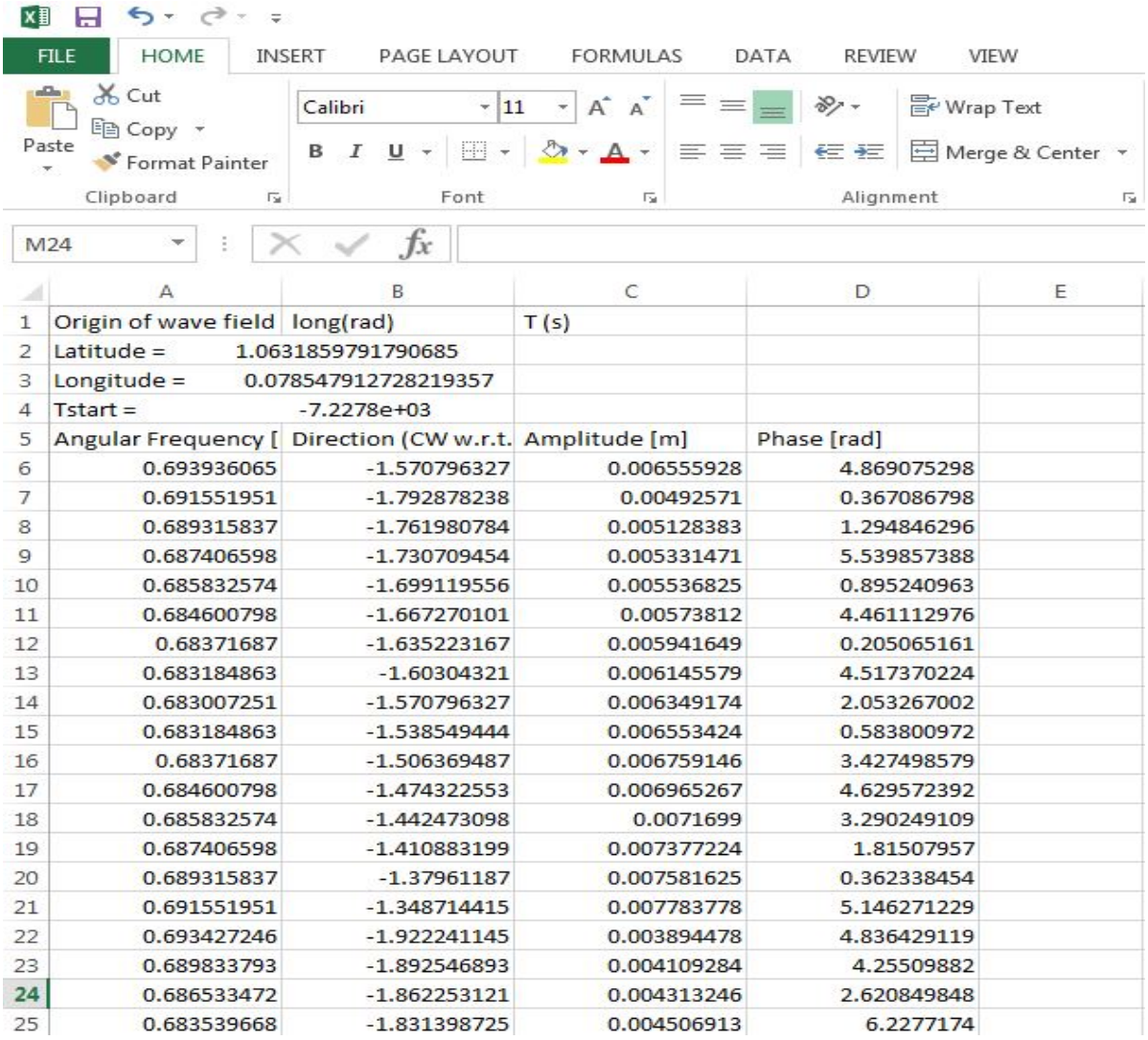

	A	B	C	D	E
1	Origin of wave field	long(rad)	T (s)		
2	Latitude =	1.0631859791790685			
3	Longitude =	0.078547912728219357			
4	Tstart =	-7.2278e+03			
5	Angular Frequency [	Direction (CW w.r.t.	Amplitude [m]	Phase [rad]	
6	0.693936065	-1.570796327	0.006555928	4.869075298	
7	0.691551951	-1.792878238	0.00492571	0.367086798	
8	0.689315837	-1.761980784	0.005128383	1.294846296	
9	0.687406598	-1.730709454	0.005331471	5.539857388	
10	0.685832574	-1.699119556	0.005536825	0.895240963	
11	0.684600798	-1.667270101	0.00573812	4.461112976	
12	0.68371687	-1.635223167	0.005941649	0.205065161	
13	0.683184863	-1.60304321	0.006145579	4.517370224	
14	0.683007251	-1.570796327	0.006349174	2.053267002	
15	0.683184863	-1.538549444	0.006553424	0.583800972	
16	0.68371687	-1.506369487	0.006759146	3.427498579	
17	0.684600798	-1.474322553	0.006965267	4.629572392	
18	0.685832574	-1.442473098	0.0071699	3.290249109	
19	0.687406598	-1.410883199	0.007377224	1.81507957	
20	0.689315837	-1.37961187	0.007581625	0.362338454	
21	0.691551951	-1.348714415	0.007783778	5.146271229	
22	0.693427246	-1.922241145	0.003894478	4.836429119	
23	0.689833793	-1.892546893	0.004109284	4.25509882	
24	0.686533472	-1.862253121	0.004313246	2.620849848	
25	0.683539668	-1.831398725	0.004506913	6.2277174	

Figure C.3: Example Wave File

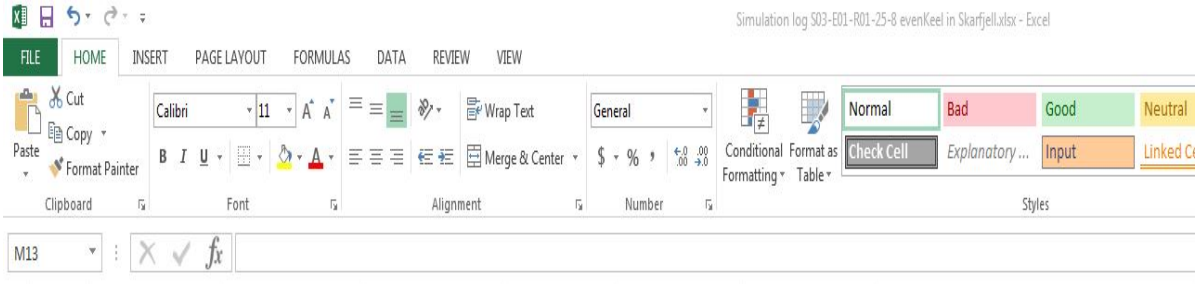

	A	B	C	D	E	F	G	H
1	Time	Thialf 1 Latitude []	Thialf 1 Longitude []	Thialf 1 Altitude [m]	Thialf 1 Roll [º]	Thialf 1 Pitch [º]	Thialf 1 Heading [º]	Thialf 1 Wave elevation for origin of the model [m]
2	00:00:00	1.063135316	0.078612509	-26.50114441	-5.08889E-14	0.003971099	89.5099979	0
3	00:00:01	1.063135316	0.078612521	-26.50331688	-0.051096495	0.000924998	89.51120002	-0.116743527
4	00:00:02	1.063135316	0.078612534	-26.54057312	-0.082572331	0.016690731	89.51193768	-0.030503746
5	00:00:03	1.063135316	0.078612546	-26.59381866	-0.106565338	0.031940192	89.51270949	0.235724732
6	00:00:04	1.063135317	0.078612555	-26.643116	-0.118088034	0.037260663	89.5135496	-0.035123911
7	00:00:05	1.063135318	0.078612563	-26.67115211	-0.117395784	0.031744365	89.51441704	-0.323343724
8	00:00:06	1.06313532	0.07861257	-26.67128372	-0.109449639	0.020571763	89.515223	-0.5109092
9	00:00:07	1.063135321	0.078612578	-26.64852524	-0.098929327	0.009848917	89.515947	-0.472159356
10	00:00:08	1.063135322	0.078612585	-26.61450958	-0.086389713	0.0038091	89.51661636	0.200679749
11	00:00:09	1.063135324	0.078612592	-26.58097839	-0.069832121	0.004890662	89.51735402	0.593464136
12	00:00:10	1.063135325	0.078612599	-26.55573654	-0.049494295	0.01465344	89.51824877	0.571795404
13	00:00:11	1.063135327	0.078612606	-26.54178238	-0.029701568	0.033522438	89.5192733	0.199204177
14	00:00:12	1.063135328	0.078612613	-26.5381813	-0.014863375	0.05897883	89.52031832	-0.320367843
15	00:00:13	1.063135329	0.07861262	-26.54135704	-0.003659329	0.084198603	89.52131553	-0.274203628
16	00:00:14	1.06313533	0.078612624	-26.54649353	0.011697068	0.099501369	89.52224443	-0.530775011
17	00:00:15	1.063135332	0.078612626	-26.54928207	0.038542394	0.096824868	89.52309821	-0.297571838
18	00:00:16	1.063135334	0.078612625	-26.54804039	0.07572416	0.074860608	89.52385636	0.301349223
19	00:00:17	1.063135336	0.078612622	-26.54482079	0.11188853	0.041032518	89.52455304	0.057509027
20	00:00:18	1.063135338	0.078612619	-26.54426575	0.131821197	0.008550088	89.52527021	-0.314550608
21	00:00:19	1.063135338	0.078612616	-26.5504818	0.126024501	-0.009876675	89.52612398	-0.111156613
22	00:00:20	1.063135337	0.078612616	-26.56417274	0.096001877	-0.008222171	89.52714851	0.507707357
23	00:00:21	1.063135335	0.078612618	-26.58215141	0.051541448	0.009829704	89.52830964	0.32298854
24	00:00:22	1.063135334	0.07861262	-26.59933662	0.003899328	0.033025826	89.52948443	0.216806024
25	00:00:23	1.063135333	0.07861262	-26.61157036	-0.038316961	0.048704688	89.5305636	-0.330025673

Figure C.4: Example Motion File

Plot Selection The sub-panel 'Plot Selection' can be used to select plotting options. Each plot can be activated by selecting the 'plot 1, 2 or 3' check box. The timespan shown in each plot can be determined by the 'Past' and 'Future' boxes. To show an envelop or/and a specified limit, the 'Envelop' and 'Limit' check boxes should be selected together with a user specified limit. When the 'limit' option is selected, the plot's will be colored with red panels when the limit is exceeded and green when not (figure: 6.2). During a simulation, the 'Plot Selection' options can be changed and updated by pressing the 'Update plot' pushbutton.

COMMAND PANEL

The command panel contains five push buttons. The 'Test' button is added for validation and verification purpose. When pressed, the input panel is filled with standard value's and preferences hard-coded inside the GUI to enable quick test runs. When the input panel is filled in (by hand or pushing 'Test'), The 'Load' button will first create the 'The Management Object' and sent the user input received through the dashboard to it. The 'Management' object creates all other objects and the user input is passed on to each object. When successfully loaded, the 'Connect' button comes available which will make a connection with the HSC. Finally when connected, the 'Start' and 'Stop' button come available allowing the user to start and stop the forecast.

SIMULATION PANEL

The simulation panel shows the forecast, specified by the user in the input panel. Figure **??** shows an example of a heave motion forecast for the CoG with a motion limit of 0.1 meter. The upper plot shows the wave elevation in the next 300 seconds. The middle plot show the motion forecast for 300 seconds. The lower plot shows the same motion forecast for 120 seconds in the future and the measured motion as a reference for the past 60 seconds (blue line). This lower plot gives the user confidence in making decisions based on the forecast (if forecast and measured motions are aligned).

C.1.2. MANAGEMENT

The Management object is the 'manager' of the data flows. Its tasks can be devided in three:

OBJECT CREATION

The Management object creates all other objects after it has been created by the GUI object and divides the users input. For objects to be able to communicate to each other (sent data from one object to another), 'handles' are made and passed on to each object.

STORE FORECAST

When a forecast is made by the Calculation object, it is stored by the Management object and marked with a time stamp. When a new forecast arrives, it is marked as 'most up to date' and displayed on the dashboard. It should be noted that since all wave components are known in the HSC and do not change during a simulation, a forecast does not change either. So an updated forecast shows the exact same motions, only further into the future.

MAKE PLOT

When displaying the wave- or motion forecast, an actual time trace moving in time is desirable. Unfortunately, matlab does not have a standard feature that enables to do so. To create a moving plot, a Timer object is created which gives a periodic signal, refreshing the data displayed. The more frequent this plotted data is refreshed, the more fluent the displayed signal.

Timer 1 Timer 1 is an object inside the Management object. It consist of a timer which refreshes the displayed plots periodically resulting in a fluent moving plot. The following specifics are hard coded in the matlab script:

C.1.3. CONNECT HSC

The Connect HSC object is only created when operating in the 'HSC mode'. When the 'Connect' button in the command panel is pushed, a pop-up dialog allows the user to chose an exercise to connect to (figure **??**). This can either be a simulation in the actual HSC or on a stand alone laptop running a K-Sim simulation. When the connection is successfully made, the wave components are downloaded and send to the Wave Data object where they are stored. Secondly a real-time connection is made to the vessel or object of interest in the simulation. Through this connection, the motions (6-Dof) are stored in a 'global variable' accessible for the Management object to plot as a reference for the forecast.

C.1.4. WAVE DATA

The Wave Data object is a 'dummy radar' which stores the wave components of a simulation. When operating in 'HSC' mode, these wave components are downloaded through the API by the Connect HSC object and sored in separate variables: Frequency, Amplitude, Phase and direction. When operating in 'Off-Line' mode, an excel file has to be submitted by the user in the 'File Selection' panel containing the wave components. To mimic an actual wave radar which has newer and more accurate data available when time passes, a timer is created sending the wave components periodically to the Calculation object to make a new forecast.

Timer 2 Timer 2 is an object inside the Wave Data object. It consist of a timer which sends wave components periodically to the calculation object to make a new forecast. To make a more realistic wave radar, noise can be added to the signal (turned off by default). The following specifics are hard coded in the matlab script:

C.1.5. CALCULATION

The Calculation object can either make a forecast of the heave-, roll-, pitch- or relative heave motion of a certain point. Depending on the user input, one of the above objects is created. Although for each motion a individual object exists, the objects are similar and will not be explained individual. During a simulation, a new data package sent from the Wave Data object arrives periodically. This data package contains the wave components. With these components, a forecast is made (chapter 4.

To align the forecast made and the simulation, the latest logging of the vessel motions in the global variable made by the HSC Connect object is accessed and the time is checked. This is necessary since time is elapsed since the whole cycle started. Now the actual time in the simulation is known, the forecast is time stamped and combined with the logged vessel motions into a 'forecast' package and sent to the Management object where it is stored ready to be plotted.

C.1.6. LOAD RAO

The Load RAO object stores the LiftDyn file uploaded by the user in the 'File Input' panel. This file contains the RAO's needed to make a forecast. The object opens the file and extracts the RAO that is needed (Heave, Roll, Pitch). The LiftDyn file only contains the RAO's for a certain amount of wave directions and frequencies. To align these directions and frequencies with the ones present in the simulation, data points are linear interpolated. When completed, the RAO is ready for use and sent to the Calculation object where it is stored.

D

THE MODEL

D.1. TEST BARGE

	Heading [deg]	Mooring [-]	Duration [min]	Object [-]	Wamit [-]
Test Barge	0	Turret (3.2.1)	60	03000 H400 V01	TestH400 linDamp

Table D.1: Summary simulation specifics K-Sim

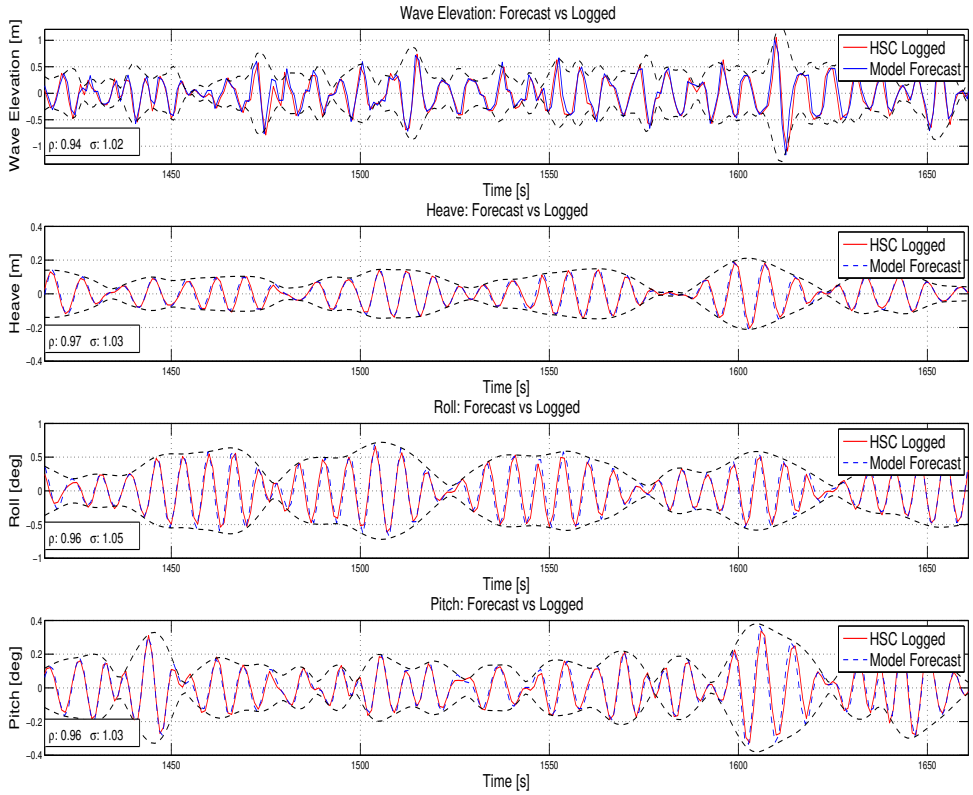

Figure D.1: Time trace of Test Barge, in head waves (0 deg)

D.2. VERIFICATION DEFAULT THIALF

	Heading [deg]	Mooring [-]	Duration [min]	Object [-]	Wamit [-]
Default Thialf	0	Net API (3.2.1)	60	1500333 V01	Thialf 26m6 WDinf

Table D.2: Summary simulation specifics K-Sim

D.2.1. MILD SEA-STATE

	Spectrum [-]	Hs [m]	Tp [sec]	$HsTp^2$ [ms^2]	Heading [deg]	Spreading [-]
Sea-State	JONSWAP	1.5	7	73.5	0:45:180	cos2

Table D.3: Mild sea-state used for verification model

WAVE HEADING: 0 DEG

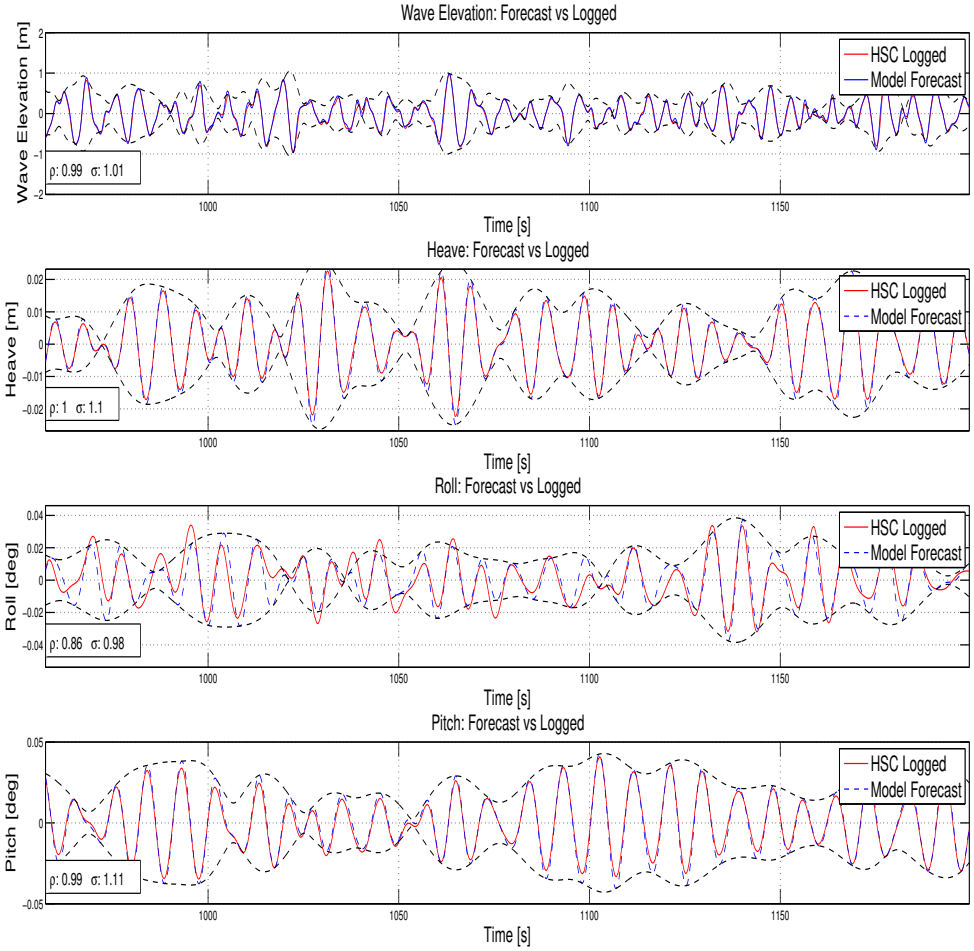

Figure D.2: Time trace verification mild sea-state, wave heading: 0 deg.

	Correlation Coefficient [-]	dT Shift [sec]	RMS Ratio [-]	Standard Deviation [*]
Wave Elevation	0.99	0.08	1.01	0.34[m]
Heave	1.00	1.18	1.10	0.01[m]
Roll	0.86	1.14	0.98	0.01[deg]
Pitch	0.99	1.23	1.11	0.02[deg]

Table D.4: Summary verification mild sea-state, wave heading: 0 deg.

WAVE HEADING: 45 DEG

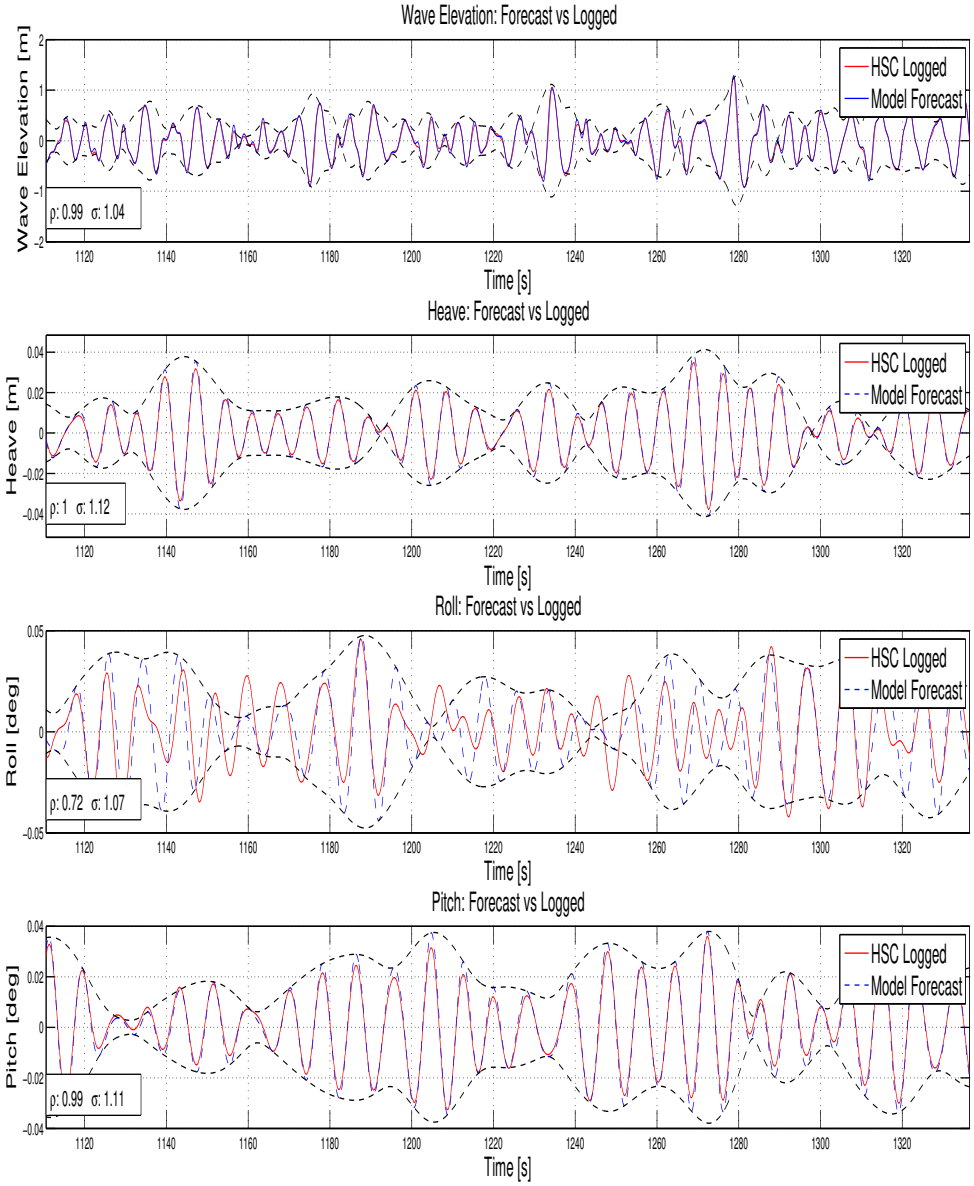

Figure D.3: Time trace verification mild sea-state, wave heading: 45 deg.

	Correlation Coefficient [-]	dT Shift [sec]	RMS Ratio [-]	Standard Deviation [*]
Wave Elevation	0.99	0.09	1.04	0.34[m]
Heave	1.00	1.17	1.12	0.01[m]
Roll	0.72	1.36	1.07	0.02[deg]
Pitch	0.99	1.20	1.11	0.02[deg]

Table D.5: Summary verification mild sea-state, wave heading: 45 deg.

WAVE HEADING: 90 DEG

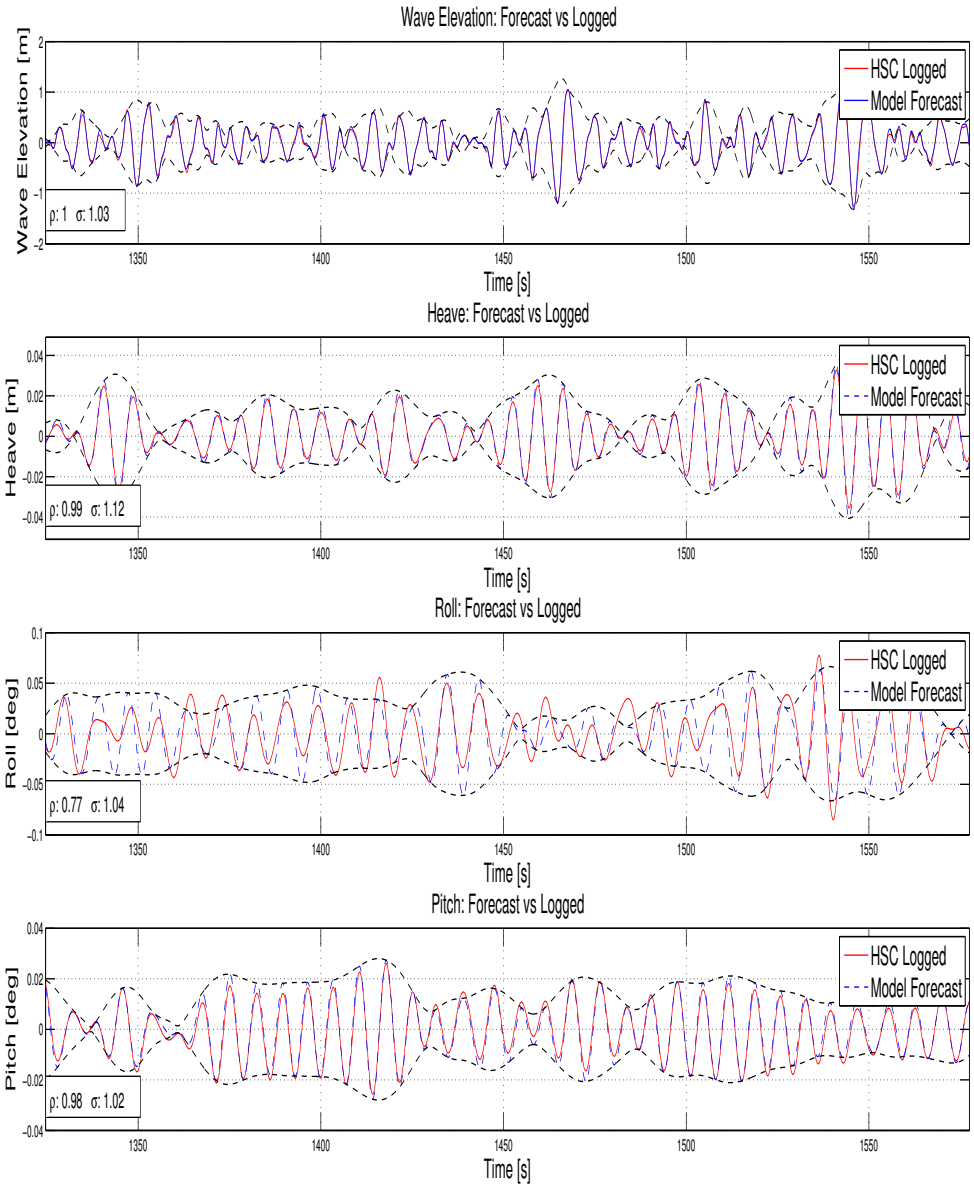

Figure D.4: Time trace verification mild sea-state, wave heading: 90 deg.

	Correlation Coefficient [-]	dT Shift [sec]	RMS Ratio [-]	Standard Deviation [*]
Wave Elevation	1.00	0.03	1.03	0.38[m]
Heave	0.99	1.23	1.12	0.01[m]
Roll	0.77	1.33	1.04	0.03[deg]
Pitch	0.98	1.21	1.02	0.01[deg]

Table D.6: Summary verification mild sea-state, wave heading: 90 deg.

WAVE HEADING: 135 DEG

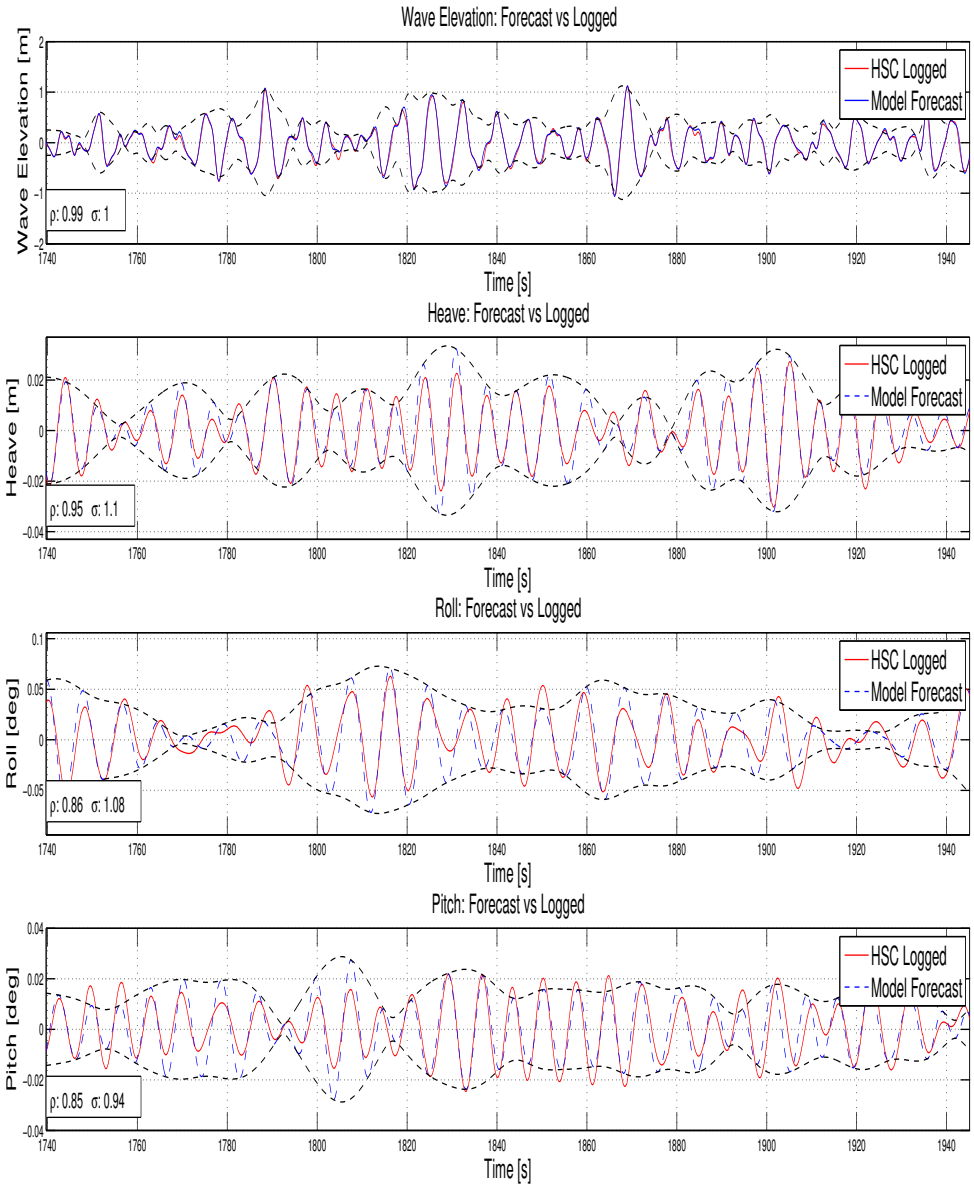

Figure D.5: Time trace verification mild sea-state, wave heading: 135 deg.

	Correlation Coefficient [-]	dT Shift [sec]	RMS Ratio [-]	Standard Deviation [*]
Wave Elevation	0.99	-0.01	1.00	0.34[m]
Heave	0.95	1.06	1.10	0.01[m]
Roll	0.86	1.30	1.08	0.03[deg]
Pitch	0.85	1.23	0.94	0.01[deg]

Table D.7: Summary verification mild sea-state, wave heading: 135 deg.

WAVE HEADING: 180 DEG

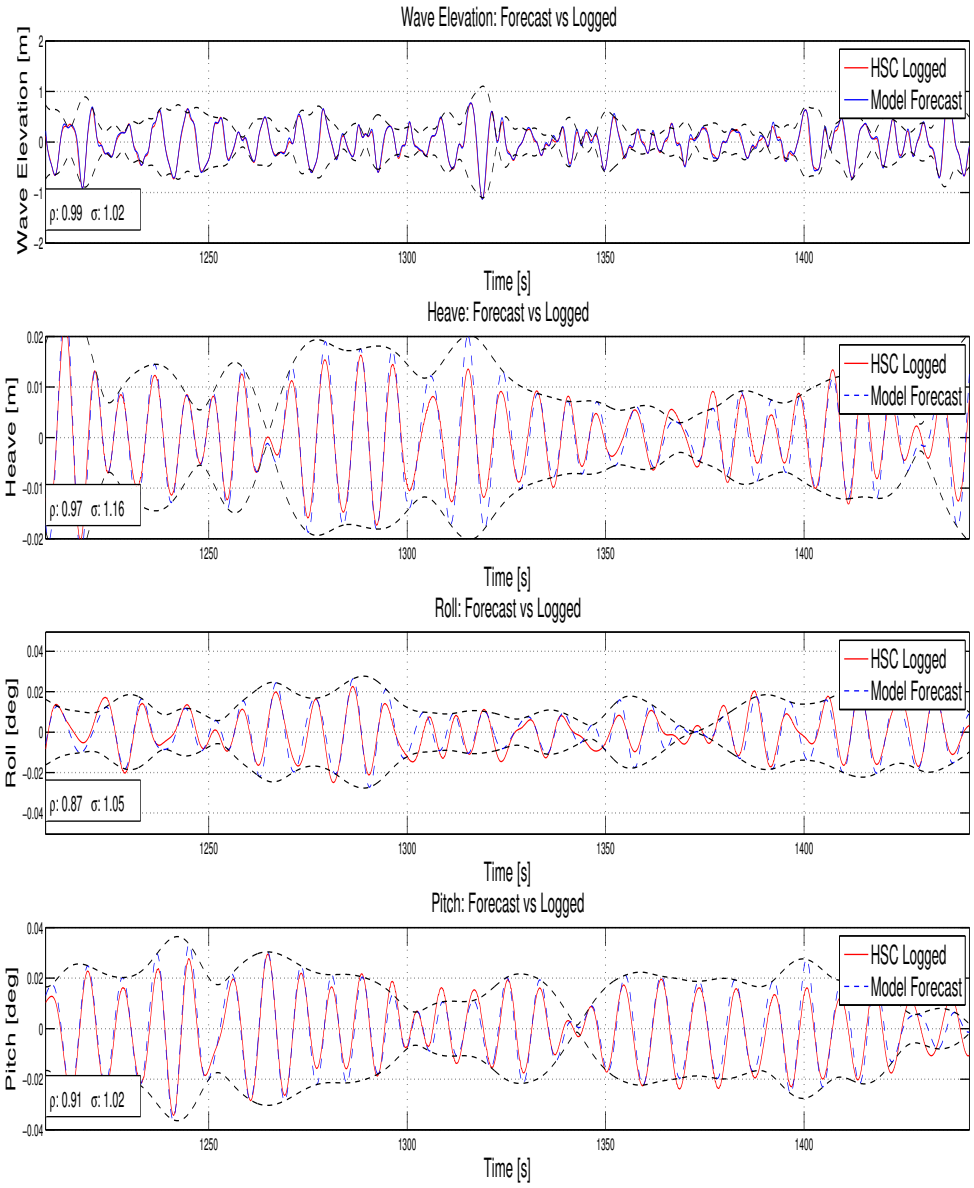

Figure D.6: Time trace verification mild sea-state, wave heading: 180 deg.

	Correlation Coefficient [-]	dT Shift [sec]	RMS Ratio [-]	Standard Deviation [*]
Wave Elevation	0.99	-0.01	1.02	0.36[m]
Heave	0.97	1.20	1.16	0.01[m]
Roll	0.87	1.15	1.05	0.01[deg]
Pitch	0.91	1.28	1.02	0.01[deg]

Table D.8: Summary verification mild sea-state, wave heading: 180 deg.

D.2.2. MODERATE SEA-STATE

	Spectrum [-]	Hs [m]	Tp [sec]	$HsTp^2$ [ms^2]	Heading [deg]	Spreading [-]
Sea-State	JONSWAP	5	10	500	0:45:135	cos2

Table D.9: Moderate sea-state used for verification model

WAVE HEADING: 0 DEG

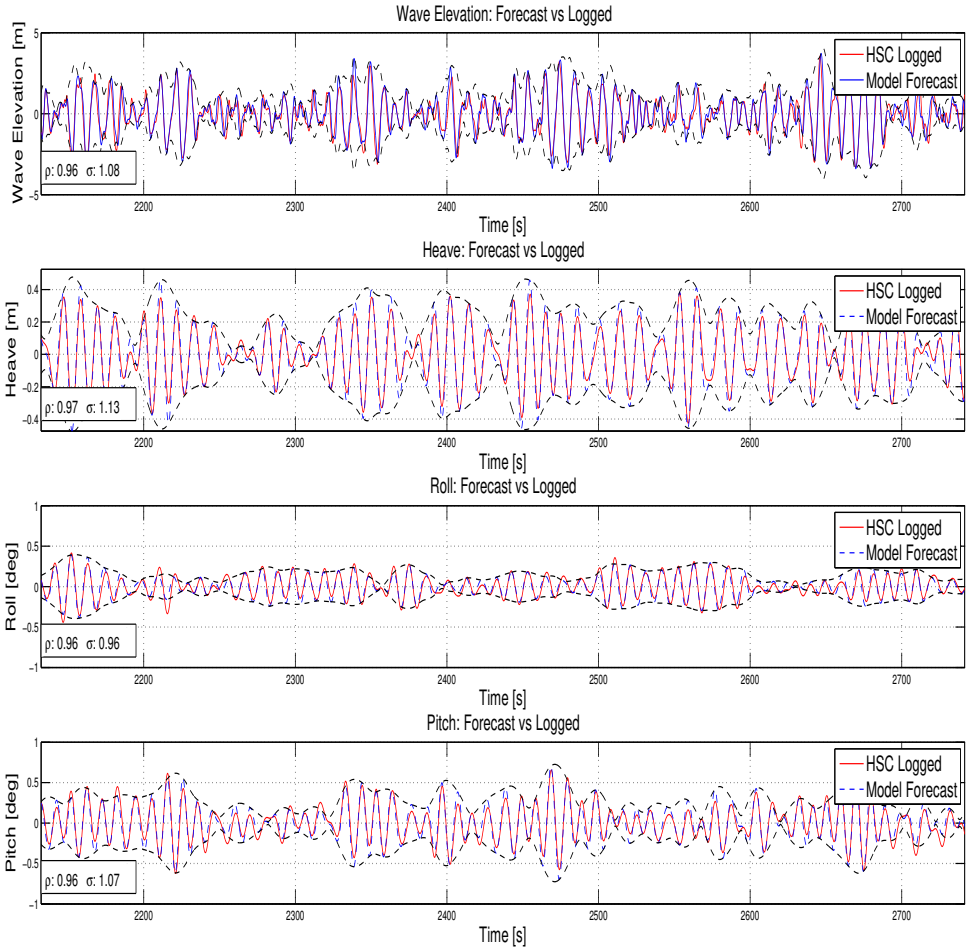

Figure D.7: Time trace verification moderate sea-state, wave heading: 0 deg.

	Correlation Coefficient [-]	dT Shift [sec]	RMS Ratio [-]	Standard Deviation [*]
Wave Elevation	0.96	-0.25	1.08	1.24[m]
Heave	0.97	1.19	1.13	0.18[m]
Roll	0.96	1.35	0.96	0.14[deg]
Pitch	0.96	1.21	1.07	0.24[deg]

Table D.10: Summary verification moderate sea-state, wave heading: 0 deg.

WAVE HEADING: 45 DEG

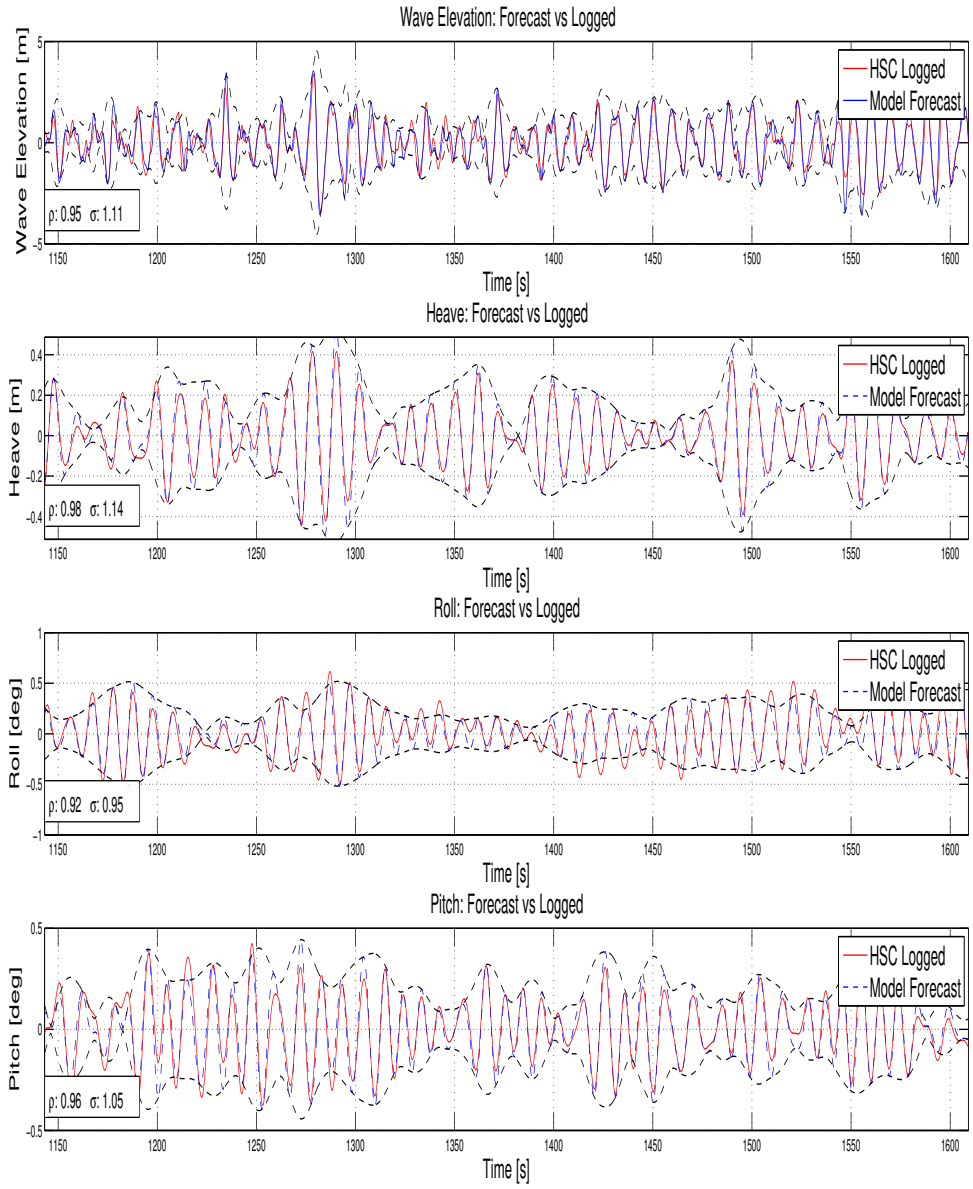

Figure D.8: Time trace verification moderate sea-state, wave heading: 45 deg.

	Correlation Coefficient [-]	dT Shift [sec]	RMS Ratio [-]	Standard Deviation [*]
Wave Elevation	0.95	-0.17	1.11	1.26[m]
Heave	0.98	0.99	1.14	0.17[m]
Roll	0.92	1.15	0.95	0.20[deg]
Pitch	0.96	0.96	1.05	0.20[deg]

Table D.11: Summary verification moderate sea-state, wave heading: 45 deg.

WAVE HEADING: 90 DEG

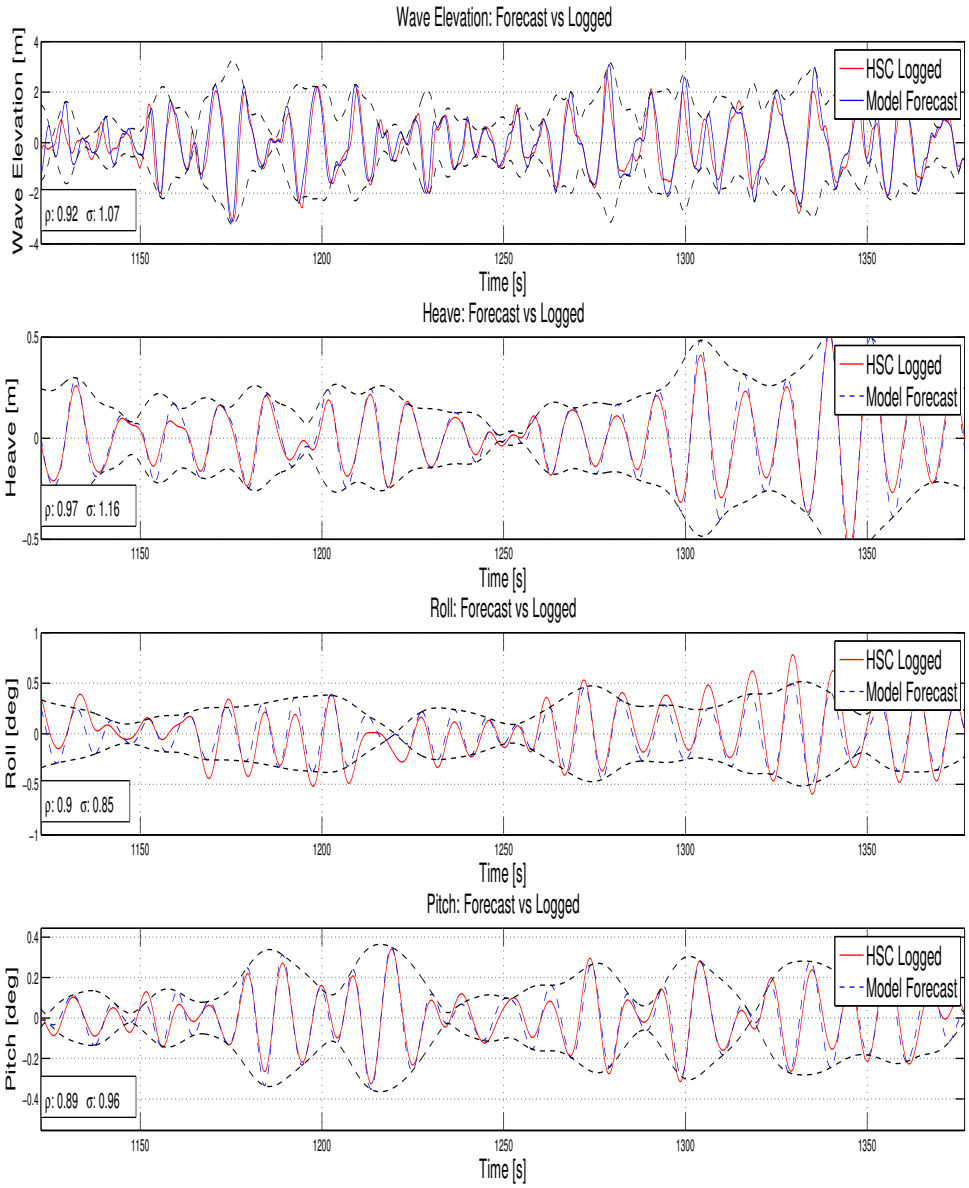

Figure D.9: Time trace verification moderate sea-state, wave heading: 90 deg.

	Correlation Coefficient [-]	dT Shift [sec]	RMS Ratio [-]	Standard Deviation [*]
Wave Elevation	0.92	-0.56	1.07	1.19[m]
Heave	0.97	1.33	1.16	0.18[m]
Roll	0.90	1.31	0.85	0.26[deg]
Pitch	0.89	1.31	0.96	0.13[deg]

Table D.12: Summary verification moderate sea-state, wave heading: 90 deg.

WAVE HEADING: 135 DEG

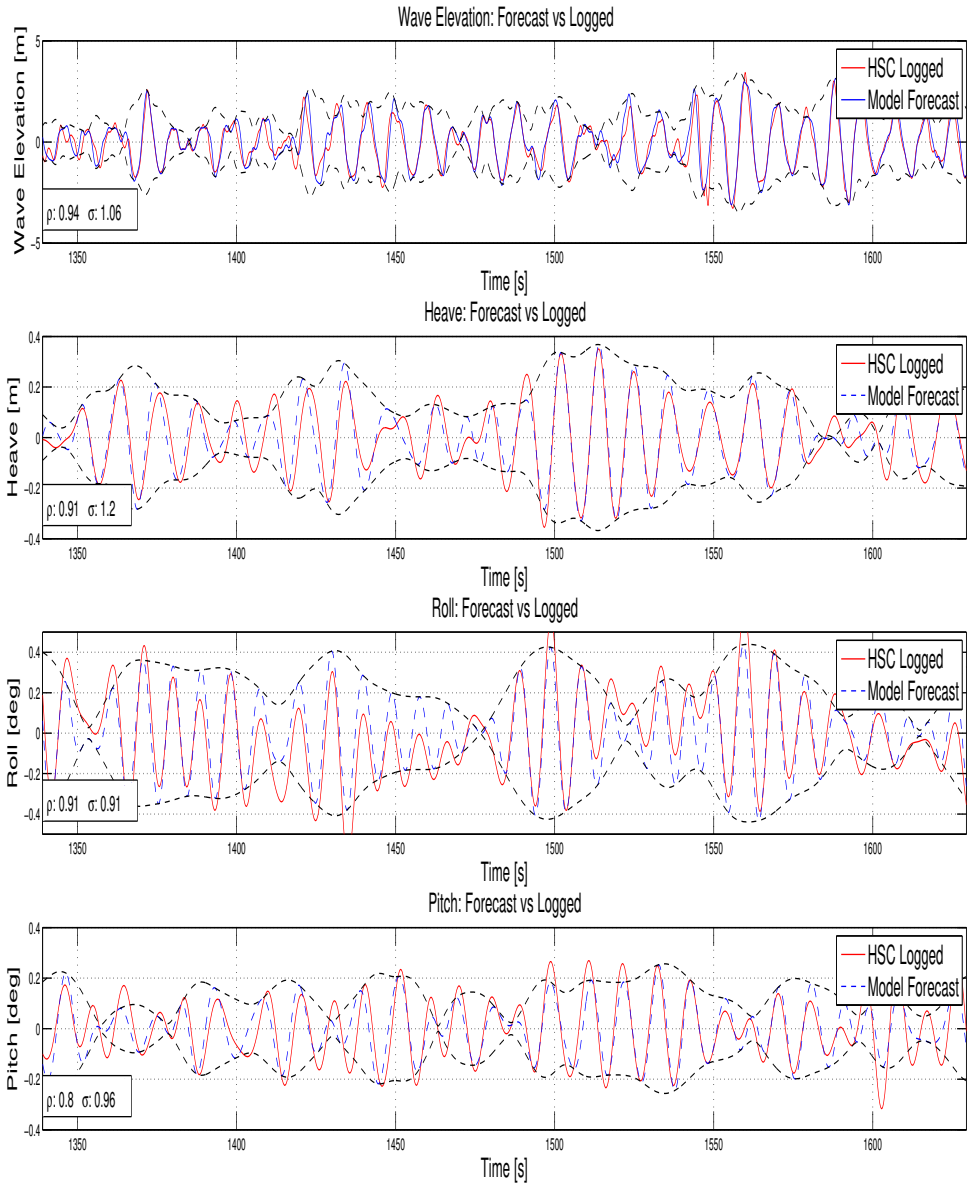

Figure D.10: Time trace verification moderate sea-state, wave heading: 135 deg.

	Correlation Coefficient [-]	dT Shift [sec]	RMS Ratio [-]	Standard Deviation [*]
Wave Elevation	0.94	0.14	1.06	1.23[m]
Heave	0.91	1.34	1.20	0.18[m]
Roll	0.91	1.36	0.91	0.25[deg]
Pitch	0.80	1.38	0.96	0.13[deg]

Table D.13: Summary verification moderate sea-state, wave heading: 135 deg.

D.2.3. COMPLEX SEA-STATE

	Spectrum [-]	Hs [m]	Tp [sec]	$HsTp^2$ [ms^2]	Rel. Heading [deg]	Spreading [-]
Sea-State	Torsethaugen	1.5	86	88	315	cos2

Table D.14: Complex sea-state used for verification model

WAVE HEADING: 315 DEG

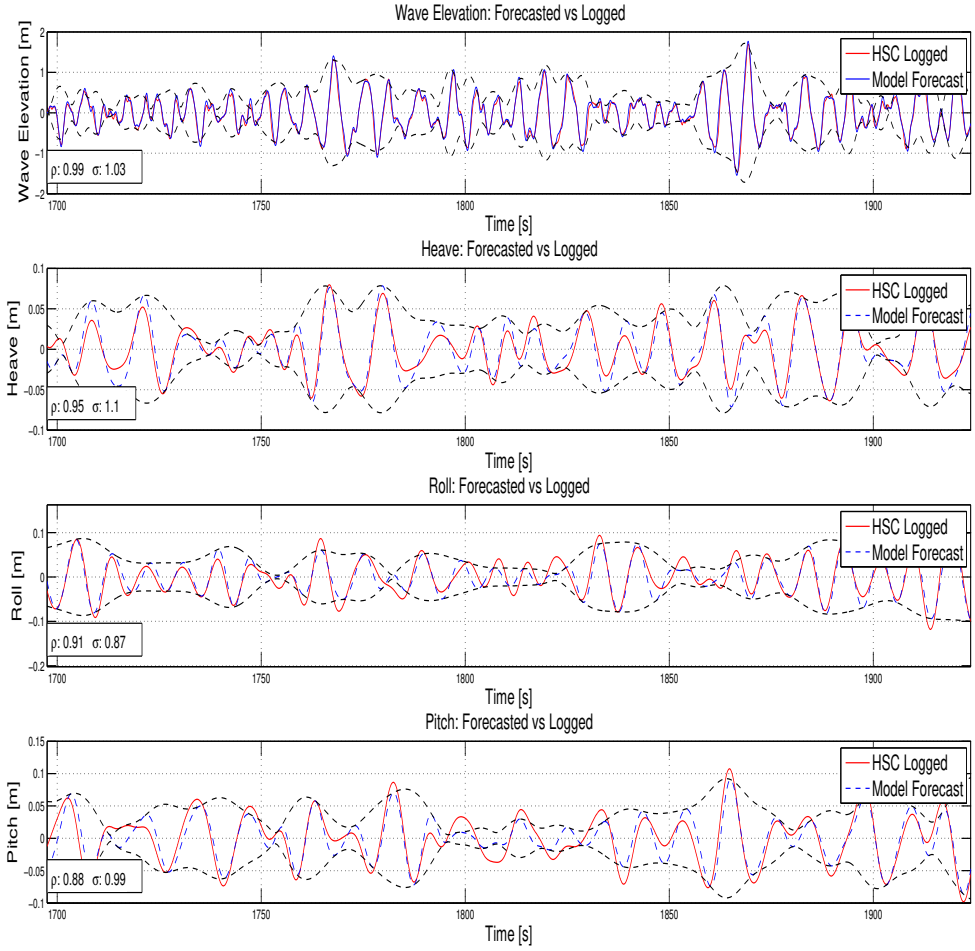

Figure D.11: Time trace verification complex sea-state, wave heading: 315 deg.

	Correlation Coefficient [-]	dT Shift [sec]	RMS Ratio [-]	Standard Deviation [*]
Wave Elevation	0.99	-0.01	1.03	0.48[m]
Heave	0.95	1.44	1.10	0.05[m]
Roll	0.91	1.43	0.87	0.05[deg]
Pitch	0.88	1.54	0.99	0.04[deg]

Table D.15: Summary verification moderate sea-state, wave heading: 315 deg.

D.3. SENSITIVITY ANALYSES

D.3.1. MILD SEA-STATE

	Spectrum [-]	Hs [m]	Tp [sec]	HsTp^2 [ms^2]	Heading [deg]	Spreading [-]
Sea-State	JONSWAP	1.5	7	73.5	0,90	cos2

Table D.16: Mild sea-state used for sensitivity analyses

COG: VERTICAL (Z) COORDINATE + 2M

0 deg	Correlation Coefficient [-]	dT Shift [sec]	RMS Ratio [-]	Standard Deviation [*]
Wave Elevation	0.99 (0.99)	-	-	-
Heave	0.98 (1)	1.2	1.02 (1.1)	0.01[m]
Roll	0.86 (0.86)	1.6	1.00 (0.98)	0.01[deg]
Pitch	0.99 (0.99)	1.22	1.14 (1.11)	0.02[deg]

Table D.17: Summary sensitivity analyses mild sea-state, Z-coordinate CoG deviated from original value with 2m, wave heading: 0 deg.

90 deg	Correlation Coefficient [-]	dT Shift [sec]	RMS Ratio [-]	Standard Deviation [*]
Wave Elevation	0.99 (1.00)	-	-	-
Heave	0.99 (0.99)	1.28	1.12 (1.12)	0.01[m]
Roll	0.77 (0.77)	1.36	1.05 (1.04)	0.03[deg]
Pitch	0.99 (0.98)	1.24	1.06 (1.02)	0.01[deg]

Table D.18: Summary sensitivity analyses mild sea-state, Z-coordinate CoG deviated from original value with 2m, wave heading: 90 deg.

RADII OF GYRATION: LONGITUDINAL (RXX) COORDINATE + 2M

0deg	Correlation Coefficient [-]	dT Shift [sec]	RMS Ratio [-]	Standard Deviation [*]
Wave Elevation	0.99 (0.99)	-	-	-
Heave	0.98 (1)	1.2	1.00 (1.1)	0.01 [m]
Roll	0.86 (0.86)	1.14	1.01 (0.98)	0.01 [deg]
Pitch	0.99 (0.99)	1.22	1.07 (1.11)	0.02 [deg]

Table D.19: Summary sensitivity analyses mild sea-state, Rxx-coordinate (radii of gyration) deviated from original value with 2m, wave heading: 0 deg.

90 deg	Correlation Coefficient [-]	dT Shift [sec]	RMS Ratio [-]	Standard Deviation [*]
Wave Elevation	0.99 (1.00)	-	-	-
Heave	0.99 (0.99)	1.28	1.12 (1.12)	0.01[m]
Roll	0.77 (0.77)	1.34	0.97 (1.04)	0.02[deg]
Pitch	0.98 (0.98)	1.24	1.07 (1.02)	0.01 [deg]

Table D.20: Summary sensitivity analyses mild sea-state, Rxx-coordinate (radii of gyration) deviated from original value with 2m, wave heading: 90 deg.

RADII OF GYRATION: TRANSVERSAL (RYY) COORDINATE + 2M

0 deg	Correlation Coefficient [-]	dT Shift [sec]	RMS Ratio [-]	Standard Deviation [*]
Wave Elevation	0.99 (0.99)	-	-	-
Heave	0.98 (1.00)	1.2	1.00 (1.10)	0.01[m]
Roll	0.86 (0.86)	1.14	1.01 (0.98)	0.01[deg]
Pitch	0.99 (0.99)	1.2	1.07 (1.11)	0.02[deg]

Table D.21: Summary sensitivity analyses mild sea-state, Ryy-coordinate (radii of gyration) deviated from original value with 2m, wave heading: 0 deg.

90 deg	Correlation Coefficient [-]	dT Shift [sec]	RMS Ratio [-]	Standard Deviation [*]
Wave Elevation	0.99 (1.00)	-	-	-
Heave	0.99 (0.99)	1.28	1.12 (1.12)	0,01[m]
Roll	0.77 (0.77)	1.36	1.05 (1.04)	0.03[deg]
Pitch	0.98 (0.98)	1.24	1.00 (1.02)	0.01[deg]

Table D.22: Summary sensitivity analyses mild sea-state, Ryy-coordinate (radii of gyration) deviated from original value with 2m, wave heading: 90 deg.

SIMULTANEOUS: Z+2M RXX+2M RYY+2M

0 deg	Correlation Coefficient [-]	dT Shift [sec]	RMS Ratio [-]	Standard Deviation [*]
Wave Elevation	0.99 (0.99)	-	-	-
Heave	0.98 (1.00)	1.2	1.01 (1.10)	0.01[m]
Roll	0.87 (0.86)	1.14	0.93 (0.98)	0.01[deg]
Pitch	0.99 (0.99)	1.22	1.04 (1.11)	0.02[deg]

Table D.23: Summary sensitivity analyses mild sea-state, Z-coordinate CoG and Rxx,Ryy-coordinate (radii of gyration) deviated from original value with 2m simultaneously, wave heading: 0 deg.

90 deg	Correlation Coefficient [-]	dT Shift [sec]	RMS Ratio [-]	Standard Deviation [*]
Wave Elevation	0.99 (1.00)	-	-	-
Heave	0.99 (0.99)	1.28	1.12 (1.12)	0.01[m]
Roll	0.84 (0.77)	1.32	0.77 (1.04)	0.02[deg]
Pitch	0.98 (0.98)	1.24	1.89 (1.02)	0.01[deg]

Table D.24: Summary sensitivity analyses mild sea-state, Z-coordinate CoG and Rxx,Ryy-coordinate (radii of gyration) deviated from original value with 2m simultaneously, wave heading: 90 deg.

D.3.2. MODERATE SEA-STATE

	Spectrum [-]	Hs [m]	Tp [sec]	$HsTp^2$ [ms^2]	Heading [deg]	Spreading [-]
Sea-State	JONSWAP	5	10	500	0, 90	cos2

Table D.25: Moderate sea-state used for sensitivity analyses, Z-coordinate CoG and Rxx,Ryy-coordinate (radii of gyration) deviated from original value with 2m simultaneously, wave heading: 90

SIMULTANEOUS: Z+2M RXX+2M RYY+2M

0 deg	Correlation Coefficient [-]	dT Shift [sec]	RMS Ratio [-]	Standard Deviation [*]
Wave Elevation	0.96 (0.96)	-	-	-
Heave	0.99 (0.97)	1.18	1.13 (1.13)	0.18[m]
Roll	0.96 (0.96)	1.31	0.77 (0.96)	0.11[deg]
Pitch	0.98 (0.96)	1.15	0.81 (1.07)	0.19[deg]

Table D.26: Summary sensitivity analyses moderate sea-state, Z-coordinate CoG and Rxx,Ryy-coordinate (radii of gyration) deviated from original value with 2m simultaneously, wave heading: 0 deg.

90 deg	Correlation Coefficient [-]	dT Shift [sec]	RMS Ratio [-]	Standard Deviation [*]
Wave Elevation	0.93 (0.92)	-	-	-
Heave	0.99 (0.97)	1.17	1.20 (1.16)	0.19[m]
Roll	0.92 (0.90)	1.33	0.71 (0.85)	0.21[deg]
Pitch	0.95 (0.89)	1.13	0.75 (0.96)	0.1[deg]

Table D.27: Summary sensitivity analyses moderate sea-state, Z-coordinate CoG and Rxx,Ryy-coordinate (radii of gyration) deviated from original value with 2m simultaneously, wave heading: 90 deg.

SIMULTANEOUS: Z+5M RXX+5M RYY+5M

0 deg	Correlation Coefficient [-]	dT Shift [sec]	RMS Ratio [-]	Standard Deviation [*]
Wave Elevation	0.96 (0.96)	-	-	-
Heave	0.99 (0.97)	1.15	1.13 (1.13)	0.18[m]
Roll	0.96 (0.96)	1.31	0.78 (0.96)	0.11[deg]
Pitch	0.98 (0.96)	1.18	0.81 (1.07)	0.19[deg]

Table D.28: Summary sensitivity analyses moderate sea-state, Z-coordinate CoG and Rxx,Ryy-coordinate (radii of gyration) deviated from original value with 5m simultaneously, wave heading: 0 deg.

90 deg	Correlation Coefficient [-]	dT Shift [sec]	RMS Ratio [-]	Standard Deviation [*]
Wave Elevation	0.93 (0.92)	-	-	-
Heave	0.99 (0.97)	1.28	1.2 (1.16)	0.19[m]
Roll	0.92 (0.90)	1.33	0.71 (0.85)	0.21[deg]
Pitch	0.95 (0.89)	1.16	0.75 (0.96)	0.1[deg]

Table D.29: Summary sensitivity analyses moderate sea-state, Z-coordinate CoG and Rxx,Ryy-coordinate (radii of gyration) deviated from original value with 5m simultaneously, wave heading: 90 deg.

E

Test Case Results

E.1. Skarfjell

	Heading [deg]	Draft [m]	Mooring [-]	Object [-]	Wamit [-]
Skarfjell	0	26.6	Net API (3.2.1)	1500333 V01	Thialf 26m6 WDinf

Table E.1: Summary simulation specifics K-Sim

Environment

	Spectrum	Hs [m]	Tp [sec]	HsTp^2 [ms^2]	Rel. Heading [deg]	Spreading [???]
Sea-State	JONSWAP 1	1.7	6	61.2	315	cos2
	JONSWAP 2	1.1	10.3	116.7	315	cos2

Table E.2: Sea-state used in Skarfjell test case

LiftDyn model input

	CoG [x,y,z] [m]	Radii of gyration [x,y,z] [m]	Local Origin [x,y,z]	Set down point [x,y,z] [m]
Platform Skarfjell	[0,0,27.6]	[37.1,39.7,42.4]	[0,0,-21]	[38.26,-18.47,50.54]

Table E.3: Summary of input LiftDyn Skarfjell, Thialf, local origin is w.r.t. global origin, set down point defined in local coordinates.

	Trim/Heel [deg]	CoG [x,y,z] [m]	Radii of gyration [x,y,z] [m]	Local Origin [x,y,z]
Thialf Skarfjell	[redacted]	[redacted]	[redacted]	[redacted]

Table E.4: Summary of input LiftDyn Skarfjell, Thialf, local origin is w.r.t. global origin.

	Slew [deg]	Radius [m]	Hookload [mT]	Hook Height [m]
PS Crane Skarfjell	45	52	7	108.2
SB Crane Skarfjell	180	68.5	1067	95.2

Table E.5: Summary of input LiftDyn Skarfjell, Cranes

E.1.1. RIGGING MODES SKARFJELL MODULE

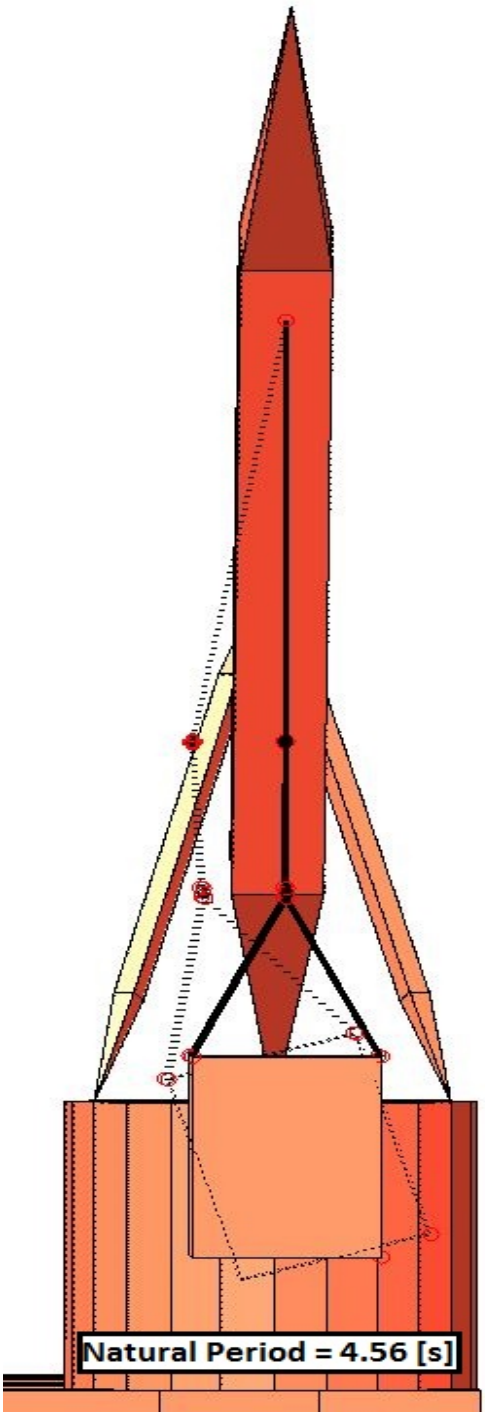

Figure E.1: Example of mode in which module can move w.r.t. rigging. Crane slewed 180 deg, view from astern.

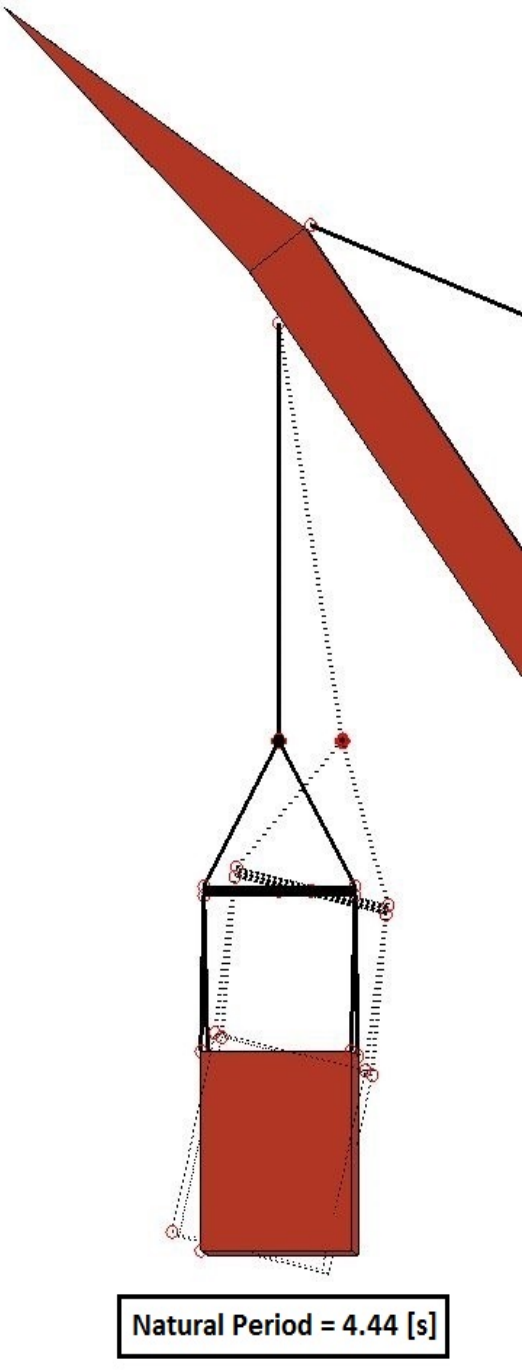

Figure E.2: Example of mode in which module can move w.r.t. rigging. Crane slewed 180 deg, view from SB.

Note: There are several other modes in which the module could move w.r.t. its rigging, all with smaller natural periods.

EFFECT TUGGER ON MODULE

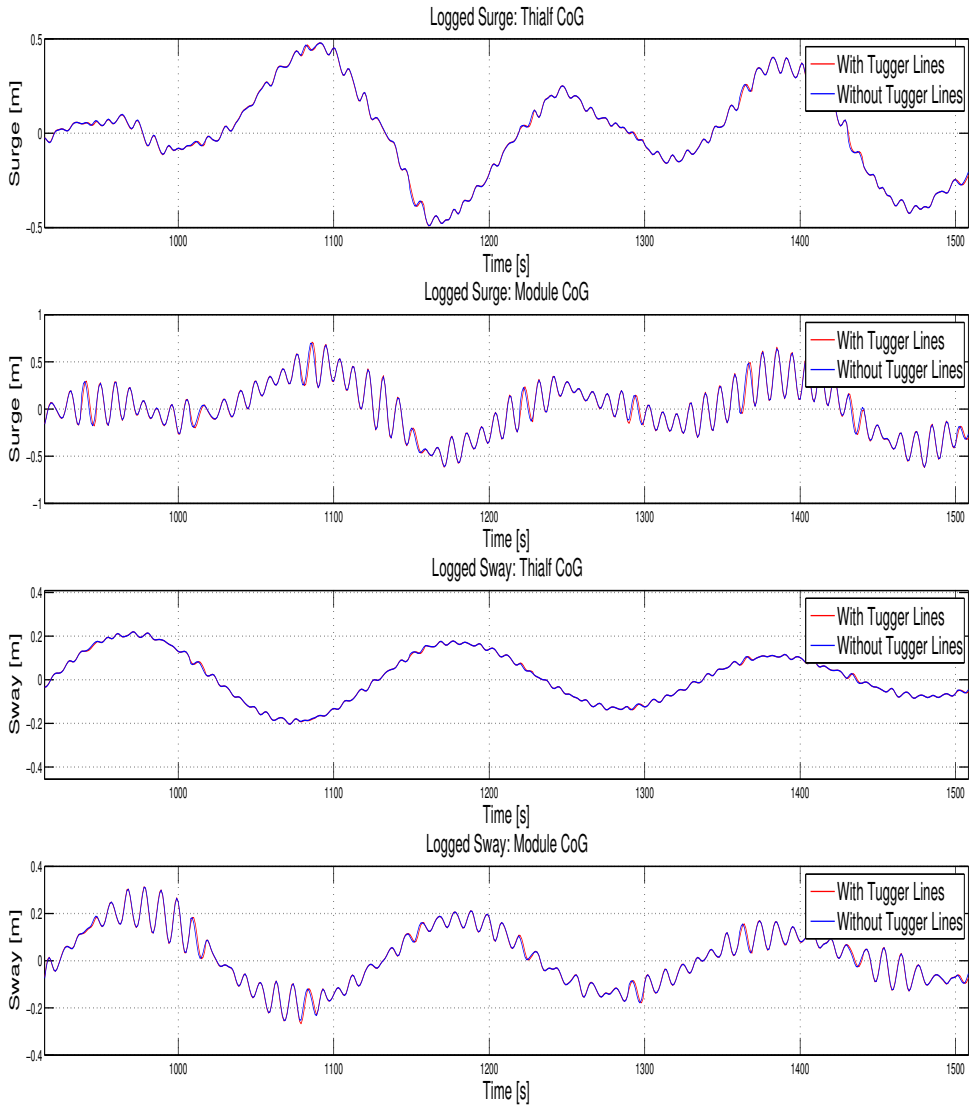

Figure E.3: Effect of tugger lines on Surge and Sway of Skarfjell module CoG, complex sea-state, wave heading: 315 deg.

Note: For the simulation run without tugger-lines, the stiffness of the module is tuned with the API preventing it from yawing. This has clearly no further effect on the motions of the module.

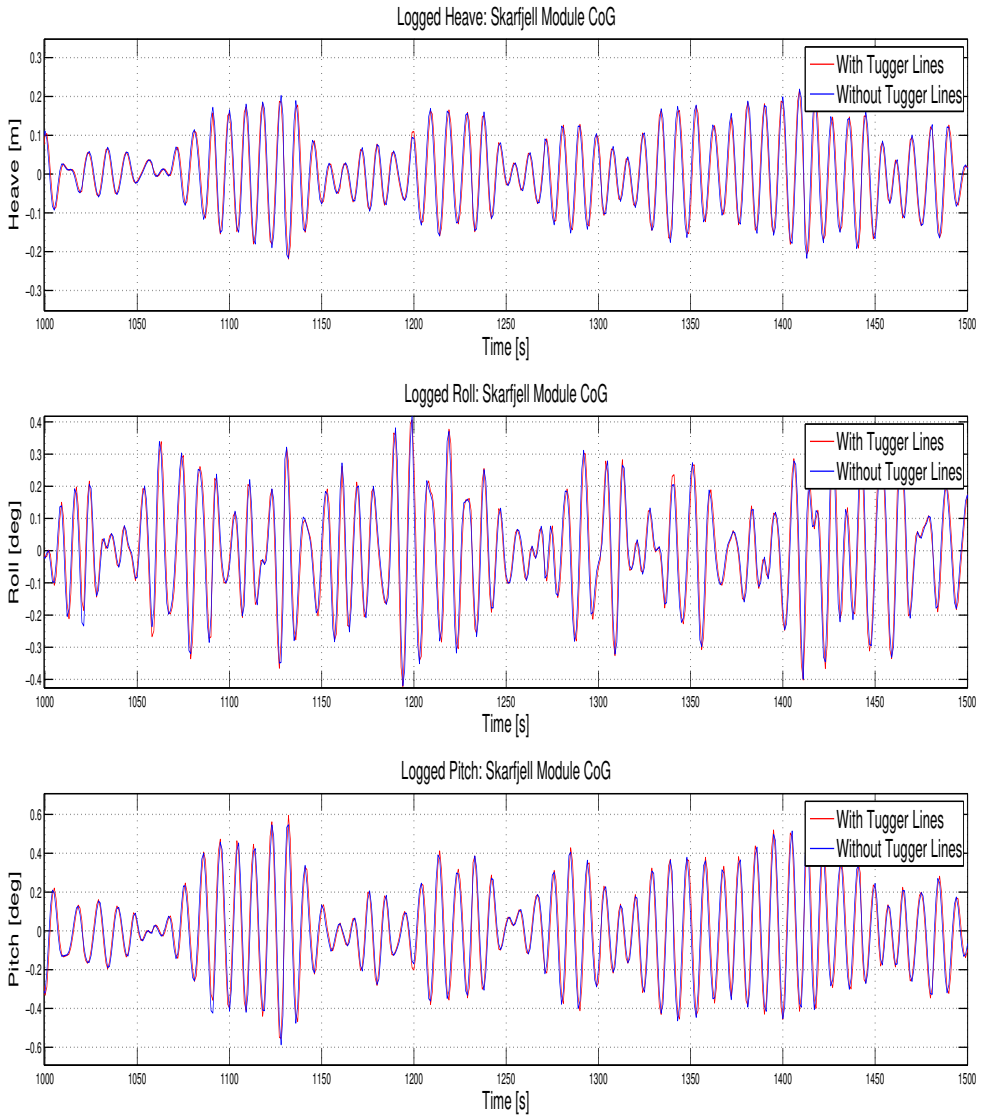

Figure E.4: Effect of tugger lines on Heave Roll and Pitch motion, Skarfjell module CoG, complex sea-state, wave heading: 315 deg.

Note: For the simulation run without tugger-lines, the stiffness of the module is tuned with the API preventing it from yawing. This has clearly no further effect on the motions of the module.

GJOA PLATFORM COG

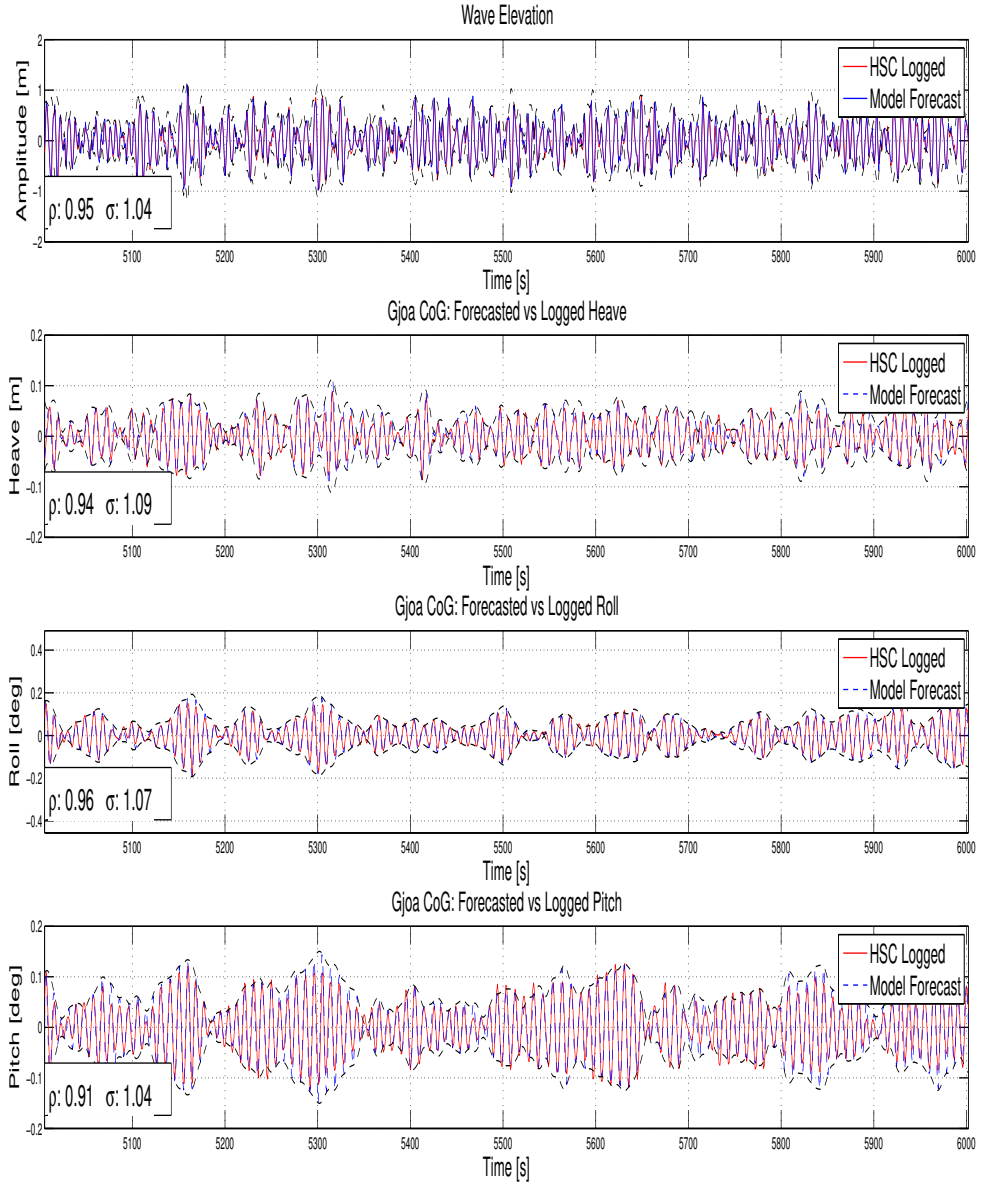

Figure E.5: Time trace test case Skarfjell, Gjoa Platform CoG, complex sea-state, wave heading: 315 deg.

	Correlation Coefficient [-]	dT Shift [sec]	RMS Ratio [-]	Standard Deviation [*]
Wave Elevation	0.95	-0.54	1.04	0.37 [m]
Heave	0.94	1.44	1.09	0.04 [m]
Roll	0.96	1.43	1.07	0.06 [deg]
Pitch	0.95	1.54	1.04	0.05 [deg]

Table E.6: Summary test case Skarfjell, Gjoa CoG, wave heading: 315 deg.

GJOA PLATFORM SET-DOWN POINT

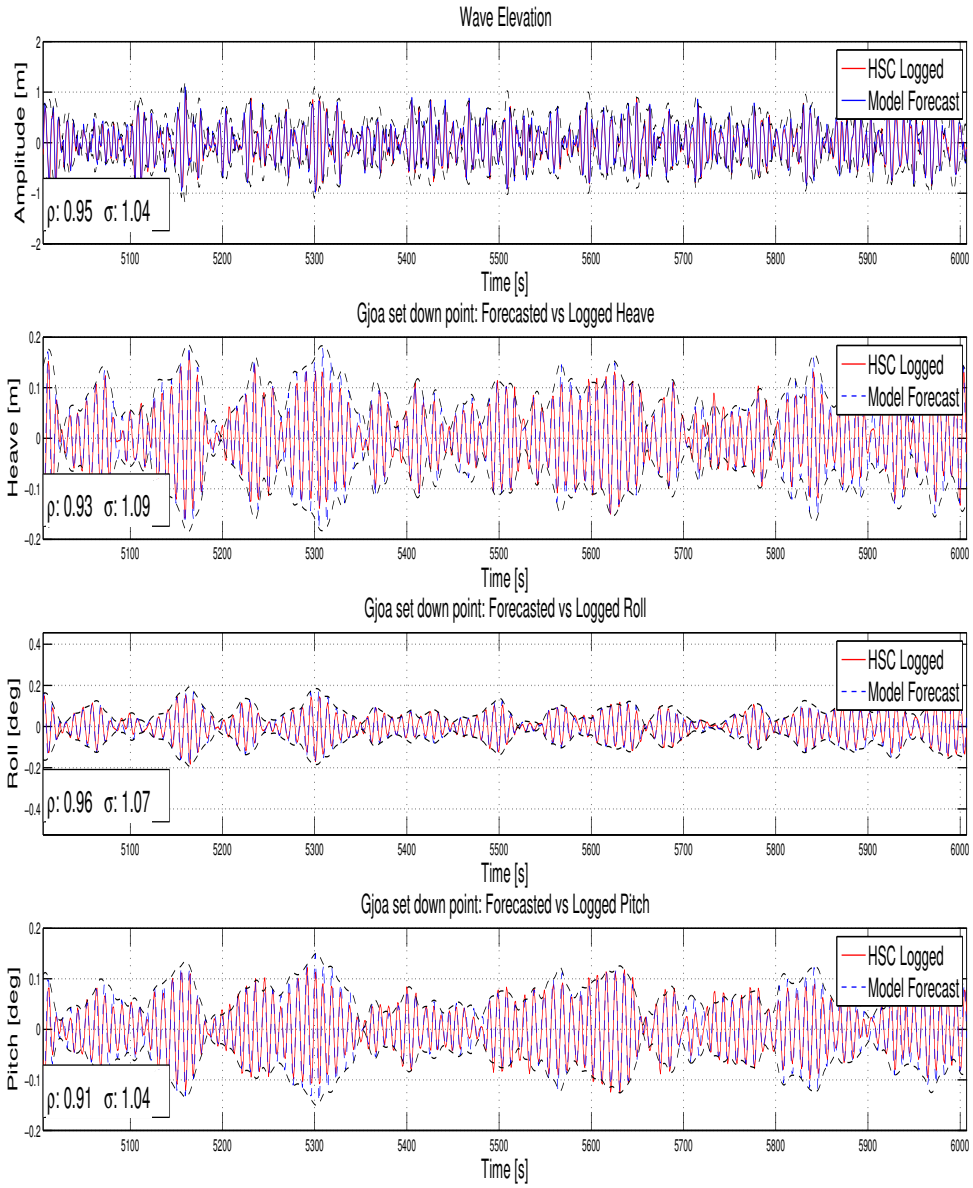

Figure E.6: Time trace test case Skarfjell, Gjoa set down point, complex sea-state, wave heading: 315 deg.

	Correlation Coefficient [-]	dT Shift [sec]	RMS Ratio [-]	Standard Deviation [*]
Wave Elevation	0.95	-0.54	1.04	0.37[m]
Heave	0.93	1.54	1.09	0.07[m]
Roll	0.96	1.51	1.07	0.06[deg]
Pitch	0.91	1.59	1.04	0.05[deg]

Table E.7: Summary test case Skarfjell, Gjoa set down point, wave heading: 315 deg.

THIALF COG

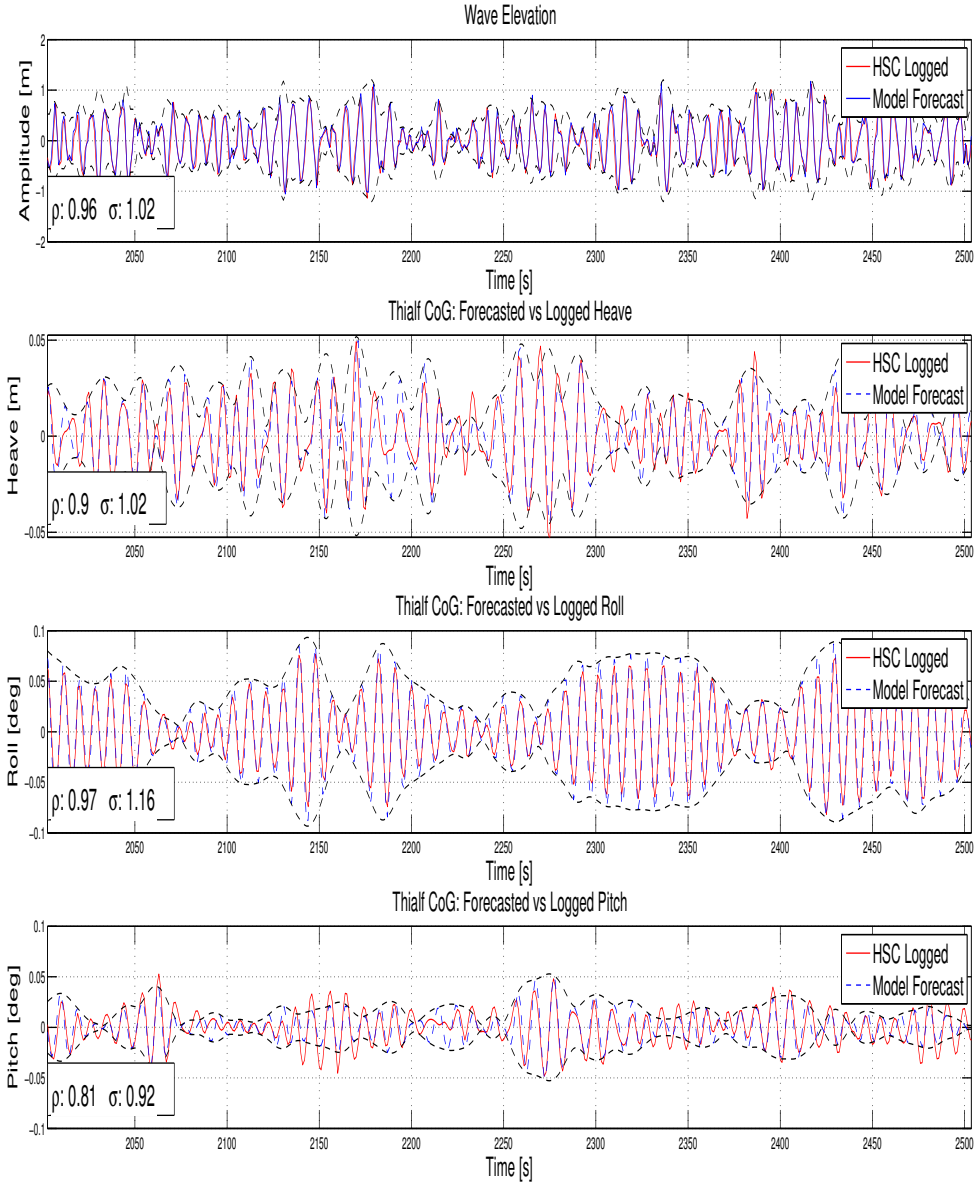

Figure E.7: Time trace test case Skarfjell, Thialf CoG, complex sea-state, wave heading: 315 deg.

	Correlation Coefficient [-]	dT Shift [sec]	RMS Ratio [-]	Standard Deviation [*]
Wave Elevation	0.95	-0.46	1.04[m]	0.44[m]
Heave	0.90	1.09	1.02	0.02[m]
Roll	0.97	0.94	1.17	0.04[deg]
Pitch	0.81	0.96	0.92	0.02[deg]

Table E.8: Summary test case Skarfjell, Thialf CoG, wave heading: 315 deg.

THIALF SKARFJELL MODULE COG

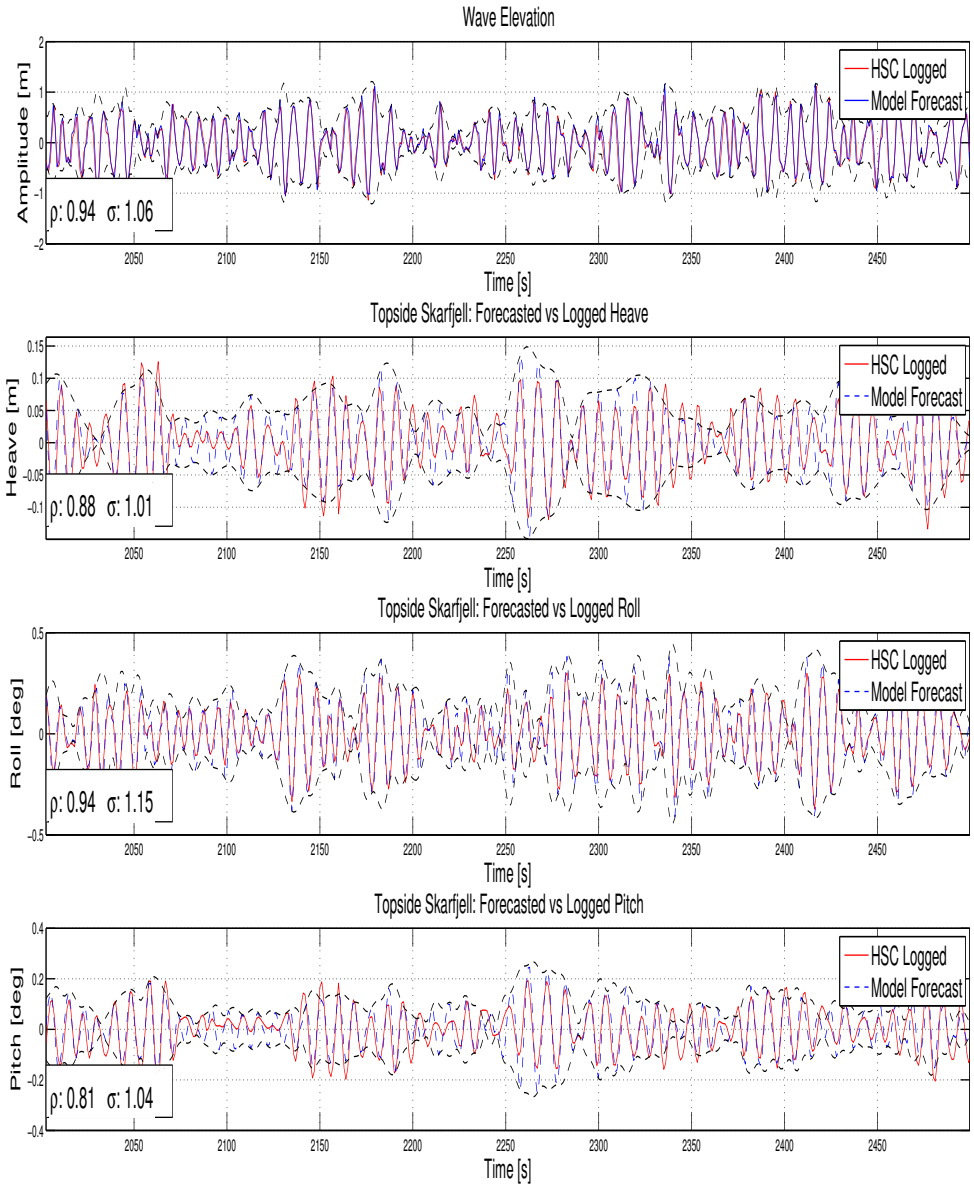

Figure E.8: Time trace test case Skarfjell, Topside CoG, complex sea-state, wave heading: 315 deg.

	Correlation Coefficient [-]	dT Shift [sec]	RMS Ratio [-]	Standard Deviation [*]
Wave Elevation	0.95	-0.46	1.04	0.44 [m]
Heave	0.88	0.85	1.01	0.05[m]
Roll	0.94	0.93	1.16	0.16[deg]
Pitch	0.81	0.83	1.04	0.07[deg]

Table E.9: Summary test case Skarfjell, Topside CoG, wave heading: 315 deg.

ENVIRONMENT

	Spectrum	Hs [m]	Tp [sec]	$HsTp^2$ [ms^2]	Rel. Heading [deg]	Spreading [???]
Sea-State	JONSWAP	1.5	8	96	0	30

Table E.10: Sea-state used for test in HSC

THIALF COG

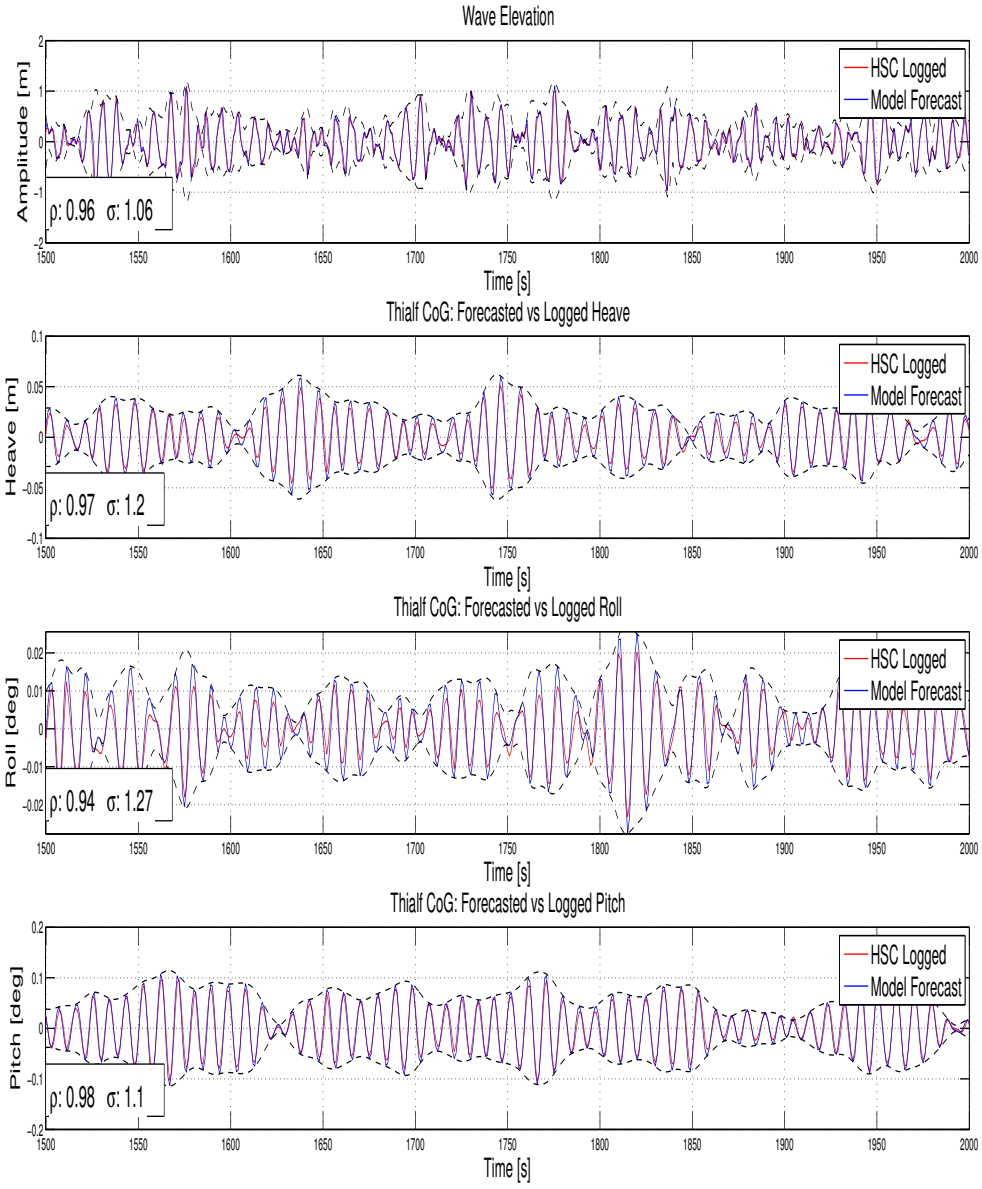

Figure E.9: Time trace Skarfjell test in HSC Skarfjell, Thialf CoG.

THIALF SKARFJELL MODULE COG

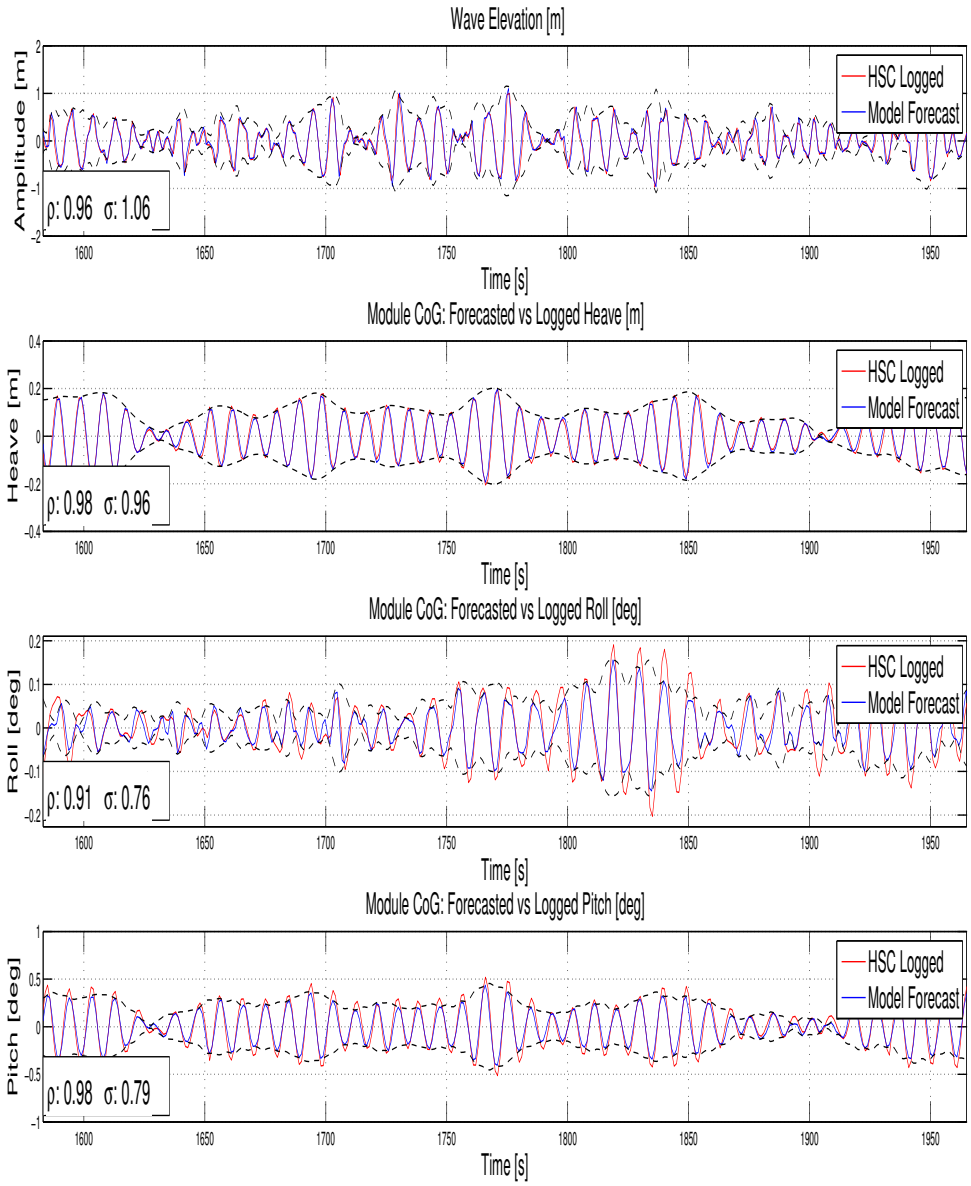

Figure E.10: Time trace Skarfjell test in HSC, Topside CoG.

E.2. SABLE ISLAND

	Heading [deg]	Draft [m]	Mooring [-]	Object [-]	Wamit [-]
Sable Island	0	26.6	Net API (3.2.1)	1500333 V01	Thialf 26m6 WDinf

Table E.11: Summary simulation specifics K-Sim

ENVIRONMENT

	Spectrum	Hs [m]	Tp [sec]	$HsTp^2$ [ms^2]	Rel. Heading [deg]	Spreading [-]
Sea-State	JONSWAP 1	1.7	6	61.2	315	cos2
	JONSWAP 2	1.1	10.3	116.7	315	cos2

Table E.12: Sea-state used in Sable Island test case

LIFTDYN MODEL INPUT

	Trim/Heel [deg]	CoG [x,y,z] [m]	Radii of gyration [x,y,z] [m]	Local Origin [x,y,z]
Thialf Sable Island	[redacted]	[redacted]	[redacted]	[redacted]

Table E.13: Summary of input LiftDyn Sable Island, Thialf, local origin is w.r.t. global origin.

	Slew [deg]	Radius [m]	Hookload [mT]	Hook Height [m]
PS Crane Skarfjell	191	52	3500	77.6
SB Crane Skarfjell	169	52	3500	77.6

Table E.14: Summary of input LiftDyn Sable Island, Cranes

THIALF COG

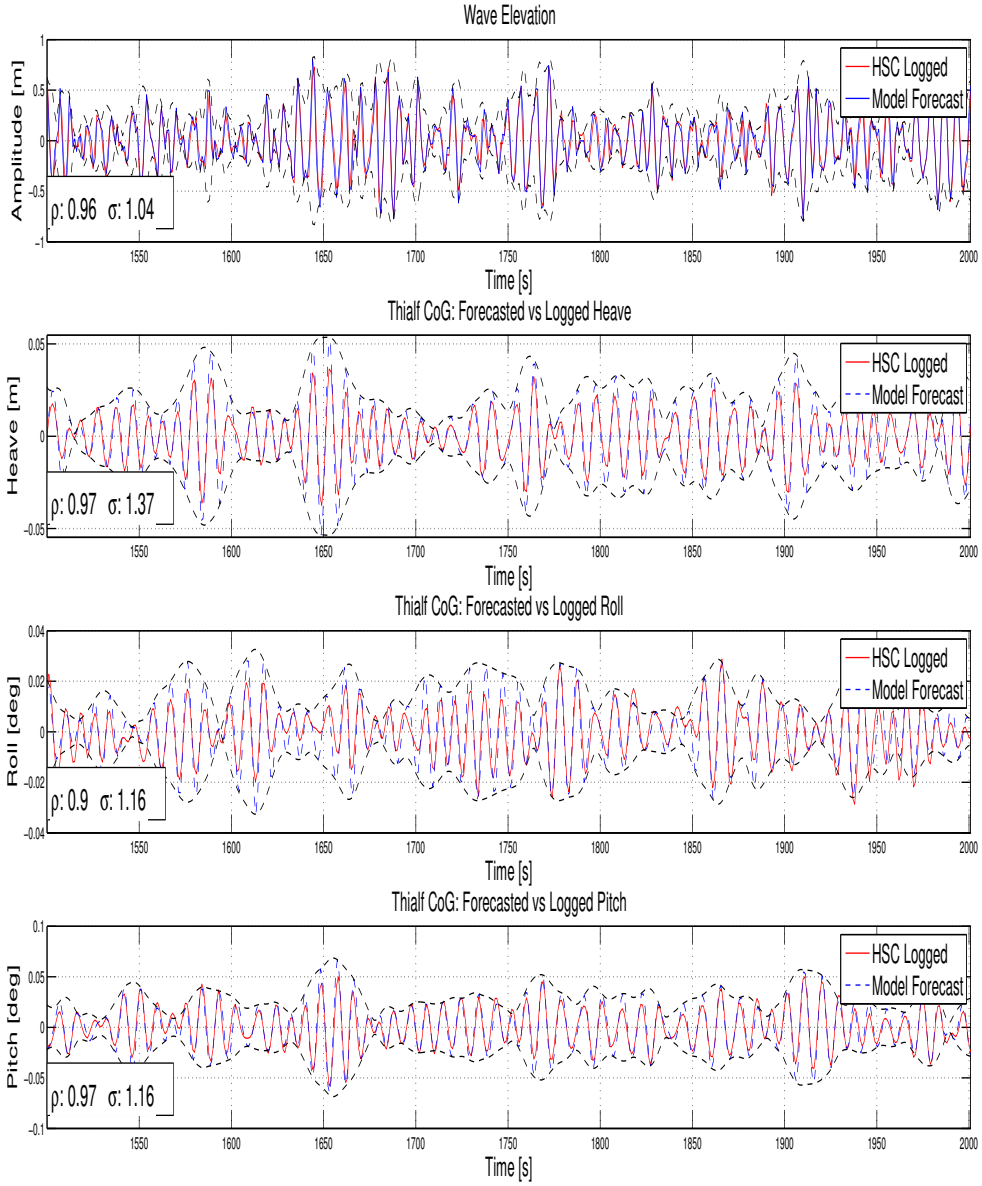

Figure E.11: Time trace test case Sable Island, Thialf CoG

	Correlation Coefficient [-]	dT Shift [sec]	RMS Ratio [-]	Standard Deviation [*]
Wave Elevation	0.96	-0.93	1.04	0.37[m]
Heave	0.97	1.65	1.37	0.02[m]
Roll	0.90	1.27	1.16	0.07[deg]
Pitch	0.97	1.36	1.16	0.01[deg]

Table E.15: Summary test case Sable Island, Thialf CoG

THIALF MODULE COG

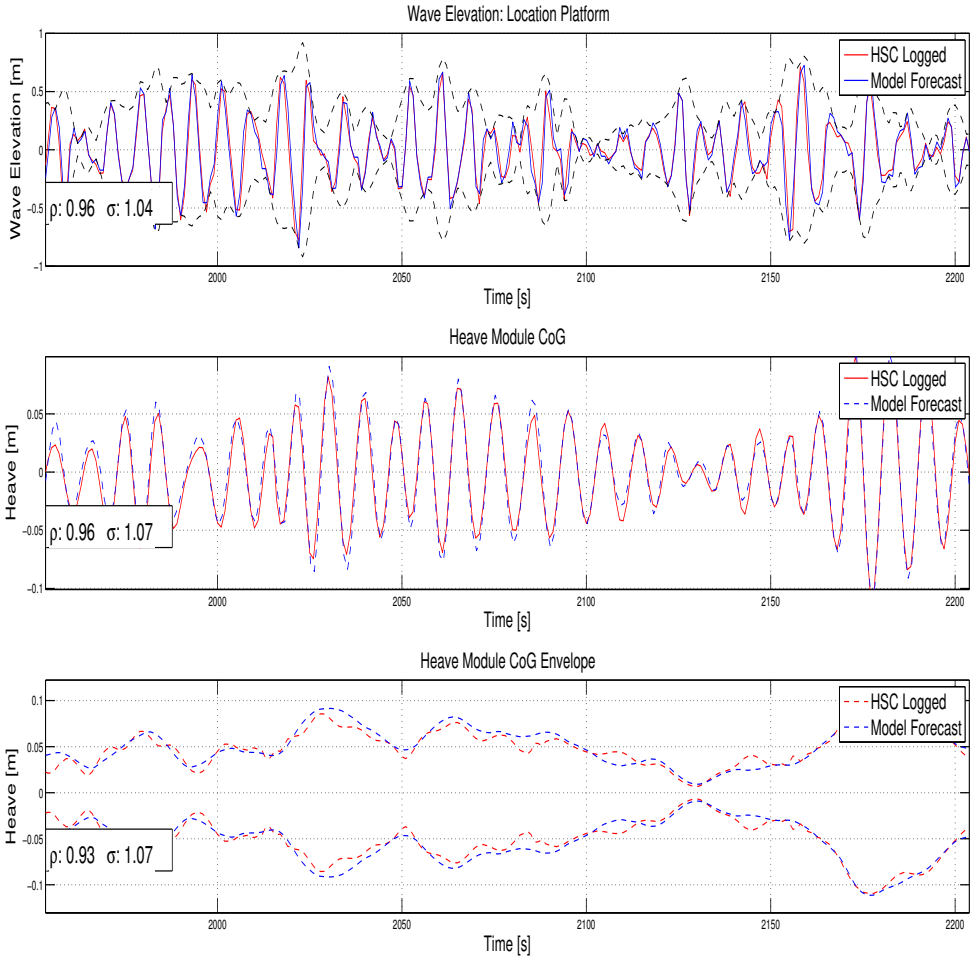

Figure E.12: Time trace test case Sable island, heave topside

	Correlation Coefficient [-]	dT Shift [sec]	RMS Ratio [-]	Standard Deviation [*]
Wave Elevation	0.96	-0.93	1.04	0.37[m]
Heave	0.96	1.26	1.07	0.04[m]
Roll	0.85	1.35	1.23	0.08[deg]
Pitch	0.89	1.35	1.2	0.05[deg]

Table E.16: Summary test case Sable Island, Module CoG

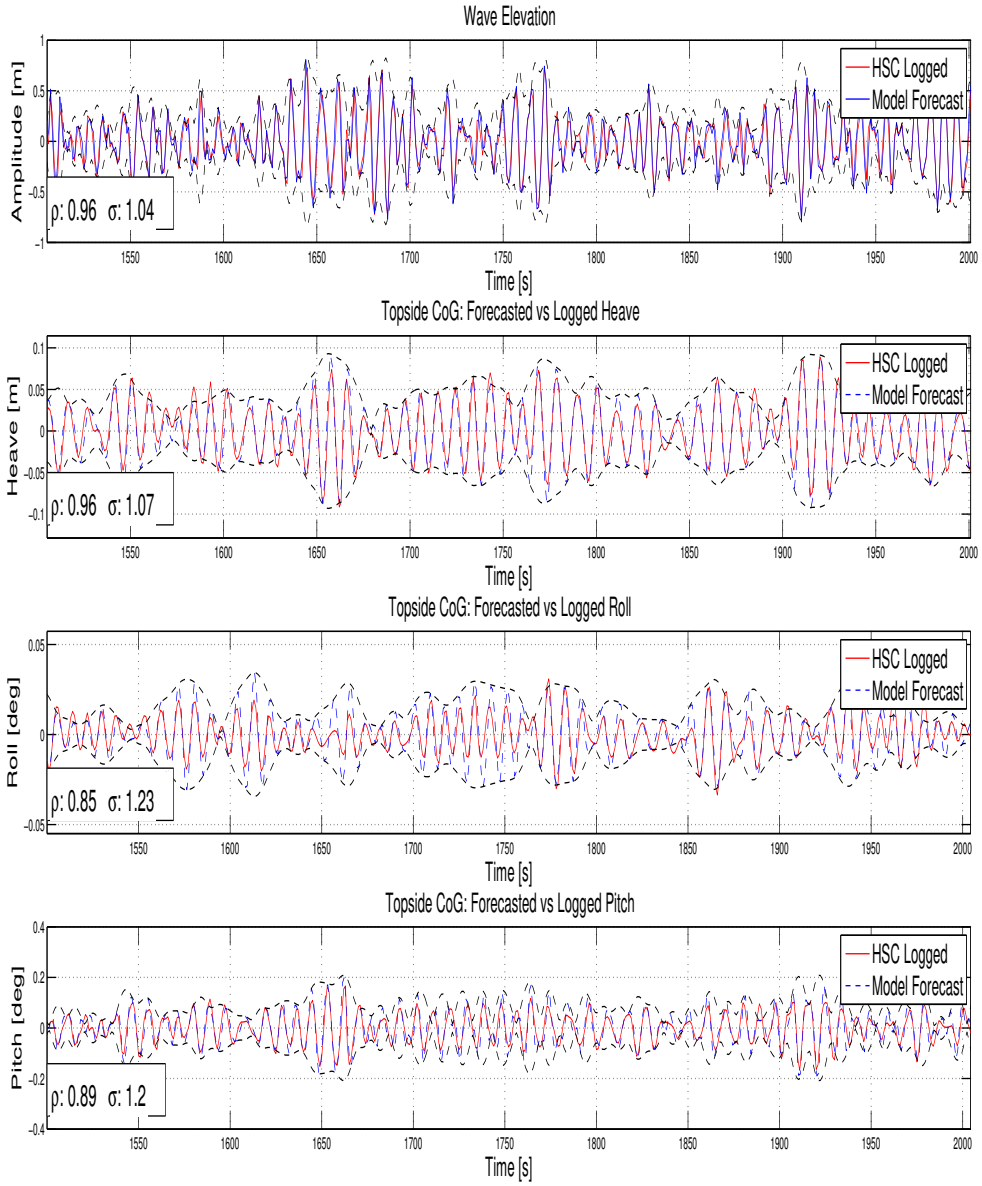

Figure E.13: Time trace test case Sable Island, Module CoG

List of Figures

List of Tables